

**Newcastle**  
University

**Treatment of Biomass Gasification Tars  
with Non-Thermal Plasmas**

Thesis submitted by:

By

**Faisal Saleem**

For the degree of

**Doctor of Philosophy**

School of Engineering,

Newcastle University, United Kingdom

September 2019



## Abstract

In this project, a non-thermal plasma dielectric barrier discharge (“DBD”) reactor was used to reduce the concentration of tar in the product gas, and its performance was evaluated at different reaction conditions. Toluene and benzene were used as tar model compounds. The effects of reaction parameters such as the residence time, concentration, wall temperature and plasma power on tar removal were studied in a tubular dielectric barrier discharge (DBD) plasma reactor at ambient pressure. The percentage removal of tar increased with increasing plasma power and residence time to as high as 99% in various carrier gases (CO<sub>2</sub>, H<sub>2</sub>, and N<sub>2</sub>) and gas mixtures. However, the decomposition of tar analogue compounds decreased with increasing concentration. It was found that most of the toluene converted into solid residue due to the polymerization of hydrocarbon radicals produced in the plasma system at ambient temperature in all carrier gases (CO<sub>2</sub>, H<sub>2</sub>, N<sub>2</sub>, and mixtures). The other products were lower hydrocarbons, CO, and H<sub>2</sub>, depending upon the type of carrier gas. The synergetic effect of power and temperature was investigated to decrease the unwanted solid deposition. It was observed that selectivity to lower hydrocarbons increased to 99% at 400 °C and 40 W, with the non-thermal plasma. In these conditions solid formation was completely prevented. The maximum selectivities to methane were 60 % and 81% for toluene and benzene, respectively. However, in other carrier gases (N<sub>2</sub> and CO<sub>2</sub>), the selectivity did not increase beyond 15 %, even with increasing temperature, and solid formation was observed even at elevated temperatures. However, in the gas mixtures, solid formation was significantly reduced when increasing the temperature due to presence of H<sub>2</sub>. Therefore, the plasma power and surrounding temperatures can be used to control the product distribution in the presence of H<sub>2</sub> carrier gas.

## **Dedication**

*I want to dedicate this work to almighty ALLAH who gave me tremendous opportunity and the brilliant people who helped me to complete my studies.*

## **Acknowledgements**

First of all, I would like to thank my supervisor Prof. Adam Harvey for his consistent support and guidance throughout this project. It would not have been possible to carry out this work without his supervision.

I would also like to thank co-supervisor Dr. Kui Zhang for his advice and knowledgeable discussion throughout my research project. His knowledge in the field of plasma was very helpful to carry out this research work in right direction. I am also thankful to him for his assistance on the lab equipment, which was new to me.

I would especially like to thank my parents, family, brothers and friends for their love, prayers, and support which helped to complete this work.

Finally, I would like to thank University of Engineering and Technology, Lahore, Pakistan and Newcastle University for financial and technical support to complete this work.



## List of Publications

### Published work

1. F. Saleem, K. Zhang, A. Harvey, Role of CO<sub>2</sub> in the Conversion of Toluene as a Tar Surrogate in a Nonthermal Plasma Dielectric Barrier Discharge Reactor, *Energy & Fuels* 32 (2018) 5164-5170.
2. F. Saleem, K. Zhang, A. Harvey, Plasma-assisted decomposition of a biomass gasification tar analogue into lower hydrocarbons in a synthetic product gas using a dielectric barrier discharge reactor, *Fuel* 235 (2019) 1412-1419.
3. F. Saleem, K. Zhang, A. Harvey, Temperature dependence of non-thermal plasma assisted hydrocracking of toluene to lower hydrocarbons in a dielectric barrier discharge reactor, *Chemical Engineering Journal* 356 (2019) 1062-1069.
4. F. Saleem, K. Zhang, A.P. Harvey, Decomposition of benzene as a tar analogue in CO<sub>2</sub> and H<sub>2</sub> carrier gases, using a non-thermal plasma, *Chemical Engineering Journal*, 360, pp. 714-720.
5. F. Saleem, K. Zhang, K. and A. Harvey, (2019a) 'Removal of Toluene as a Tar Analogue in a N<sub>2</sub> Carrier Gas Using a Non-thermal Plasma Dielectric Barrier Discharge Reactor', *Energy & Fuels*, 33(1), pp. 389-396.
6. F. Saleem, K. Zhang, A.P. Harvey, The direct conversion of benzene to methane using Non-thermal plasma, *Energy and fuel*, 33(3), pp. 2598-2601.
7. F. Saleem, K. Zhang, A.P. Harvey, Low temperature Conversion of Toluene to Methane using Dielectric Barrier Discharge reactor, *Fuel*, 248, pp. 258-261.
8. F. Saleem, J. Kennedy, U.H. Dahiru, K. Zhang, A. Harvey, Methane conversion to H<sub>2</sub> and higher hydrocarbons using Non-thermal plasma dielectric barrier discharge reactor, *Chemical Engineering and Processing-Process Intensification* (2019) 107557.



## Table of Contents

<b>Abstract</b> .....	iii
<b>Dedication</b> .....	iv
<b>Acknowledgements</b> .....	v
<b>List of Publications</b> .....	vii
<b>Published work</b> .....	vii
<b>List of Figures</b> .....	xiii
<b>List of Abbreviations</b> .....	xix
<b>Nomenclature</b> .....	xix
Chapter 1. Introduction .....	1
1.1 Biomass and its conversion technologies .....	1
1.2 Aims and objectives .....	4
1.3 Thesis structure .....	4
Chapter 2. Tar formation .....	7
2.1 Tar formation and its drawbacks .....	7
2.2 Tar Removal Techniques .....	8
2.2.1 Primary Methods .....	9
2.2.2 Secondary Methods .....	11
2.3 Plasma .....	18
2.3.1 Thermal plasma .....	18
2.3.2 Non thermal plasmas (NTPs) for treatment of biomass gasification tars .....	19
Chapter 3. Materials and methods .....	37
3.1 Chemicals and gases .....	37
3.2 Experimental setup .....	37
3.3 Experimental procedure .....	38
3.4 Definitions .....	40
Chapter 4. The role of CO <sub>2</sub> in the conversion of toluene as a tar surrogate .....	43

4.1	Introduction .....	43
4.2	Results and discussion.....	44
4.2.1	Effect of Power .....	44
4.2.2	Effect of concentration.....	46
4.2.3	Effect of residence time .....	47
4.2.4	Effect of Temperature .....	51
4.3	Conclusions .....	52
Chapter 5.	Decomposition of toluene as a tar analogue in H <sub>2</sub> carrier gas .....	55
5.1	Introduction .....	55
5.2	Results and Discussion.....	55
5.2.1	Effect of Power .....	55
5.2.2	Effect of concentration.....	59
5.2.3	Effect of residence time .....	60
5.2.4	Effect of temperature .....	62
5.3	Conclusions .....	65
Chapter 6.	Removal of toluene as a tar analogue in a N <sub>2</sub> carrier gas using a non-thermal plasma dielectric barrier discharge (DBD) reactor .....	67
6.1	Introduction .....	67
6.2	Results and discussion.....	68
6.2.1	Effect of power and residence time .....	68
6.2.2	Effect of toluene concentration.....	72
6.2.3	Effect of temperature .....	74
6.3	Comparative decomposition of toluene in different carrier gases.....	76
6.4	Conclusions .....	79
Chapter 7.	Plasma-assisted decomposition of toluene in a mixture of gases .....	81
7.1	Introduction .....	81
7.2	Results and discussion.....	81
7.2.1	Effect of Power .....	81

7.2.2	Effect of residence time .....	84
7.2.3	Effect of concentration .....	85
7.2.4	Effect of temperature .....	87
7.3	Conclusions.....	91
Chapter 8. Decomposition of benzene as a tar analogue in CO <sub>2</sub> and H <sub>2</sub> carrier gases, using a non-thermal plasma.....		93
8.1	Introduction.....	93
8.2	Results and discussion .....	94
8.2.1	Effect of carrier gas and SIE.....	94
8.2.2	Effect of residence time.....	97
8.2.3	Effect of Concentration .....	98
8.2.4	Effect of temperature .....	99
8.3	Conclusions.....	102
Chapter 9. Role of methane in the product gas towards the formation of lower hydrocarbons during the decomposition of different tar analogues .....		105
9.1	Introduction.....	105
9.2	Results and discussion .....	105
9.2.1	Effect of SIE .....	105
9.2.2	Effect of residence time .....	110
9.2.3	Effect of temperature .....	112
9.3	Conclusions.....	114
Chapter 10. Conclusions and Further Work.....		117
10.1	Conclusions.....	117
10.2	Future recommendations.....	119
10.2.1	Kinetic and scale up study .....	119
10.2.2	Formation of valuable lower hydrocarbons (C <sub>1</sub> -C <sub>5</sub> ).....	120
10.2.3	Synthesis of nano crystals and valuable solid products using Non-thermal plasmas	120



## List of Figures

Figure 1.1. Process steps in gasification (Ruiz <i>et al.</i> , 2013).....	3
Figure 2.1. Effect of temperature changes on various factors (Hallgren, 1997). ....	10
Figure 2.2. Schematic Diagram of a Catalytic Candle Filter (Draelants <i>et al.</i> , 2000).....	13
Figure 2.3. Steam gassification with wet gas scrubbing and dry dust removal in Gussing, Austria (Lettner <i>et al.</i> , 2007). ....	14
Figure 2.4. Strategy of Catalytic Tar removal (Schmidt <i>et al.</i> , 2011). ....	16
Figure 2.5. Wire cylinder configuration of pulsed corona discharge with preheating (Fridman <i>et al.</i> , 2005). ....	20
Figure 2.6. Energy consumed to decompose Napthalene. Conc., 500-600 ppm; T, 200-210°C (Nair <i>et al.</i> , 2003c). ....	22
Figure 2.7. Tar removal in pure N <sub>2</sub> . Phenol, 1000 ppm; Naphthalene 500-600 ppm; Toluene, 700 ppm (Nair <i>et al.</i> , 2003a). ....	22
Figure 2.8. Toluene decomposition. T, 773 K; He, carrier gas (Tao <i>et al.</i> , 2013). ....	24
Figure 2.9. Common dielectric barrier discharge configurations (Kogelschatz, 2003) ....	25
Figure 2.10. NTP Benzene Degradation Comparison (Kim, 2004a).....	25
Figure 2.11. Toluene decomposition and energy efficiency. Power, 35 W; toluene concentration, 17.7 g/Nm <sup>3</sup> (Liu <i>et al.</i> , 2017b). ....	27
Figure 2.12. The yield of gaseous products. Power, 35 W; toluene concentration, 17.7 g/Nm <sup>3</sup> (Liu <i>et al.</i> , 2017b). ....	27
Figure 2.13. Suggested Toluene Decomposition Pathway (Liang <i>et al.</i> , 2013) ....	28
Figure 2.14. Photo image of the gliding arc discharge in the parallel flow reactor (Fridman <i>et al.</i> , 2005).....	29
Figure 2.15. Effect of benzene concentration (Chun <i>et al.</i> , 2013) ....	30
Figure 2.16. Effect of total gas flow rate (Chun <i>et al.</i> , 2013). ....	31
Figure 2.17. Effect of specific energy input(Yang and Chun, 2011). ....	31
Figure 2.18. Effect of various electrode length (Yang and Chun, 2011).....	32
Figure 2.19. Effect of the oscillation amplitude (Chun <i>et al.</i> , 2012) ....	33
Figure 2.20. Pressure drop measured with respect to time. SIE, 360J/L; Gas flow rate, 6.6 L/min; conc., 100 ppm <sub>v</sub> (Karatum and Deshusses, 2016). ....	35
Figure 3.1. Schematic diagram of the experimental setup. ....	38
Figure 4.1. Effect of plasma power on the (a) conversion of toluene, (b) selectivity of CO, H <sub>2</sub> and LHC at residence time 4.23 s, (c) yield of CO and H <sub>2</sub> at 4.23 s, and (d) decomposition of	

CO <sub>2</sub> . Reaction conditions: gas flow rate, 40.6 ml/min; concentration, 82g/Nm <sup>3</sup> ; temperature, ambient; and residence time, 4.23 s. ....	44
Figure 4.2. Effect of concentration on the (a) conversion of toluene, (b) selectivity of CO, H <sub>2</sub> and LHC at 10 W, (c) decomposition of CO <sub>2</sub> , and (d) energy efficiency. Reaction conditions: gas flow rate, 40.6 ml/min; residence time, 4.23 s; concentration, 82g/Nm <sup>3</sup> ; and Temperature, ambient.....	46
Figure 4.3 Effect of residence time on the (a) conversion of toluene and towards selectivity of CO, H <sub>2</sub> and LHC (C <sub>1</sub> -C <sub>5</sub> ), (b) decomposition of CO <sub>2</sub> and towards yield of CO and H <sub>2</sub> . Reaction conditions; temperature, ambient; gas flow rate, 40.6-120 ml/min; concentration, 82g/Nm <sup>3</sup> ; and Power, 40 W. ....	48
Figure 4.4. Reaction mechanism.....	50
Figure 4.5. Effect of temperature on (a) the conversion of toluene, (b) selectivity of CO, H <sub>2</sub> and LHC (C <sub>1</sub> -C <sub>5</sub> ), and (c) the yield of CO, H <sub>2</sub> and decomposition of CO <sub>2</sub> . Reaction conditions: input power, 40 W; gas flow rate, 40.6 ml/min; concentration, 82g/Nm <sup>3</sup> ; and residence time, 4.23 s.....	51
Figure 5.1. Effect of plasma power on the conversion, energy efficiency and selectivity to LHC; bars represent standard deviation. Reaction conditions: concentration, 33 g/Nm <sup>3</sup> ; Temperature, ambient; flow rate, 40.6 ml/min; residence time, 4.23 s; and SIE, 7.39-59.11 kJ/L. ....	56
Figure 5.2. Selectivity of different LHC at 4.23 s. Reaction conditions: concentration, 33 g/Nm <sup>3</sup> ; Temperature, ambient; residence time, 4.23 s; and SIE, 7.39-59.11 kJ/L. ....	57
Figure 5.3. Effect of specific input energy (SIE) on the remaining fraction of toluene (Reaction conditions: concentration, 33 g/Nm <sup>3</sup> ; Temperature, ambient; and residence time, 1.43 s).....	59
Figure 5.4. Effect of concentration on the conversion of toluene and energy efficiency of the plasma process; bars represent standard deviation. Reaction conditions: input power, 10 W; residence time, 4.23 s; flow rate, 40.6 ml/min; ambient temperature; and SIE, 14.77 kJ/L....	60
Figure 5.5. Effect of residence time (a) on the conversion of toluene, energy efficiency and selectivity to LHC; bars represent standard deviation, and (b) selectivity to individual lower hydrocarbons. Reaction conditions: concentration, 33 g/Nm <sup>3</sup> ; flow rate, 40.6-120 ml/min; Temperature, ambient; and Power, 20 W; and SIE, 10-29.6 kJ/L. ....	61
Figure 5.6. Effect of temperature on (a) the conversion of toluene, (b) total selectivity LHC; (c) selectivity to various LHCs at 10 W, (d) selectivity to various LHCs at 20 W, (e) selectivity to various LHCs at 30 W, and (f) selectivity to various LHCs at 40 W. Reaction	

conditions: concentration, 33 g/Nm <sup>3</sup> ; flow rate, 40.6 ml/min; residence time, 4.23 s; and SIE, 14.77-59.11 kJ/L.....	63
Figure 6.1. Effect of plasma power on the conversion of toluene. Reaction conditions: ambient temperature; Concentration, 33 g/Nm <sup>3</sup> ; flow rate, 40.6 ml/min; residence time, 4.23 s; carrier gas, N <sub>2</sub> ; and SIE, 7.39-59.11 kJ/L. ....	68
Figure 6.2. Effect of plasma power on selectivity of gaseous products. Reaction conditions: ambient temperature; toluene concentration, 33 g/Nm <sup>3</sup> ; flow rate, 40.6 ml/min; residence time, 4.23 s; carrier gas, N <sub>2</sub> ; and SIE, 7.39-59.11 kJ/L. ....	69
Figure 6.3. Effect of residence time on the conversion and towards the selectivity of gaseous products. Reaction conditions: input power, 20 W; ambient temperature; concentration, 33 g/Nm <sup>3</sup> ; carrier gas, N <sub>2</sub> ; and flow rate, 40.6-120 ml/min.....	70
Figure 6.4. Effect of concentration on the conversion and energy efficiency. Reaction conditions: input power, 10 W; ambient temperature; flow rate, 40.6 ml/min; residence time, 4.23 s; carrier gas, N <sub>2</sub> ; and SIE, 14.77 kJ/L.....	72
Figure 6.5. Effect of concentration on the selectivity of gaseous products. Reaction conditions: input power, 10 W; ambient temperature; flow rate, 40.6 ml/min; carrier gas, N <sub>2</sub> ; and residence time, 4.23 s.....	73
Figure 6.6. Effect of temperature on (a) the conversion of toluene, (b) total selectivity to LHCs formation (C <sub>1</sub> -C <sub>6</sub> ), (c) selectivity to individual LHCs, 15% H <sub>2</sub> , (d) selectivity to individual LHCs, 25% H <sub>2</sub> , and (e) selectivity to individual LHCs, 35% H <sub>2</sub> . Reaction conditions: input power, 40 W; and concentration, 33g/Nm <sup>3</sup> ; and residence time, 4.23 s; and SIE, 14.77-59.11 kJ/L.....	75
Figure 6.7 Reaction mechanism at high temperature .....	76
Figure 6.8. Effect of (a) power on the conversion of toluene, (b) power on the total selectivity to LHC; (c) RT on the toluene conversion, (d) concentration on toluene conversion, (e) temperature on toluene conversion, and (f) temperature on the selectivity to LHCs at 40 W. Reaction conditions: concentration, 33 g/Nm <sup>3</sup> .....	77
Figure 7.1. Effect of plasma power on (a) the conversion and energy efficiency of toluene, (b) the selectivity and yield of different gaseous products, and (c) individual lower hydrocarbons. Reaction conditions: Concentration, 33g/Nm <sup>3</sup> ; residence time, 2.82 s; flow rate, 40.6 ml/min; SIE, 2.05-16.4 kWh/m <sup>3</sup> ; and Temperature, ambient. ....	82
Figure 7.2 Reaction mechanism .....	83
Figure 7.3. Effect of residence time (a) on the conversion and energy efficiency of toluene, (b) on the selectivity and yield of different gaseous products, and (c) on individual lower	

hydrocarbons. Reaction conditions: concentration, 33g/Nm <sup>3</sup> ; Power, 20 W; flow rate, 40.6-120 ml/min; and Temperature, ambient. ....	85
Figure 7.4. Effect of concentration (a) on the conversion and energy efficiency of toluene, (b) on the selectivity and yield of different gaseous products, and (c) on individual lower hydrocarbons. Reaction conditions: residence time, 2.82 s; power, 10 W; flow rate, 40.6 ml/min; and temperature, ambient. ....	86
Figure 7.5. Effect of temperature on (a) the conversion of toluene, (b) total selectivity and yield of LHC and CO at 20 W; selectivity and yield of different LHC at (c) 10 W, (d) 20 W, (e) 30 W, and (f) 40 W. Reaction conditions: concentration, 33 g/Nm <sup>3</sup> ; residence time, 2.82 s; flow rate, 40.6 ml/min. ....	88
Figure 7.6 Reaction mechanism at elevated temperature .....	89
Figure 7.7. Effect of (a) power on the conversion of toluene (b) power on the total selectivity to C <sub>2</sub> -C <sub>5</sub> , (c) residence time on the conversion of toluene at 20 W, and (d) temperature on the conversion and selectivity at 40 W. Reaction conditions: concentration of toluene, 33 g/Nm <sup>3</sup> .....	90
Figure 8.1. Effect of carrier gas and SIE on (a) the conversion and energy efficiency of benzene, (b) selectivity of products in H <sub>2</sub> carrier gas, (c) selectivity of products in CO <sub>2</sub> carrier gas, and (d) detailed selectivity to LHC. Reaction conditions: concentration, 36 g/Nm <sup>3</sup> ; temperature, ambient; and residence time, 4.23 s. ....	94
Figure 8.2 General Mechanism for benzene decomposition .....	96
Figure 8.3. Effect of residence time on (a) the conversion and energy efficiency of benzene, and (b) selectivity and yield of products, in H <sub>2</sub> and CO <sub>2</sub> . Reaction conditions: concentration, 36 g/Nm <sup>3</sup> ; temperature, ambient; and plasma power, 20 W. ....	97
Figure 8.4. Effect of concentration in each carrier gas on (a) the conversion and energy efficiency of benzene, and (b) products selectivity and yield. Reaction conditions: SIE, 14.7 kJ/ L; temperature, ambient; and power, 10 W. ....	99
Figure 8.5. Effect of temperature and carrier gas on (a) the conversion and energy efficiency of benzene, (b) selectivity to lower hydrocarbons, and (c) selectivity to individual LHC in H <sub>2</sub> carrier gas .Reaction conditions: concentration, 33 g/Nm <sup>3</sup> ; residence time, 4.23 s; power, 40 W; and SIE, 59.1 kJ/L. ....	100
Figure 8.6 Effect of specific input energy (SIE) on the remaining fraction of benzene. Reaction conditions: concentration, 36 g/Nm <sup>3</sup> ; Temperature, ambient; and residence time, 4.23 s. ....	102

Figure 9.1. Effect of SIE on (a) the conversion and energy efficiency of tar representatives, (b) the selectivity and decomposition of gaseous products (benzene), and (c) the selectivity and decomposition of gaseous products (toluene). Reaction conditions: concentration, 33g/Nm <sup>3</sup> ; residence time, 2.82 s; flow rate, 40.6 ml/min; SIE, 2.05-16.4 kWh/m <sup>3</sup> ; and temperature, ambient. ....	106
Figure 9.2. Effect of SIE on (a) the individual selectivity to C <sub>2</sub> -C <sub>5</sub> (toluene), (b) the individual selectivity to C <sub>2</sub> -C <sub>5</sub> (benzene), (c) composition of permanent gas (toluene), and (d) the composition of permanent gases (benzene). Reaction conditions: concentration of benzene and toluene, 33 g/Nm <sup>3</sup> ; residence time, 2.82 s; flow rate, 40.6 ml/min; SIE, 2.05-16.4 kWh/m <sup>3</sup> ; and temperature, ambient. ....	108
Figure 9.3. Effect of specific input energy (SIE) on the remaining fraction of toluene. Reaction conditions: concentration, 33 g/Nm <sup>3</sup> ; temperature, ambient; and residence time, 2.82 s.....	109
Figure 9.4. Effect of residence time on (a) the conversion of toluene, benzene and energy efficiency, (b) Decomposition of CO <sub>2</sub> and CH <sub>4</sub> and selectivity to LHC, (c) Individual selectivity to LHC for benzene, and (d) individual selectivity to LHC for toluene; bars represent standard deviation. Reaction conditions: concentration, 33 g/Nm <sup>3</sup> ; flow rate, 40.6-120 ml/min; ambient temperature; and power, 20 W.....	111
Figure 9.5. Effect of temperature on the conversion of toluene and benzene. Reaction conditions: concentration, 33 g/Nm <sup>3</sup> ; residence time, 2.82 s; flow rate, 40.6 ml/min, SIE, 16.40 kWh/m <sup>3</sup> .....	112
Figure 9.6. Effect of temperature on (a) the products distribution (toluene), (b) the product distribution (benzene) ;(c) the individual selectivity to LHC (toluene); (d) the individual selectivity to LHC (benzene). Reaction conditions: concentration, 33 g/Nm <sup>3</sup> ; residence time, 2.82 s; flow rate, 40.6 ml/min.....	113



## List of Abbreviations

### *Nomenclature*

B	Intermediate product
C	Concentration (g/Nm <sup>3</sup> )
C <sub>0</sub>	Initial concentration (g/Nm <sup>3</sup> )
d <sub>B</sub>	Decomposition of benzene
d <sub>T</sub>	Decomposition/conversion efficiency of toluene
k <sub>SIE</sub>	Energy constant (L/kJ)
m	Number of carbon atoms
M	Background gas
n	Reaction order
P	Power (W)
R	Radicals
S	Selectivity (%)
T	Temperature (°C) otherwise mentioned
Y	Yield (%)

### *Acronyms*

CR	Catalytic reforming
DBD	Dielectric barrier discharge
DD	Direct decomposition
EE	Energy efficiency (g/kWh)
EOPR	Externally oscillated plasma reformer
FID	Flame ionization detector
GAD	Gliding arc discharge
GC	Gas chromatography
LHC	Lower hydrocarbons (<C <sub>6</sub> and <C <sub>7</sub> )
MFC	Mass flow controller
PCR	Plasma enhanced catalytic reforming (PCR)
PD	Plasma assisted decomposition
RDF	Refuse-derived fuel

RGAD	Rotating gliding arc discharge
RT	Residence time (s)
SD	Surface discharge
SIE/SEI	Specific input energy (kJ/L)
TCD	Thermal conductivity detector
UV	Ultraviolet
VOC	Volatile organic compound

# Chapter 1. Introduction

## 1.1 Biomass and its conversion technologies

Organic material derived from plants (including, trees and crops) is known as “biomass”. Green plants convert sunlight into plant material by a photosynthetic process and produce biomass. The organic matter produced is usually considered to be a source of renewable energy, because it releases the solar energy stored in chemical bonds. The biomass can release stored energy by breaking these chemical bonds through combustion, digestion or decomposition (McKendry, 2002a). Hence, biomass has always been considered as a main source of renewable energy for human being.

There are different ways to obtain biomass, such as cultivation of “energy crops”, harvesting plants and forestry residues, and from organic wastes. After collection of the biomass, it is transported and stored for selection of suitable energy conversion process. The energy from the biomass can be extracted by various processes. The conversion process of biomass depends upon many factors, such as quantity and nature of feedstock, environmental regulations, the required energy form, requirements for end use, and economic conditions. In many cases the required form of energy decides the process path (McKendry, 2002b).

There are three major products usually produced from biomass: transportation fuel, heat/power generation and chemical feedstock. The first two types of products are energy related, and could be produced from biomass through thermo-chemical technology. There are four different conversion processes available within thermo-chemical technology. These processes are combustion, gasification, pyrolysis and liquefaction. In combustion, biomass is burned in air and the temperature of the hot gases reaches 800–1000 °C. The stored energy of the biomass is converted to heat, electricity or mechanical power via various downstream steps. The combustion of the biomass is only feasible when the moisture contents are below 50%. However, the conversion efficiencies of biomass to bioenergy vary from 20–40 % and the fuel produced from combustion is not appropriate for use in a gas turbine (Bridgwater and Evans, 1993; Rampling and Gill, 1994; Livingston *et al.*, 1997).

Pyrolysis is the process of heating biomass to 500 °C in the absence of air. It produces liquid, gaseous and solid products. It can be used for the production of bio-oil, through flash pyrolysis, resulting in a yield near 80% (Bridgwater and Evans, 1993; Bridgwater *et al.*,

1996). The product oil has its applications in turbines and engines and can be used in refineries as a feed stock. However, the major problems associated with bio-oil are corrosivity and low thermal stability. Therefore, it is necessary to upgrade bio-oils by reducing the oxygen percentage and eliminating alkalis through e.g. catalytic cracking and hydrogenation (McKendry, 2002b).

Biomass gasification is a method for producing alternative, eco-friendly fuels for power generation and transport. It is an indirect combustion process in which solid biomass is converted to valuable synthesis gas ( $H_2 + CO$ ) or gaseous fuel by partial oxidation at high temperatures (Basu, 2010). The partial oxidation of biomass can be performed in air, oxygen or steam.

Air gasification does not produce high quality gas in terms of heating value (higher heating value ranges from 4–7 MJ m<sup>-3</sup>), so is not suitable for pipeline distribution due to its low energy density. However, it is good for turbines, engines and boiler operations. Higher gas qualities are achieved when using oxygen as the gasifying medium (10–18 MJ m<sup>-3</sup>), which is better for limited pipeline transportation and for conversion of synthesis gas to valuable chemicals, such as methanol and gasoline. Steam gasification can also be used to produce higher quality gas, with the process energy possibly provided by the combustion of by-product char in another reactor. The twin fluid bed system is the typical example of this. However, air is widely used as a gasifying medium because of the costs and hazards associated with the oxygen gasification; and the complexity and cost of multiple reactors are the drawbacks of steam gasification (Bridgwater, 1995).

As shown in Figure 1.1, during gasification, biomass is decomposed according to the following sequence: drying, pyrolysis and partial oxidation of solid char and pyrolysis products. Pyrolysis takes place at 423–673 K, and the biomass decomposes into char, gases (non-condensable) and volatile hydrocarbons (Ruiz *et al.*, 2013). Then, these products react with the oxidizing agent to produce CO, CO<sub>2</sub>, H<sub>2</sub> and smaller amounts of lower hydrocarbon gases (C<sub>1</sub>–C<sub>4</sub>). CO and CO<sub>2</sub> are produced by the oxidation of carbon in char, whereas H<sub>2</sub> is produced through water gas shift reaction. There are many factors, such as moisture contents, composition of feed, and reaction temperatures, which affect the composition of product gas.

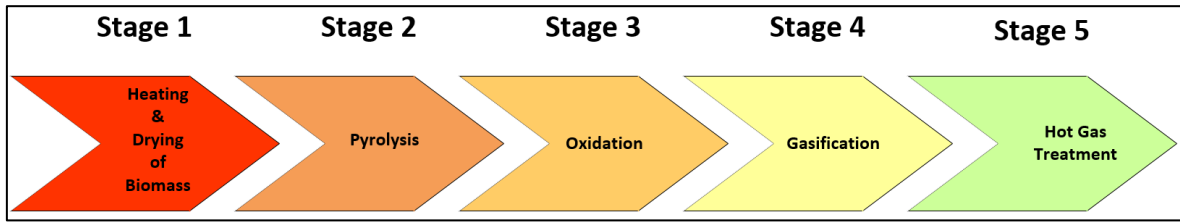


**Figure 1.1. Process steps in gasification (Ruiz *et al.*, 2013).**

Final product gas contains tar compounds due to incomplete conversion of the liquid products produced from the pyrolysis. This happens due to chemical limitations of reactions and geometrical limitations of reactors. These tar compounds tend to be refractory due to the higher temperatures involved in gasification than pyrolysis. So, it becomes very difficult to remove these tar compounds by physical, thermal or catalytic process (Bridgwater, 1995).

Generally, decomposition of tar is applied after the gasifier and there are a variety of methods that can be used to eliminate tar compounds, such as mechanical separation, thermal cracking and catalytic cracking. In mechanical separation, tar is removed by: Venturi scrubbers, water scrubbers, ESP, rotational particle separators or cyclones. However, these methods only remove or capture the tar from producer gas, causing secondary pollution. Moreover, the chemical energy associated with tars is also wasted (Richardson *et al.*, 2012). Thermal and catalytic cracking can be used to decompose tar compounds, but these technologies also have disadvantages: operating cost, for instance, is significantly increased by maintaining high temperature in thermal cracking (Chen *et al.*, 2009). Catalytic cracking is a good way to decompose tar into valuable products and operates at lower temperatures than thermal decomposition of tar (Chen *et al.*, 2015). However, various catalysts may be poisoned due to their high affinity for sulphur and chlorine. Fouling, which arises due to coking, is another problem, and it is difficult to control unless the feed of the gasifier is well tested. The major contaminants of the product gas are chlorine, sulphur and nitrogen compounds (Chun and Lim, 2012). Hence, it is a significant challenge to decompose the tar completely, due to its complex nature and the unavailability of proven, efficient technology.

Downstream non-thermal plasma (NTP) treatment of tar is a possible solution due to its high removal efficiency and compact design. The NTP produces high energy electrons (1–10 eV) that decompose the carrier gas and generate reactive species at normal temperature (Yan *et al.*, 2002). It consists of many active species, which cause electron impact excitation, light excitation, dissociation excitation, ionization, radiative recombination and atomic photoionization, etc. These phenomena or combinations of them can convert the tar into lighter hydrocarbons.

## 1.2 Aims and objectives

The main aims of this work are

1. To investigate the feasibility of treating biomass gasification tars with non-thermal plasmas.
2. To develop a dielectric barrier discharge reactor as novel technology to decompose heavy hydrocarbons to lower hydrocarbons.

To this end, the following objectives have been defined:

1. To investigate the applications of non-thermal plasmas dielectric barrier discharge reactor for different tar analogues (benzene and toluene).
2. To study the effects of various reaction parameters, such as residence time, discharge power, concentration of tar compounds and wall temperature on the performance of DBD reactor and products distribution.
3. To study the effect of different carrier gases individually and collectively towards the tar conversion and products distribution.
4. To develop a non-thermal plasma based technology to eliminate residue and toxic compounds formation by controlling the reaction parameters.

## 1.3 Thesis structure

Most researchers in the field of non-thermal plasma processing have focused on the decomposition of tar analogue compounds in N<sub>2</sub> carrier gas. However, product gas from gasifiers contains various different gases (CO<sub>2</sub>, H<sub>2</sub>, N<sub>2</sub>, CO and CH<sub>4</sub>), all of which may influence the performance of the plasma system. Therefore, it is very important to investigate the effect of individual carrier gases to study the contribution towards the products distribution and tar decomposition.

Toluene and benzene were selected as tar analogue compounds. Toluene was selected due to its simple structure, high thermal stability and low boiling point. Its simple structure aids understanding of the mechanism involved in the cracking of tar under non-thermal plasma conditions at low temperatures and ambient pressure. For these reasons many studies have used toluene as a tar analogue to investigate the performance of the system (Taralas *et al.*, 2003; Zhu *et al.*, 2016; Liu *et al.*, 2017a; Liu *et al.*, 2017b; Sun *et al.*, 2017). Benzene has a higher thermal stability than toluene. It was reported that high temperatures are required

(>760 °C) for ring opening products to be formed during the decomposition of benzene (Brooks *et al.*, 1979). Therefore, to investigate the performance of the DBD reactor benzene was also used as a tar model compound.

**Chapter 2** explains the background of the study.

**Chapter 3** explains all materials and methods used in this research.

In **Chapter 4**, the role of CO<sub>2</sub> was studied by varying different parameters such as, power, residence time, concentration and temperature. CO<sub>2</sub> is present in significant amount in the gasifier product gas, ranges from 15–25% depending upon gasification conditions. Therefore, it was necessary to investigate the contribution of CO<sub>2</sub> towards the product distribution and decomposition of toluene.

In **Chapter 5**, the contribution of H<sub>2</sub> was studied, as it has an even higher percentage (25–50%) than CO<sub>2</sub> in “real” product gas from gasifier.

If air was used as a gasifying medium, then N<sub>2</sub> is the most significant component of typical biomass gasifier product gas (around 50%) (Narvaez *et al.*, 1996). Therefore, N<sub>2</sub> was used as a carrier gas in **Chapter 6**. Various percentages (15–25%) of H<sub>2</sub> were added to N<sub>2</sub> carrier gas to try to increase the selectivity to LHC (C<sub>1</sub>-C<sub>6</sub>), rather than solid residues.

In **Chapter 7**, a mixture of gases (CO<sub>2</sub>: 30%; CO: 20 %; H<sub>2</sub>: 50%) was used, as a “synthetic product gas”. The typical mixture was selected because, in steam gasification, the gasifier product gas is a mixture of CO<sub>2</sub>, H<sub>2</sub>, CO, and various by-products (Luo *et al.*, 2009).

Benzene has relatively high thermal stability than toluene. It has been reported that soot formation occurred when benzene is used as a tar representative (Jamróz *et al.*, 2018).

Therefore, benzene was used as a model compound to test H<sub>2</sub> and CO<sub>2</sub> at elevated temperature in **Chapter 8**. A parametric study (power, residence time, concentration and temperature) was also conducted to investigate the performance of DBD reactor.

In **Chapter 9**, methane was used as an additive to observe its effect on product selectivity during the decomposition of benzene *and* toluene. This was of interest, as methane percentages can increase to as high as 12% at lower gasification temperatures (700–800 °C) (Luo *et al.*, 2009)

**Chapter 10** summarises the conclusions and proposes future work.



## Chapter 2. Tar formation

### 2.1 Tar formation and its drawbacks

Lignin, cellulose and hemicellulose are the major components of biomass. Lignin is the only fraction of the biomass that is aromatic in nature and a precursor for polycyclic aromatic hydrocarbons (Palma, 2013). Lignin is the most difficult to crack of the biomass components. Lignin pyrolysis produces tars consisting of phenolic compounds of various molecular weights (Jegers and Klein, 1985). Cellulose and hemicellulose are responsible for the production of acetic acid, formic acid, furfural, methanol and acetone (Hosoya *et al.*, 2008; Palma, 2013)

Experiments were performed to compare steam gasification, pyrolysis and partial oxidation conditions by using hinoki cypress sawdust (Zhang *et al.*, 2010). It was observed that primary tar compounds were produced at 600 °C. These compounds include methanol, acetaldehyde, acetic acid, methyl furfural, and small quantities of aromatic compounds (toluene, phenol and benzene). However, at higher temperatures (900–1000 °C), fewer oxygenated compounds (phenol and benzo furan) were produced during steam gasification and pyrolysis. The main compounds produced at this temperature included benzene, toluene, styrene, naphthalene, indene and pyrene. Most tar compounds were decomposed by partial oxidation at temperature above 1100 °C, except for stable aromatic hydrocarbons (toluene, phenol and naphthalene) (Zhang *et al.*, 2010).

A typical composition of biomass tars is shown in Table 1. It can be observed from the figure that tars are complex mixtures of aromatic hydrocarbons. It shows that the one ring aromatic hydrocarbons are found in maximum concentration in tars.

Tar formation is a significant problem in gasification systems. It causes problems, such as blocking of pores of filters due to formation of coke and plugging in cold spots due to condensation. Moreover, the condensation of tar components can foul the turbines and engines downstream. If the tars are dealt with correctly, their associated energy can be recouped by converting them to producer gas as CO, hydrogen and methane. Hence, selection of the most suitable method for removing tar is a significant challenge to the utilization of syngas (Han and Kim, 2008).

Compound name	Percentage (weight)
Benzene	37.9
Toluene	14.3
Other single ring aromatic compounds	13.9
Naphthalene	9.6
Other two-ring aromatic compounds	7.8
Heterocyclic compounds	6.5
Phenolic compounds	4.6
Three ring aromatic compound	3.6
Four ring aromatic compounds	0.8
Others	1.0

**Table 2.1: Biomass gasification tar composition (Milne *et al.*, 1998).**

Application	Particles mg/Nm <sup>3</sup>	Size of particle $\mu$ m	tars mg/Nm <sup>3</sup>	Alkali metals mg/Nm <sup>3</sup>
Gas turbine	<30	<5	<40	0.24
Gas engine	<50	<10	<100	

**Table 2.2: Quality of gas required for power generation (Stassen, 1993; Milne *et al.*, 1998).**

## 2.2 Tar Removal Techniques

There are many approaches which can be employed to reduce the amount of tars in product gas. The selection of the suitable method is based on economic feasibility, efficiency for tar

removal and minimum effect on gaseous products. The available tar removal methods can be classified as primary methods and secondary methods.

### **2.2.1 Primary Methods**

In primary methods, tar formation is reduced by controlling the operation parameters during the gasification step. Operating conditions, bed additives and design of the gasifier were the main factors to control the quality of producer gas. Pressure, temperature, residence time and gasifying medium have been shown to be the most important parameters affecting the product gas quality (Devi *et al.*, 2003). In a study, pyrolysis of birch wood was performed in a free-fall reactor to investigate the effect of temperatures on the process and it was noted that higher temperatures favoured the production of gaseous species. It was observed that tar could be eliminated by maintaining high temperatures in a fluidized bed gasifier. The yield of the tar decreased by up to 40 % by increasing the temperature from 700–900 °C (Yu *et al.*, 1997). The amount of oxygen-containing hydrocarbons and aromatic compounds (1 and 2 ring) significantly decreased when increasing the temperature. However, the production of 3-ring and 4 ring aromatic compounds increased with temperature. In another study, nearly complete removal of phenol and 50 % removal of toluene was observed at high temperature during the pyrolysis of birch wood. However, a significant increase in naphthalene and benzene was observed as the temperature increased from 700–900 °C (Brage *et al.*, 2000). Kinoshita *et al.* (1994) also found that the amount of tar decreased by increasing the temperatures in a fixed bed gasifier during the gasification of sawdust. Significant quantities of compounds containing oxygen (cresol, phenol and benzo furan) were observed at temperature <800 °C. It has also been reported that decomposition of aromatic tar compounds decreases at temperatures >850 °C. However, there are many other factors like, char conversion, risk of sintering and gas heating value that limit the range of operating temperature (Fig. 2.1) (Hallgren, 1997).

The effect of pressure on biomass gasification has been well-studied. Knight (Knight, 2000) studied the effect of pressure on the gasification of chips of Wisconsin whole tree and noted that when increasing the pressure up to 21 bar the amount of the polycyclic aromatic hydrocarbons also increased (Knight, 2000). In another study, it was noted that concentration of tars and LHC (lower hydrocarbons as compared to naphthalene) decreased by increasing the pressure during gasification with 100 % conversion of carbon (Wang *et al.*, 2000).

It has been reported that amount of tar decreases to  $2 \text{ g/m}^3$  quickly as the equivalence ratio increases and also affects the products composition when air was used as a gasifying medium (Narvaez *et al.*, 1996). The concentration of  $\text{CO}_2$  increased, whereas  $\text{H}_2$  and  $\text{CO}$  concentration decreased at high values of equivalence ratio, which ultimately reduced the heating value of the product gas. It was reported that the availability of  $\text{O}_2$  increased at high equivalence ratio, which increased oxidation of the products. At  $700 \text{ }^\circ\text{C}$ , almost 30 % of the tar concentration decreased by increasing the equivalent ratio from 0.22 to 0.32 (Kinoshita *et al.*, 1994; Narvaez *et al.*, 1996). However, the low gas quality and lower heating value limit the significant increase in equivalent ratio.

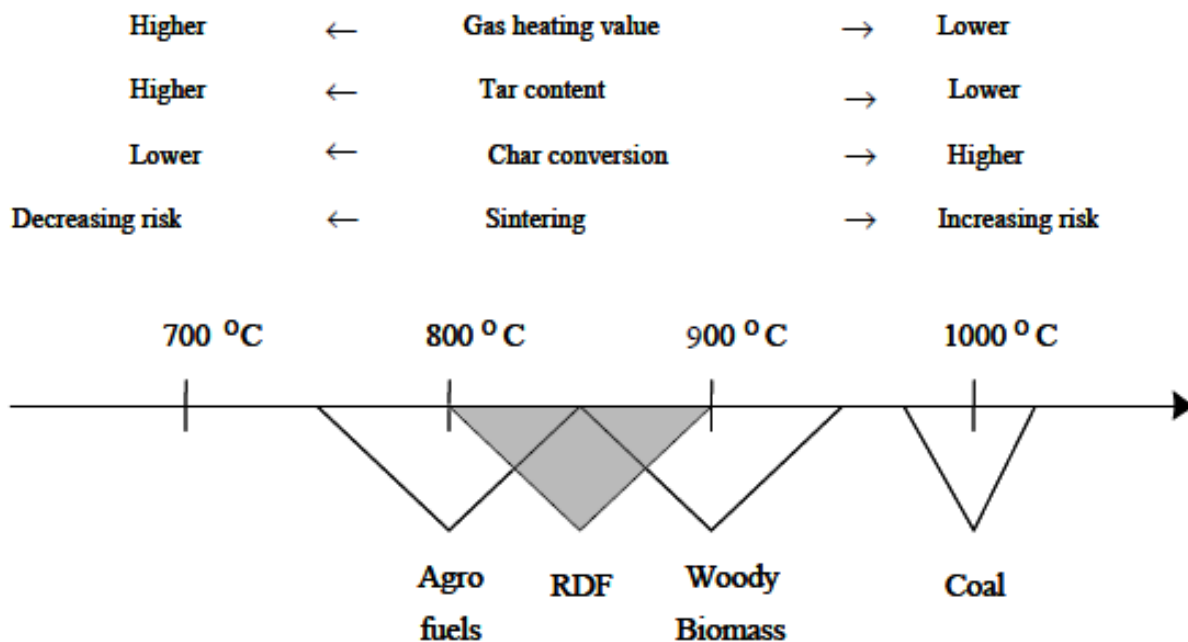


**Figure 2.1. Effect of temperature changes on various factors (Hallgren, 1997).**

The use of catalysts as bed additives to reduce tar compounds has been reported in literature. Several experiments were performed using limestone (bed additive) in a gasifier (fluidized bed) to improve the quality of gasification. The bed material was the mixture of silica sand (75 wt %) and limestone (25 wt %). This was used to investigate the gasification (steam) of manure and alpha cellulose (Walawender and Fan, 1981; Walawender *et al.*, 1985). It was observed that heating value, yield and gas composition were affected by the presence of limestone. In another study, it was reported that the tar amount decreased from 6.5 wt% to 1.3 wt% by using the calcined dolomite in the gasifier (Corella *et al.*, 1988) . Narvaez *et al.*

(Narvaez *et al.*, 1996) observed that the 40 % decrease in the tar when adding 3 % of calcined dolomite of the biomass. However, carryover of the fine particles and catalysts deactivation are the major drawbacks of using bed additives.

### 2.2.2 *Secondary Methods*

These methods are employed for the treatment of product gas from the gasifier. They can be divided into physical and chemical treatments. In mechanical/physical methods, cyclones, fabric filters, scrubber, electrostatic filters and ceramic filters are used (Han and Kim, 2008), whereas in chemical treatments, cracking of tar compounds can be performed by using high temperatures (thermally) or catalysts (catalytically) at the outlet of the gasifier. It has been found that secondary methods are very useful in terms of tar reduction. In additions, these methods are also found to be efficient for ammonia reduction (Simell *et al.*, 1997a; Simell *et al.*, 1997b)

#### *Mechanical/Physical methods.*

Physical methods are mainly used to remove particles from the product gas. However, it was reported that these methods were effective to capture tar as well as particles physically (Thambimuthu, 1993). Bakers *et al.* (1986) suggested that tar could be found in two different forms, depending upon the exit temperature from the gasifier (Baker *et al.*, 1986). At higher temperatures, tar could be observed as vapour, whereas it might be present in the gas as entrained droplets of liquid where the temperature is low. So, at higher temperatures, tar and particle removal could be decoupled. At lower temperatures, if tar and oil condensed together then their removal could not be separated from particulate removal. Mechanical methods are classified as wet gas cleaning and dry cleaning. Wet gas cleaning was used after the cooling of gas (20-60 °C), whereas dry cleaning was employed before the gas cooling where the temperature was higher than 500 °C (Anis and Zainal, 2011).

#### *Dry Gas Cleaning*

Various types of equipment can be used for dry gas cleaning, including cyclones, fabric filters, rotating particle separators, sand bed filters, and activated carbon based absorbers. There is not enough data to analyse the tar removal efficiency of these equipments from gasification of biomass (Anis and Zainal, 2011). However, the efficiency of coal tar removal was about 50-90 % in a cyclone/humidifier combination downstream of a coal gasifier (Baker *et al.*, 1986). Similarly, the removal efficiency of tar was found to be 0–50 % and 30–70 % in fabric filters and rotating particles separator (RPS) after the exit from fixed bed

biomass gasifier (Hasler and Nussbaumer, 1999), respectively. It was reported that RPS and fabric filters were not efficient at removing tars independently and extra tar reduction technology was required. In another study, it was reported that the concentration of tar decreased from 8 g/Nm<sup>3</sup> to 4.5 g/Nm<sup>3</sup> using RPS (Rabou *et al.*, 2009). Glass fibre and quartz ceramic filters were used to clean hot gases and significant removal of tar (75.6 to 78.9 %) was observed in both types of ceramic filters (de Jong *et al.*, 2003). However due to high investment and their complexity, ceramic filters are not considered as an alternative to capture the tar. The sand filters can also be used for tar removal. It has also been reported that 50–97 % of tar removal could be achieved using sand filters (Hasler and Nussbaumer, 1999). Meanwhile, the deposition of the tars on the filters causes plugging, which cannot be cleaned easily.

Equipment	Tar removal (%)	Drawback	Ref
RPS	30-70	Additional tar removal necessary	(Hasler and Nussbaumer, 1999)
Fabric filters	0-50	Additional tar removal necessary	(Hasler and Nussbaumer, 1999)
Ceramic filters (quartz)	75.6-94	Expensive and complex	(de Jong <i>et al.</i> , 2003)
Sand filters	50-97	Plugging difficult to clean	(Hasler and Nussbaumer, 1999)
Ceramic filters (glass)	77-97.4	Expensive and complex	(de Jong <i>et al.</i> , 2003)

**Table 2.3: Methods for tar removal**

Catalytic filters have been used to clean gasifier product gases. Cracking of tar using catalysts and removal of particles with the help of filtration were accomplished in one step. The method was effective for removal of tar and particles (Engelen *et al.*, 2003). A nickel-based catalyst was used in the support body of ceramic candle filter (Draelants *et al.*, 2000). Draelants *et al.* (2000) found that the performance of the candle filter improved above 850 °C in terms of benzene and naphthalene conversion. Figure 2.2, below, shows a schematic representation of catalytic candle filter (Draelants *et al.*, 2000).

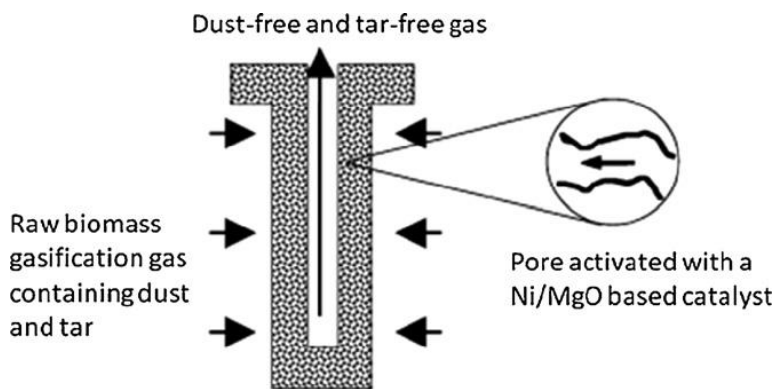


**Figure 2.2. Schematic Diagram of a Catalytic Candle Filter (Draelants *et al.*, 2000).**

### *Wet Gas Cleaning*

Wet gas technology can remove particles and tar droplets effectively. It was demonstrated that 99 % of the particles and 40-70 % of tar were removed using a wet electrostatic precipitator (ESP) for different types of gasifiers, including updraft and downdraft (Van Paasen *et al.*, 2004). A corona discharge ionizes the gas as it passes through the grounded electrode and high voltage electrode. The tar droplets or dust particles and water attached with ions and attracted towards the grounded electrode in an electric field. The capital cost and large size of the wet ESP are the major disadvantages of this technology (Kumar *et al.*, 2009).

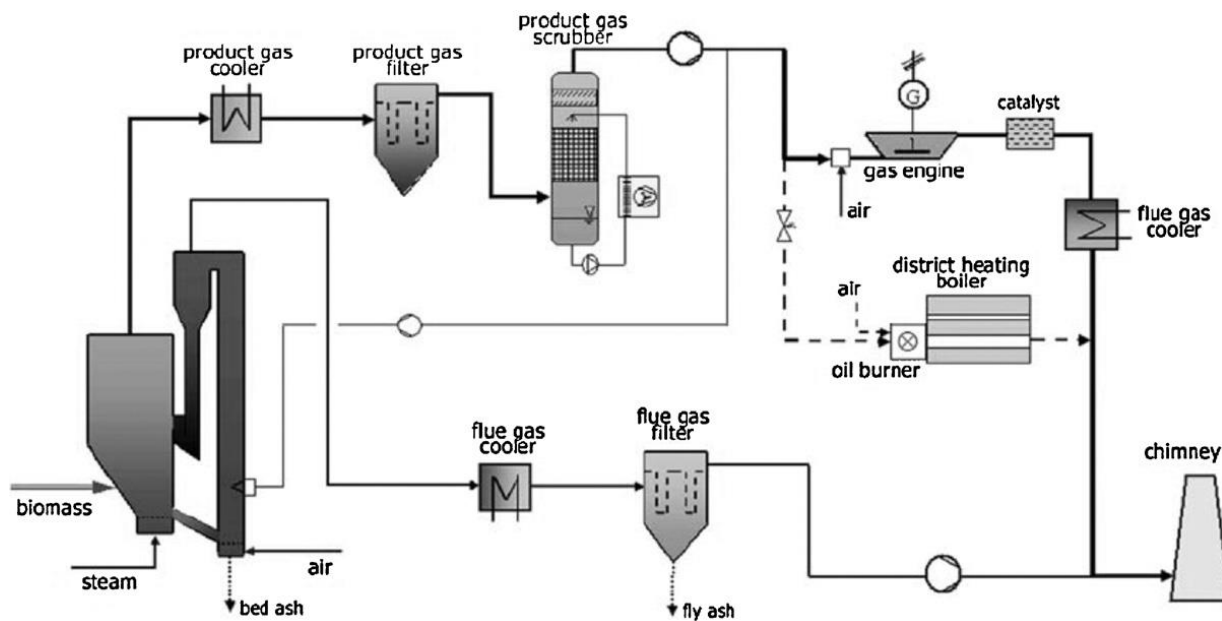


**Figure 2.3. Steam gasification with wet gas scrubbing and dry dust removal in Gussing, Austria (Lettner *et al.*, 2007).**

Wet scrubbers can also be used to clean product gas. Water was used in wet scrubbers to remove tars and particles. Venturi scrubbers were found to be the most effective for tars and particles removal and their tar removal efficiency could be as high as 90% to clean product gas from the gasification of rice husk (Hasler *et al.*, 1997). Figure 2.3 shows the industrial application of wet gas scrubbing and dry dust removal in steam gasification plant in Gussing, Austria (Lettner *et al.*, 2007).

Gas cleaning technology	Tar removal (%)	Particle removal (%)
Wash tower	10-25	60-98
Wet electrostatic precipitator	0-60	>99
Rotational particle separator	30-70	85-90
Wash tower	10-25	60-98
Venturi scrubber	50-90	

**Table 2.4 Removal of tar by various methods of wet gas cleaning (Hasler and Nussbaumer, 1999).**

There are many problems associated with the use of water as a scrubbing medium, including low solubility of hydrocarbons, plugging of apparatus, saponification, and the cost of

treatment of water (Lettner *et al.*, 2007). Moreover, there was salt formation on the parts of scrubber which could result in fouling and clogging (Lee *et al.*, 2008). In addition, the cost of the treatment of sludge also made it uneconomical.

### *Chemical methods*

The chemical removal of tar usually performs inside a secondary reactor. Unlike mechanical techniques, chemical removal methods do not produce any residual waste stream. The successful application of chemical techniques produces combustible species such as CO and H<sub>2</sub> and increases the calorific content of the syngas (Basu, 2010). Chemical removal methods can be categorised as thermal decomposition, catalytic decomposition and plasma decomposition.

### *Thermal decomposition*

Thermal decomposition of tar compounds involves the cracking of compounds into lighter gases by the effect of temperature alone. The elevated temperature affects the stability of tars, cracking them into lighter components. In a gasifier (two-stage), pyrolysis of *pinus pinaster* was performed and it was noted that increasing residence time and temperature improved gas production, tar decomposition and quality of char (Fassinou *et al.*, 2009). In another process, 88 % conversion of the tar was observed at 900 °C from the pyrolysis of woodchips (Morf *et al.*, 2002). El-Rub *et al.* (2008) investigated the thermal cracking of phenol at 700-900 °C, and only 6.3 % conversion was observed at 700°C, and it increased up to 98% at 900 °C (El-Rub *et al.*, 2008). In another study, it was reported that 78 % of the tar converted to lighter hydrocarbon gases at 800 °C (Phuphuakrat *et al.*, 2010).

It has been reported that adding air or oxygen to the gasifier product gas effectively cracks the tar compounds through partial oxidation. However, the partial oxidation of the components of the product gas reduced heating value possibly leading to further complications when using the gas in conventional gas turbines or engines (Fjellerup *et al.*, 2005).

It was investigated that the quality of char, the amount of lighter gases, and the conversion of tar improved by increasing the residence time and temperature in a two-stage gasifier (Fassinou *et al.*, 2009). Fagbemi *et al.* (2001) performed the pyrolysis of three different biomasses (coconut shell, wood and straw) and investigated the thermal decomposition of tars from 400 to 900 °C. It was reported that effective removal of tar required higher reaction temperatures (> 700°C) (Fagbemi *et al.*, 2001). Bridgwater *et al.* (1995) reported that biomass-derived tar was very hard to crack by thermal methods alone, and additional process modifications were required, such as the use of catalysts, or reactor modifications that result

in an increased residence time of the syngas (Bridgwater, 1995). Furthermore it was reported that in addition to high operational costs (associated with high temperature operations), thermal cracking could also increase soot formation, which increased particulate load on processing equipment, requiring further clean-up (Fjellerup *et al.*, 2005).

### *Catalytic Cracking*

Secondary catalytic cracking is performed to decompose tar compounds after the exit from the gasifier in a separate process unit. Catalysts reduce the activation energy for tar decomposition, therefore the required temperatures for tar cracking is significantly lower than that of thermal cracking alone.

In downstream reactors, different types of catalysts have been employed to decompose tars. These include metallic, natural minerals and metal oxide synthetic catalysts. These catalysts can be categorized into four groups: alkali metal catalysts, nickel catalysts, novel metal catalysts and dolomite catalysts (Han and Kim, 2008).

There are many types of catalyst that can be used for decomposition of tar compounds (Milne *et al.*, 1998). The criteria for the selection of catalysts was summarized by Sutton *et al.* (2001) (Sutton *et al.*, 2001; Anis and Zainal, 2011), as follows:

- the catalyst should be efficient in removing tar
- it must be resistant to deactivation due to deposition of carbon
- regeneration should be inexpensive and facile
- it must be inexpensive
- the catalyst should cause a suitable syngas ratio.

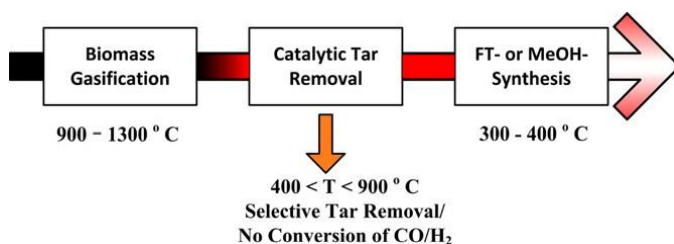


**Figure 2.4. Strategy of Catalytic Tar removal (Schmidt *et al.*, 2011).**

In the petrochemical industry, Ni-based catalysts are widely used for methane and naphtha reforming (Bridgwater, 1984; Strom *et al.*, 1985; Ekstrom *et al.*, 1988; Aznar and Delgado, 1992; Marino *et al.*, 1998; Hepola *et al.*, 1999; Coll *et al.*, 2001; Dayton, 2002; Lappas *et al.*, 2002; Dou *et al.*, 2003; Engelen *et al.*, 2003; De Filippis *et al.*, 2004; Taralas and Kontominas, 2004; Zhang *et al.*, 2004; Furusawa and Tsutsumi, 2005; Han and Kim, 2008).

Nickel catalysts were successfully used for both hot gas cleaning and in bed conversion of tar (Anis and Zainal, 2011). One of the major advantages of using nickel-based catalysts is the ability to use commercially available steam reforming catalysts, thus reducing cost. These catalysts can efficiently convert any CH<sub>4</sub> presents, to syngas (H<sub>2</sub>, CO), increasing the quality of product gas (Kinoshita *et al.*, 1995; Skoblia *et al.*, 2015). Furthermore, it was reported that nickel catalysts are very effective in decomposing heavy hydrocarbons such as naphthalene or toluene (Sutton *et al.*, 2001)

Zhang *et al.* (2004) investigated the decomposition of tar from product gas using three nickel based catalysts, Z409, ICI46-1, and RZ409, all of which have the active component nickel oxide, in a gasification product stream having 51.2 % N<sub>2</sub>, 14.2 % CO<sub>2</sub>, 15.7 % CO, 6.5 % hydrogen, 4.8 % methane and 4% heavy hydrocarbons. It was noted that 99 % of the tar decomposed in all catalysts, at temperatures up to 800 °C. The reactivity and performance of the tar decomposition system did not measurably diminish during 12–18 hours of experiments (Zhang *et al.*, 2004). However, it was noted that small pores in the catalysts were converted to larger pores due to the high temperature operation.

It has been found that alkali metal catalysts are also effective for cracking of tars (Sinaž *et al.*, 2006; Jiménez *et al.*, 2008; Yanik *et al.*, 2008; Huang *et al.*, 2009; Xie *et al.*, 2009; Wang *et al.*, 2010). The decomposition of lignin, hemicellulose and cellulose has been shown to be substantial in the presence of K<sub>2</sub>CO<sub>3</sub>. It increased the yield of gaseous products and reduced the formation of liquid products due to secondary reactions. It was observed that the yield of alkane and phenols increased by adding 17.7 wt.% of K<sub>2</sub>CO<sub>3</sub>, whereas formation of acids, alcohols and aldehydes reduced (Wang *et al.*, 2010).

It was reported that dolomite-type catalysts were efficient in cracking tar compounds (Pérez *et al.*, 1997; Seshadri and Shamsi, 1998; Corella *et al.*, 1999; Gil *et al.*, 1999; Myrén *et al.*, 2002; He *et al.*, 2009; Li *et al.*, 2009; Yu *et al.*, 2009b). Gusta (2009) reported that dolomite enhanced tar decomposition by an average of 21% over thermal cracking at 750 °C (Gusta *et al.*, 2009). Tar conversion and water-gas shift reaction were promoted due to presence of iron contents in dolomite. In other research it was shown that a modified dolomite (Fe<sub>2</sub>O<sub>3</sub> mixed with natural dolomite) increased the decomposition of tar up to 97% (Wang *et al.*, 2005).

Novel metal catalysts (Rh, Ru, Pd, Pt, etc.) have been developed to decrease tar from biomass gasification. Several studies showed that these catalysts were efficient in decomposing tars into fuel gas (Asadullah *et al.*, 2002; Asadullah *et al.*, 2003; Polychronopoulou *et al.*, 2004; Tomishige *et al.*, 2004; Miyazawa *et al.*, 2005; Ammendola *et al.*, 2009). However, these

catalysts are more expensive than nickel catalysts or conventional catalysts (Anis and Zainal, 2011).

Catalytic cracking is a good way to decompose tar into valuable products and operates at lower temperatures than thermal decomposition of tar (Chen *et al.*, 2015), thus it has significant advantages when considering operational costs. However, the complexity of the process increases when using catalysts, along with other operational challenges such as fragmentation, poisoning, fouling and carbon deposition (Bosmans, 2013).

## **2.3 Plasma**

Plasma is a fully or partially ionized gas. It can be produced by several methods, such as flames, combustion, electric furnace, shocks (electrically, chemically and magnetically driven) and electric discharges (glow, corona, microwave, arc, electron beam, etc.) of matter (Liu *et al.*, 1999). It is highly reactive and conductive due to the presence of excited molecules, atoms, radicals, ions and neutral particles. Plasmas can be classified as thermal or non-thermal.

### **2.3.1 Thermal plasma**

In thermal plasmas, the temperature of the background gas is very high and all neutral and charged particles are in thermal equilibrium. It has been observed that chemical reactions significantly increase in a hot medium due to presence of reactive species, such as electrons, ions and radicals. However, the consumption of energy is very high (Petitpas *et al.*, 2007). It has been reported that non-thermal plasmas consume less energy as compared to thermal plasma to produce comparable yield of H<sub>2</sub> (Bromberg *et al.*, 2001).

Thermal plasmas are commonly used for the treatment of solid or municipal wastes. It is similar to thermal degradation techniques, as the waste is degraded by raising the temperature of the entire plasma. However, useful energy can be extracted from these wastes when using plasma gasification. H<sub>2</sub>O/Ar plasma torches have been applied to convert waste plastic and wood into product gas. High concentrations of CO and H<sub>2</sub> (90 %) were produced with very low contents of condensable tar, but the high energy use made it uneconomical (Hlina *et al.*, 2014). The production of high quality syngas was studied in a two-stage steam plasma system. In the first stage, steam and small concentrations of hydrogen and CO<sub>2</sub> were produced using contact glow discharge electrolysis of an electrolyte. These gases were used to gasify

the biomass in a second stage. It was observed that the production of hydrogen was higher than in conventional gasification processes (Diaz *et al.*, 2015).

In another study, plasma was used in a two-stage fluidized bed gasifier to convert solid waste into syngas (Materazzi *et al.*, 2016). The carbon conversion efficiency and syngas composition were investigated in this process. It was observed that the two-stage gasifier was efficient in reducing the concentration of tar. The plasma converter helped to reduce/decompose the condensable tar. The synergic effect of high temperature and plasma converted the residual carbon to CO which ultimately increased the yield of the process.

Interest in applying plasma for the decomposition of biomass has been continuously increasing because it can, in principle, produce tar-free syngas. The smaller size of equipment, and handling of a wide range of hazardous and heterogeneous materials are advantages of this process (Kim, 2004b). Thermal plasma was used in a gasification reactor to enhance the quality of the syngas. It was observed that the yield of CO and H<sub>2</sub> were increased by the application of thermal plasma (Cho *et al.*, 2015). However, it was viewed as too complex system for the reduction of condensable tar. A significant amount of energy is required to clean the large volumes of gases which makes this technology uneconomical for cleaning purposes.

### ***2.3.2 Non thermal plasmas (NTPs) for treatment of biomass gasification tars***

NTPs have been used for treatment of fuel gas and for production of valuable organic compounds due to highly non-equilibrium conditions and requirement of low power. The plasma has the ability to initiate reactions (physical and chemical) at lower temperatures, whereas the electron temperature can reach to 10<sup>4</sup>-10<sup>5</sup> K (Petitpas *et al.*, 2007; Tao *et al.*, 2013). Due to the very high temperatures of the electrons generated, thermodynamically unfavourable reactions can occur. Hence, thermal equilibrium does not exist in non-thermal plasmas, as the electron temperature is not the same as the ambient temperature. The most common examples of NTPs are dielectric barrier discharge, microwave, radio frequency, and corona plasma.

#### *Pulsed corona discharge*

The pulse corona discharge NTP reactor has proved useful in various industrial applications, for example, in cleaning of liquid and gas exhaust streams, and in surface treatments (Chang *et al.*, 1991; Bellakhal *et al.*, 1997). It produces significant numbers of reactive species (radicals and atoms) at ambient conditions. In this technique, weakly luminous discharge

appears near the thin wires or sharp edges where the strength of electric field is highest (Fridman *et al.*, 2005; Moreau *et al.*, 2008). Therefore, these discharges are non-uniform, as high strength of electric field, luminosity and ionization are located near just the one electrode. The electric circuit is completed by movement of charged particles from electrode to electrode in a weak electric field. Fig. 2.5 shows a wire cylinder configuration of pulsed corona discharge with preheating.

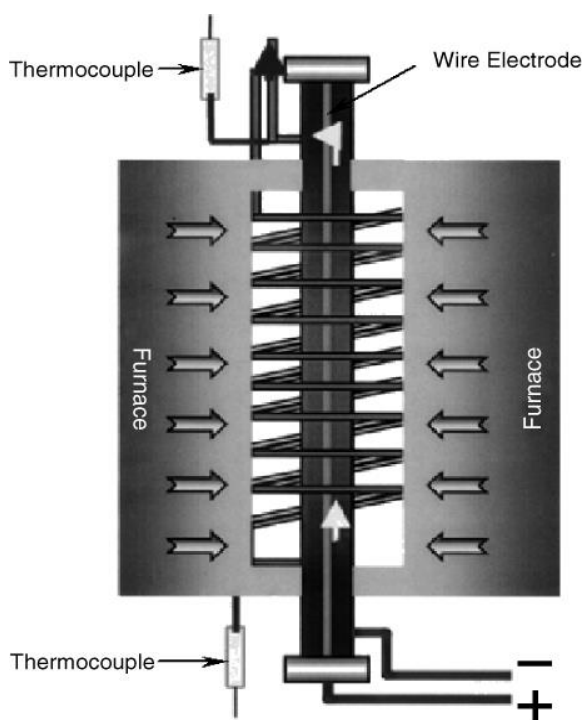
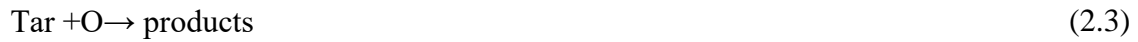


**Figure 2.5. Wire cylinder configuration of pulsed corona discharge with preheating (Fridman *et al.*, 2005).**

Pulse voltages are applied below the frequency of ions, which implies that motion of ions is restricted to reduce the energy loss and only electrons followed the applied electric field. It is difficult to scale up this reactor, because the electrode system's impedance is proportional to the size of reactor (Urashima and Chang, 2000). Therefore, investigation is required to increase the strength of local electric field by matching the impedance and electrode shapes. However, the corona discharge system is better, in terms of chemical efficiency, than other non-thermal plasma processes (Yamamoto and Futamura, 1998). The high cost of the pulsed power devices is the greatest drawback of this technology (Nair *et al.*, 2003a).

Nair (2004) investigated the decomposition of tar using pulsed corona discharges. He used different mixture of gases to identify the primary processes involved in the decomposition of tar compounds. Fig. 2.6 below presents the energy consumption

in different mixtures for the removal of naphthalene. It can be observed that in the presence of moisture less energy was required to decompose the naphthalene. The primary processes involved for the decomposition of naphthalene are as follows.



Where M is the background gas

Nair also investigated the decomposition of different tar analogue compounds in pure N<sub>2</sub> and fuel gas mixtures (CO:20%, CO<sub>2</sub>:12%, H<sub>2</sub>:17%, CH<sub>4</sub>:1%, rest N<sub>2</sub>) (Nair *et al.*, 2003b). They showed that removal of tar compounds required less energy in N<sub>2</sub> than in fuel gases, due to termination reactions of radicals (eq. 2.5 and 2.6). Figure 2.7 below shows that single ring compounds need higher energy than two-ring aromatic compounds. It was reported that this is due to the higher reaction rate constant for naphthalene decomposition as compared to phenol. For toluene, there was a chance of re-formation of toluene due to recombination reactions of fragments.



Where R-Radical produced, B and C show intermediates.

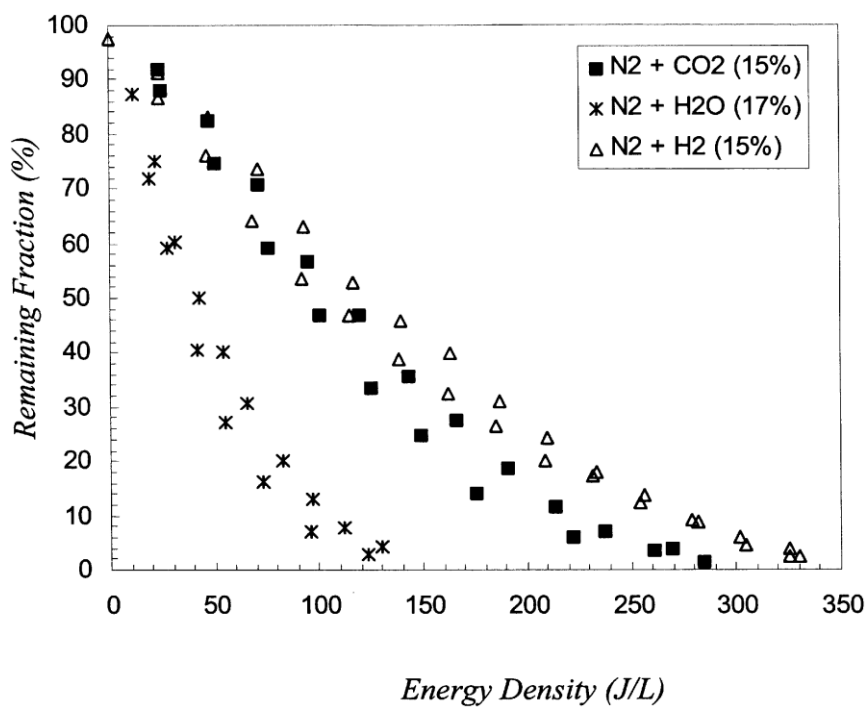


Figure 2.6. Energy consumed to decompose Naphthalene. Conc., 500-600 ppm; T, 200-210°C (Nair *et al.*, 2003c).

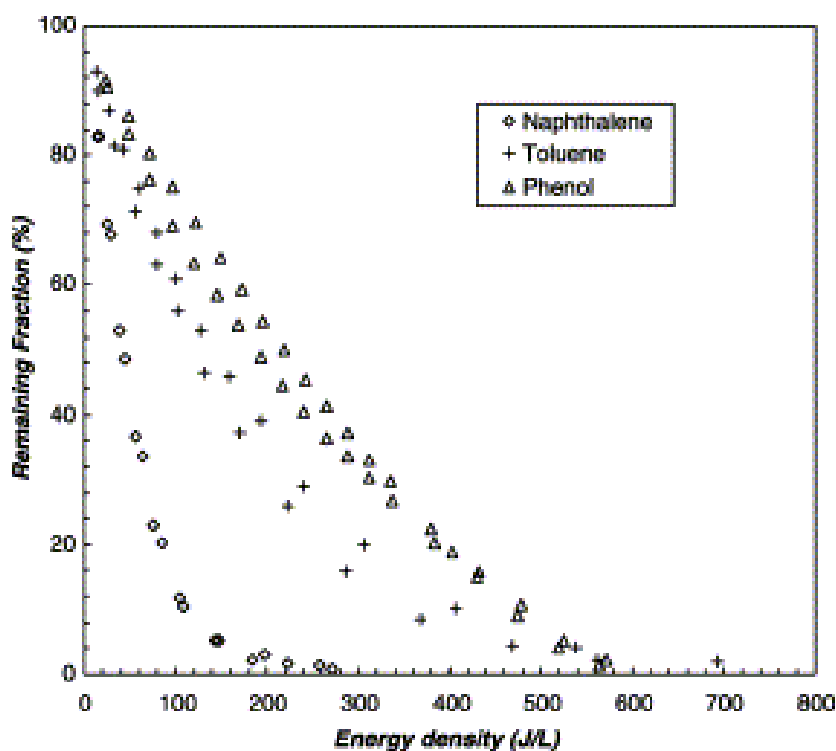


Figure 2.7. Tar removal in pure N<sub>2</sub>. Phenol, 1000 ppm; Naphthalene 500-600 ppm; Toluene, 700 ppm (Nair *et al.*, 2003a).

Pemen *et al.* (2003) investigated the kinetics of tar cracking (toluene, phenol and naphthalene) in a mixture of the product gas (CO<sub>2</sub> (12%), CO (20%), H<sub>2</sub> (17%), CH<sub>4</sub> (1%)), and balance

N<sub>2</sub>) using a pulsed corona discharge. The study was conducted to investigate the possible reaction routes, mechanisms and kinetics occurring within NTP for tar decomposition. It was reported that decomposition of tar compounds was governed by oxidation reaction, due to the presence of CO<sub>2</sub> (reaction 2.7 and 2.8) generating O radicals:



It was observed that the overall conversion efficiency of tar increased with increasing concentration of CO<sub>2</sub> in the product gas. The study also reported that the tar cracking efficiency was negatively affected by the presence of CO as a carrier gas, which terminated the reactions of O radicals via the reverse reaction of 2.7.



The chemical kinetics of the removal of naphthalene in synthetic fuel gas by using pulsed corona discharge at 200 °C have also been studied (Nair *et al.*, 2004). They reported the following reactions as being more sensitive to the overall process for tar (naphthalene) removal.



Nair reported that reactions 2.10-2.13 and 2.15 reduced the rate of decomposition of naphthalene, whereas reaction 2.14 and 2.16 increased it (Nair *et al.*, 2004). He concluded that the major reaction for decomposition of tar was via oxidation

Tao *et al.* (2013) studied the plasma-assisted catalytic decomposition of a tar analogue (toluene) in a He carrier gas using DC (direct current) non-thermal pulsed plasma (Tao *et al.*, 2013). He observed that using plasma before the catalytic steam reforming reactions increased the cracking of toluene. The amount of tar cracked increased from 32 % to 57 % when using NTP before the catalyst bed (Tao *et al.*, 2013). Fig. 2.8 shows that the cracking of toluene increases in the following order: direct decomposition (DD) < plasma assisted decomposition (PD) < catalytic reforming (CR) < plasma enhanced catalytic reforming (PCR) (Yang and Chun, 2011).

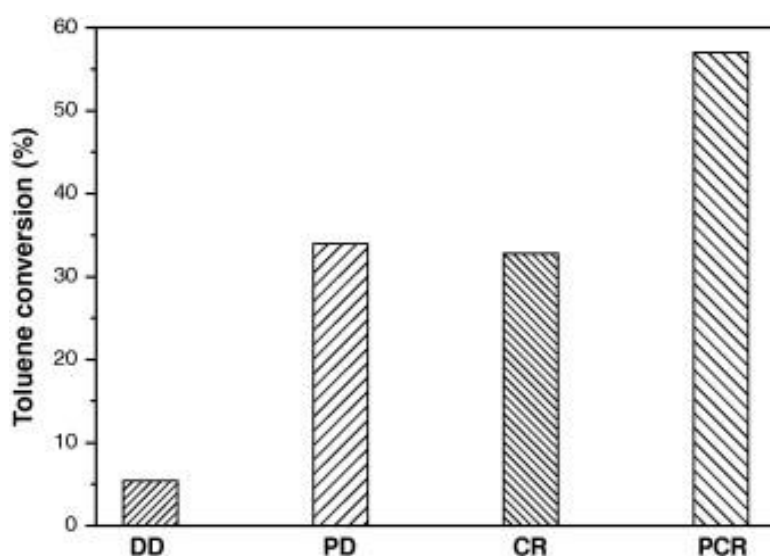


**Figure 2.8. Toluene decomposition. T, 773 K; He, carrier gas (Tao *et al.*, 2013).**

#### *Dielectric barrier discharge (DBD) reactor*

In a DBD, the dielectric barrier is used in the discharge gap to stop the electric currents and eliminates the production of sparks (Moreau *et al.*, 2008). The dielectric barrier consists of one or more layers of dielectric, which is placed between the metal electrodes. The dielectric material must have high breakdown strength and low dielectric loss. Glass ceramics and quartz are mostly used as dielectric materials and the typical discharge gap ranges from 0.1 mm to several centimetres. The operating frequency usually ranges from 0.05 to 500 kHz and the required operating voltage is about 10 kV if the discharge gap is few millimetres (Fridman *et al.*, 2005). DBD discharges operate at atmospheric pressure and have strong non-equilibrium conditions, without using expensive pulsed power supplies. For this reason, this technique has various industrial applications, for example, CO<sub>2</sub> lasers, ozone generation, and UV source in excimer lamps. In addition, many researchers have investigated using this

technique for the removal of VOCs and tars. Planar and cylindrical configurations of DBD reactor are shown in Figure 2.9.

Kim *et al.* (2004) compared the performance of different NTP technologies for the cracking of tar. The study investigated the performance of a Pulsed Corona Discharge, DBD, a ferroelectric pellet packed bed reactor, a plasma-driven catalytic reactor (PDC), and a surface discharge reactor (SD). Benzene was used as a model compound to investigate the performance of various reactors in  $N_2/O_2$  carrier gas. Fig 2.10 shows the decomposition of benzene with respect to specific input energy.

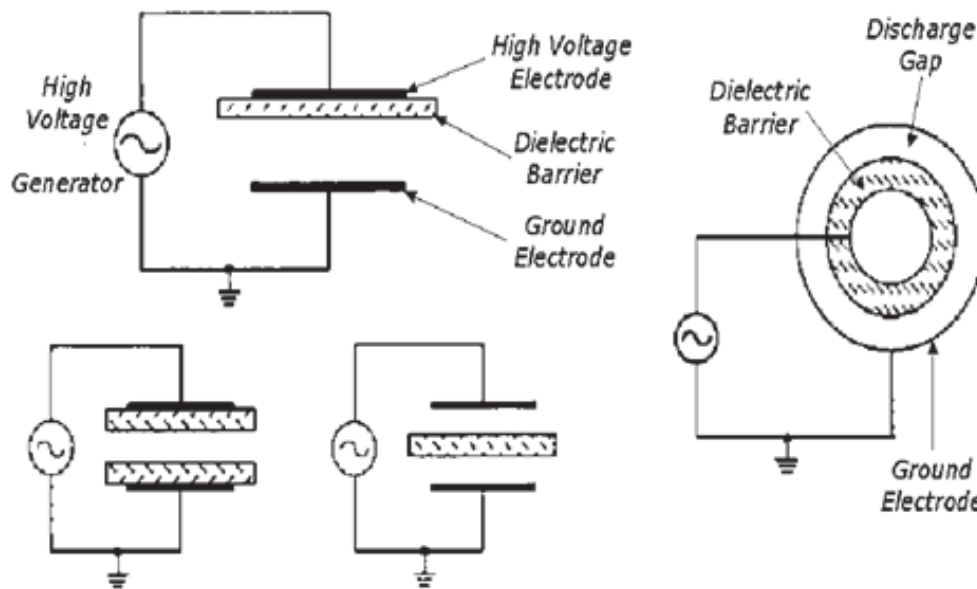


Figure 2.9. Common dielectric barrier discharge configurations (Kogelschatz, 2003)

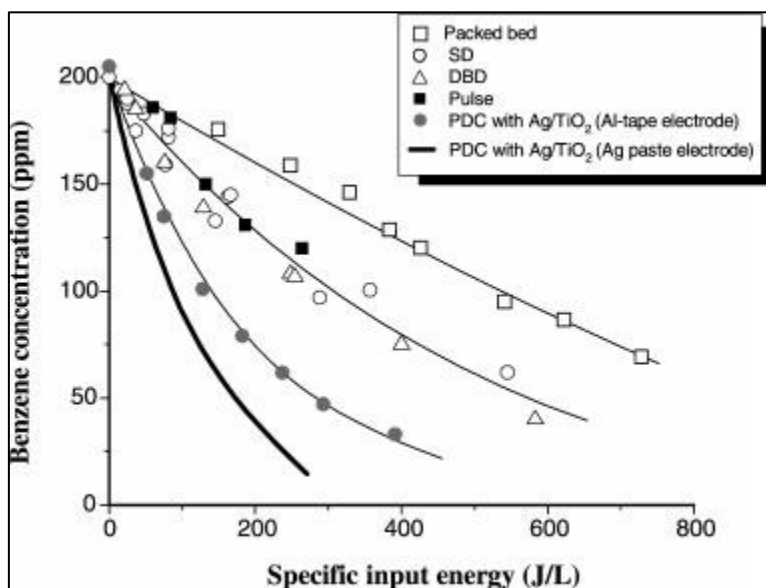
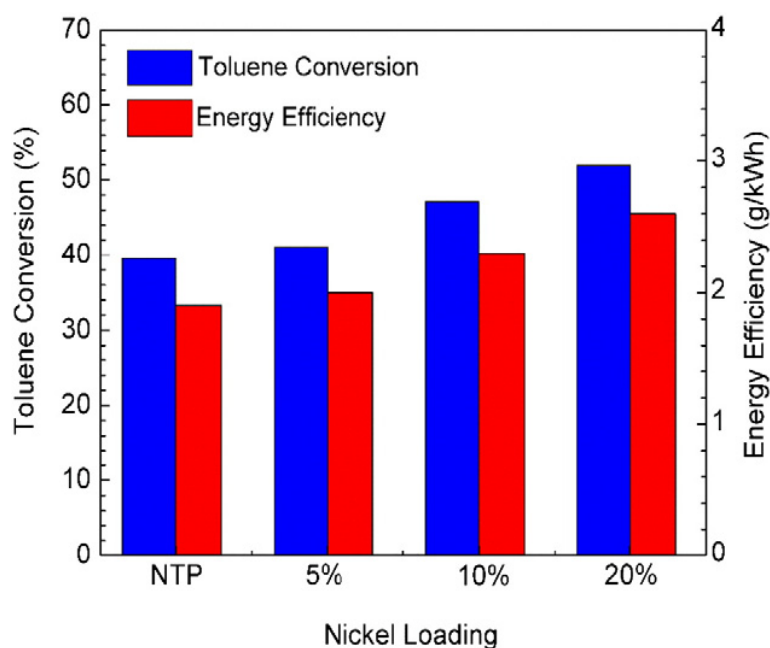


Figure 2.10. NTP Benzene Degradation Comparison (Kim, 2004a)

It can be observed that nearly 75% conversion of benzene obtained at 600 J/L in the DBD reactor. In addition, it can be noted that increase in SIE promotes the conversion of benzene directly (Kim, 2004a). Kim *et al.* (2004) discussed the selectivity to CO and CO<sub>2</sub> in the presence of oxygen, produced from the decomposition of benzene. The surface discharge reactor and DBD reactors exhibited similar selectivity for CO (40 %) and CO<sub>2</sub> (40 %), whereas the remainder was aerosols. The PDC (plasma driven catalyst) showed 28% and 72 % selectivity to CO and CO<sub>2</sub> respectively, and formation of aerosols completely disappeared. However, it was noted that selectivity to CO<sub>2</sub> remained constant with respect to SEI.

The plasma-assisted catalytic steam reforming of a tar analogue (toluene) was performed in a DBD reactor using Ni/Al<sub>2</sub>O<sub>3</sub> (Liu *et al.*, 2017b). It was shown that the synergetic effect of Ni catalysts and plasma increased the decomposition of toluene and yield of hydrogen, and reduced the generation of unwanted by-products. It is shown in Fig. 2.11 that increasing the Ni percentage increased the decomposition efficiency and energy efficiency.

Fig. 2.12 below shows the effect on the yield of products. It is evident from figure that the yield of permanent gases and lower hydrocarbon increases with increasing the Ni loading. Therefore it was concluded that reaction route shifted from oxygenation or dehydrogenation of methyl group to opening of aromatic ring, which increased the yield of products (Liu *et al.*, 2017b)



**Figure 2.11. Toluene decomposition and energy efficiency. Power, 35 W; toluene concentration, 17.7 g/Nm<sup>3</sup> (Liu *et al.*, 2017b).**

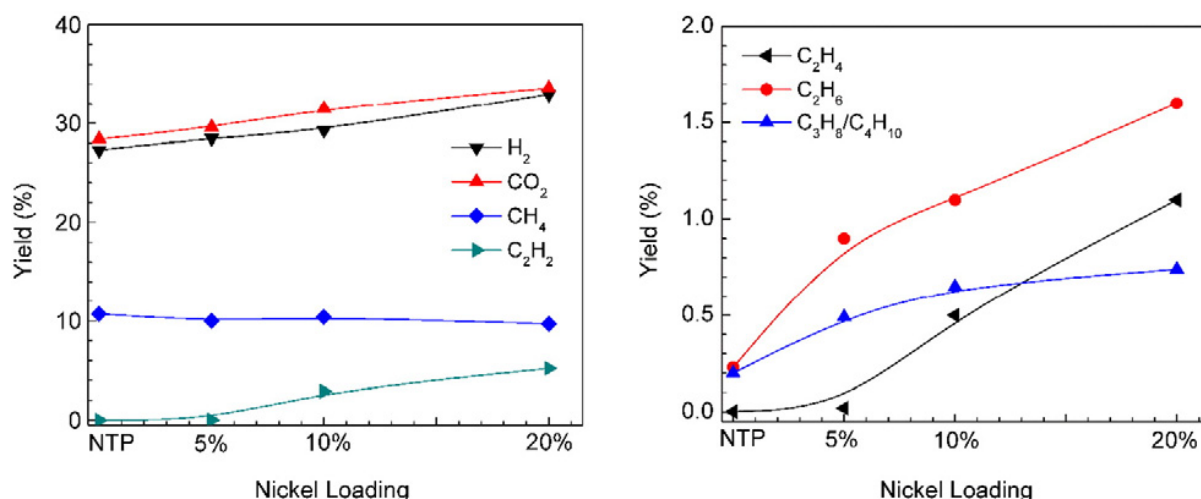


**Figure 2.12. The yield of gaseous products. Power, 35 W; toluene concentration, 17.7 g/Nm<sup>3</sup> (Liu *et al.*, 2017b).**

It was reported that two different mechanisms were involved in the decomposition of toluene. They were direct impact of electrons, and collision of gas-phase radicals (HO<sup>·</sup>, ·OH, O<sup>·</sup>, H<sup>·</sup>) with toluene (Liang *et al.*, 2013). Reaction route 1 is initiated by collisions between toluene molecule and energetic electrons in the plasma discharge zone, resulting in the production of intermediate radicals (phenyl and benzyl). These unstable intermediates lead to the formation of several aliphatic carbonyls by rupture of the aromatic ring. The CO<sub>2</sub> formation occurred due to series of oxidation reactions with O and OH radicals.

Reaction route 2 is initiated by collision of reactive radicals (O and OH) with toluene. Initially, cresol formation occurred due to the addition of OH radicals, or the abstraction of H from methyl group of toluene by ·OH radicals formed benzyl alcohol. This was further oxidized to benzaldehyde and later onto benzoic acid, further undergoing a Photo-Kolbe reaction, to form CO<sub>2</sub> and benzene. Similar to route 1, rapid opening of the aromatic ring takes place followed by a series of hydroxylations of the aromatic ring to produce several hydroxylated intermediates, which are slowly mineralized to CO<sub>2</sub>.

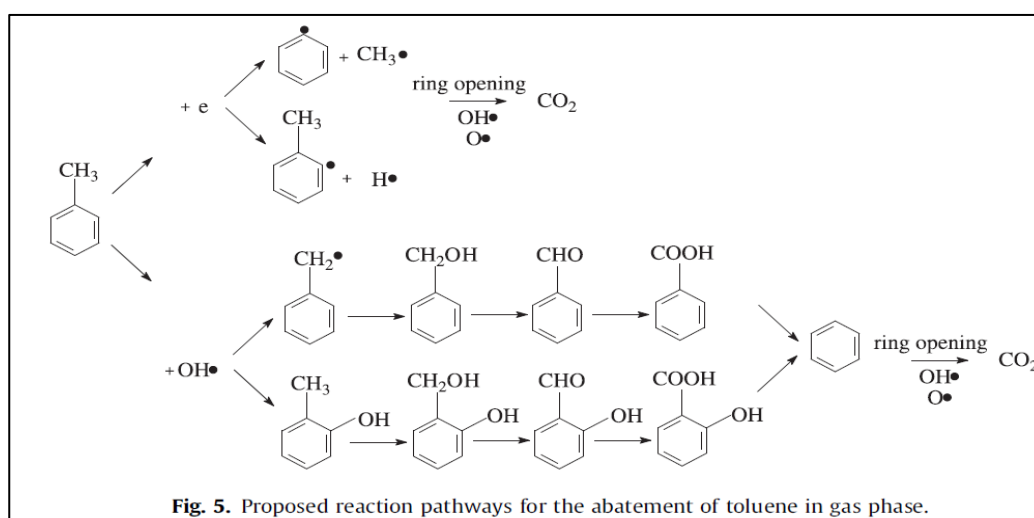


**Figure 2.13. Suggested Toluene Decomposition Pathway (Liang *et al.*, 2013)**

Liang *et al.* (2013) provide a good insight into the potential pathways and mechanisms for toluene cracking, showing that both electrons and radicals contribute to the tar analogue decomposition process (Liang *et al.*, 2013)

### *Gliding arc discharge*

Conventional non thermal and thermal plasmas are not able to simultaneously provide high electron temperatures, high densities of electrons and a highly non-equilibrium systems. Many plasma–chemical applications need a high level of non-equilibrium and a high power. The high power helps to increase the reactor productivity, whereas non-equilibrium conditions are necessary for selectivity of chemical processes. Therefore, it is very important to combine the advantages of thermal and non-thermal discharges, which can be used for large-scale pollution control, exhaust gas cleaning, conversion of fuel, surface treatment and hydrogen production.

The gliding arc discharge (GAD) has the properties of both thermal and non-thermal plasmas (Czernichowski, 1994; Fridman *et al.*, 1994; Fridman *et al.*, 1999). The GAD is highly non-

equilibrium in nature, with a relatively high electron density. Therefore, GAD is very efficient for the above mentioned applications. The GAD discharge is organized in a gas flow between two divergent electrodes (figure 2.14) and is produced at the minimum distance between the electrodes, then moves with the flow of the gas, and the arc column length increases simultaneously with the voltage.

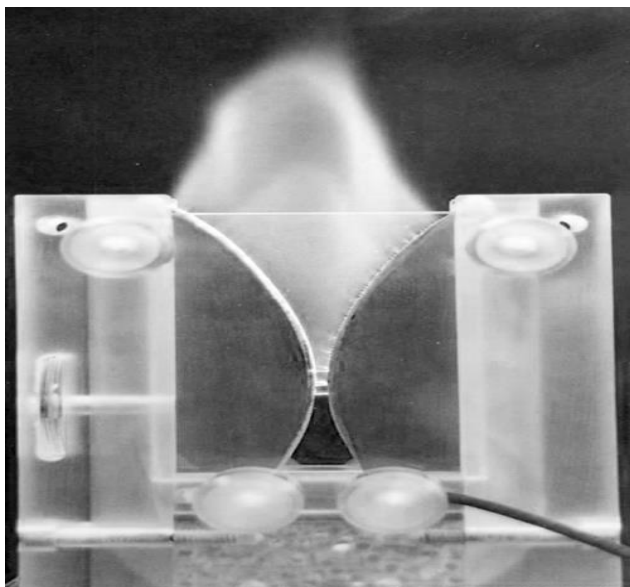


**Figure 2.14. Photo image of the gliding arc discharge in the parallel flow reactor (Fridman *et al.*, 2005)**

The thermodynamic equilibrium state of the plasma becomes difficult to sustain, when heat losses from the plasma column started to increase as compared to energy transferred by the source. Thereby, a quick transition of equilibrium to non-equilibrium phase takes place. The plasma discharge cools suddenly to gas temperature, and the conductivity of plasma is maintained by a high electron temperature:  $T_e \sim 1$  eV. After this transition, the evolution of GAD continues under non-equilibrium conditions ( $T_{\text{gas}} \ll T_e$ ) (Fridman *et al.*, 2005). The losses due to heat in this phase are much lower than in equilibrium phase (numerically nearly three times lower). After the termination of this phase (non-equilibrium), the evolution repeats from the initial breakdown.

A study by Chun *et al.* (2002) investigated the decomposition of benzene as a tar analogue in a gliding arc plasma. The maximum removal of tar compound was 82.6 %. He also studied parameters such as, benzene concentration, steam flow rate, electrode gap, nozzle diameter and specific input energy. Fig. 2.15 (a) shows the effect of concentration on the decomposition of benzene and energy efficiency. It was observed that increasing the concentration reduces removal efficiency and increases the energy efficiency of the process. At constant power, the plasma-generated reactive species react with the benzene to

decompose it. However, when the concentration is increased whilst keeping the others parameters constant, the relative amount of benzene molecules increases with respect to reactive species. Therefore, as the concentration of benzene increases, the ratio of plasma-activated reactive species to benzene molecules will decrease, which will reduce the benzene conversion

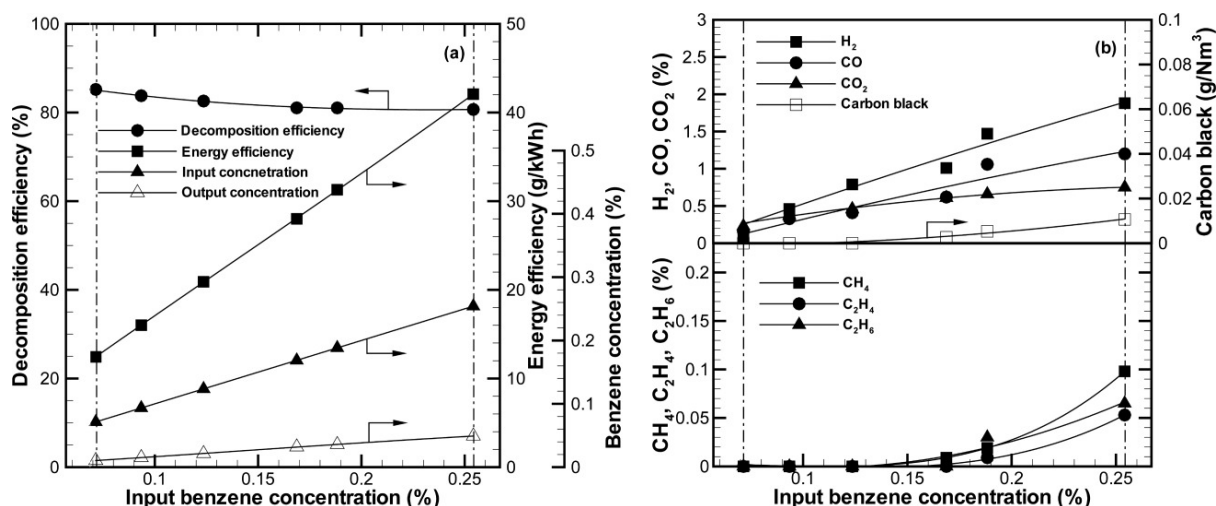


**Figure 2.15. Effect of benzene concentration (Chun *et al.*, 2013)**

The experimental results (Fig. 2.16) showed that with increasing total gas flow rate removal of benzene slightly decreased, the energy efficiency increased (Chun *et al.*, 2013). At higher flow rates, the tar compound and carrier gas are subjected to plasma discharge zone for shorter residence times, which can decrease the number of collisions between reactive species and tar compounds. Yang and Chun (2010) investigated the cracking of naphthalene as tar analogue in gliding arc plasmas (Yang and Chun, 2011). The maximum conversion and energy efficiency were 79 % and 47 g/kWh respectively.

Fig. 2.17 shows that the decomposition efficiency of naphthalene increases with increasing the specific input energy, while energy efficiency decreases with respect to SEI. A similar trend was reported previously in many publications (Guo *et al.*, 2006; Chun and Lim, 2012; Nunnally *et al.*, 2014). The plasma power played a key role in the decomposition of the tar analogue compounds. It was reported that plasma power increased the electron density, electric field and gas temperature (Tu and Whitehead, 2012)

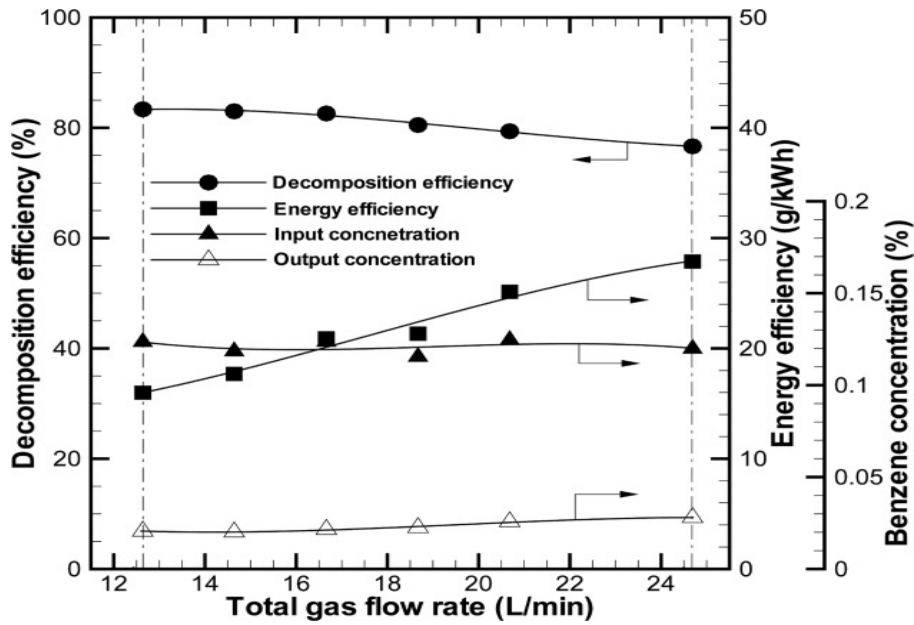


Figure 2.16. Effect of total gas flow rate (Chun *et al.*, 2013).

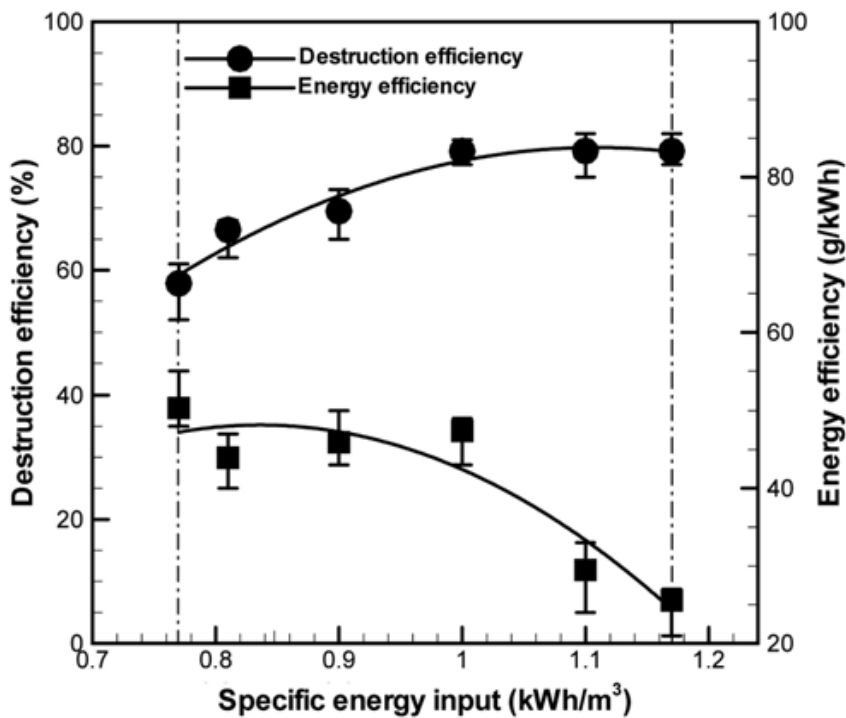
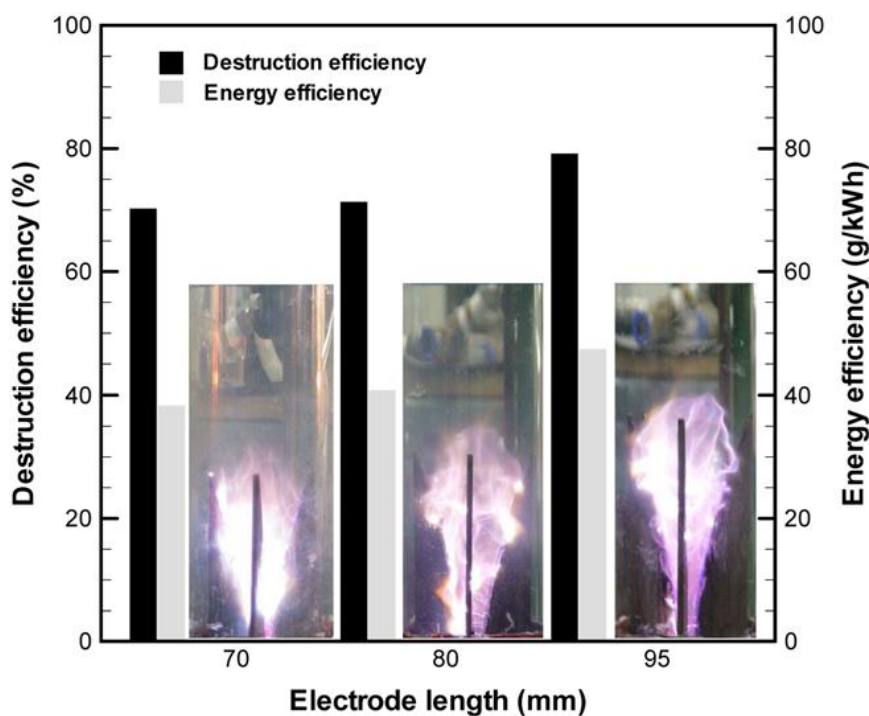


Figure 2.17. Effect of specific energy input (Yang and Chun, 2011).

The effect of electrode length (Fig. 2.18) was also studied and results showed that with increasing electrode length, both destruction efficiency and energy efficiency increased. This was possibly due to increase in the length of discharge, which ultimately increased the residence time of the gas.



**Figure 2.18. Effect of various electrode length (Yang and Chun, 2011)**

In another study, decomposition of naphthalene was studied in a two-stage gliding arc plasma. It was reported that decomposition of tar (naphthalene) could be achieved in the range of 70-95% in a single stage reactor. However, complete removal was achieved using two stages (Tippayawong and Inthasan, 2010).

The gliding arc plasma was used to investigate the decomposition of benzene and naphthalene as tar surrogates. It has been noted that removal efficiency and energy efficiency of benzene were 95% and 120 g/kWh respectively, whereas for naphthalene these were 79% and 68 g/kWh (Chun and Lim, 2012). It was observed that increasing the power increased the removal of tar compounds, whereas energy efficiency decreased. A similar effect of power was reported by Nunnally *et al.* (2014) who used gliding arc plasma to perform oxidative steam reforming of toluene and naphthalene in simulated fuel gas (Nunnally *et al.*, 2014). However, tar concentration also plays an important role in the performance of the plasma process. It was reported that at low concentration ( $30 \text{ g/m}^3$ ) more than 90% of toluene and naphthalene were decomposed, whereas at high concentration ( $75 \text{ g/m}^3$ ) it reduced to nearly 70%. A study by Zhu *et al.* (2016) explored steam reforming of toluene as a biomass tar analogue using gliding arc discharge reactor (Zhu *et al.*, 2016). The conversion of toluene in  $\text{N}_2$  carrier gas reached 95%.  $\text{C}_2\text{H}_2$  and  $\text{H}_2$  were the major gaseous products having selectivity 27% and 39.35% respectively. Further, it was observed that removal efficiency of toluene reduced with increasing the concentration. However, energy efficiency was shown to increase with increasing concentration. Similar

behaviour with regard to concentration was reported in many other studies (Chun *et al.*, 2013; Wang *et al.*, 2017b).

The externally oscillated plasma reformer (EOPR) was constructed to study the decomposition of benzene as tar analogue. The device was attached to a gliding arc plasma to produce oscillation to increase the discharge area. It was reported that the destruction efficiency of benzene was higher (90.7 %) in the presence of external oscillations. The major products were permanent gases (CO, H<sub>2</sub> and CO<sub>2</sub>), lower hydrocarbons (methane, C<sub>2</sub>H<sub>4</sub> and C<sub>2</sub>H<sub>6</sub>) and carbon black. As shown in Fig. 2.19(a), the decomposition efficiency increases with increasing the oscillation amplitude, which also increases the energy efficiency. It was reported that oscillation amplitude increased the neutral, positive and negative ion, which may contribute to the decomposition of benzene (Šícha *et al.*, 1968; Chun *et al.*, 2012). Fig. 2.19(b) shows that the concentration of CO, CO<sub>2</sub> and H<sub>2</sub> is low, due to low concentration of benzene. The concentration of CO<sub>2</sub> and H<sub>2</sub> was unaffected by the oscillation amplitude. However, concentration of CO slightly increased with oscillation amplitude, whereas the lower hydrocarbons were not detected.

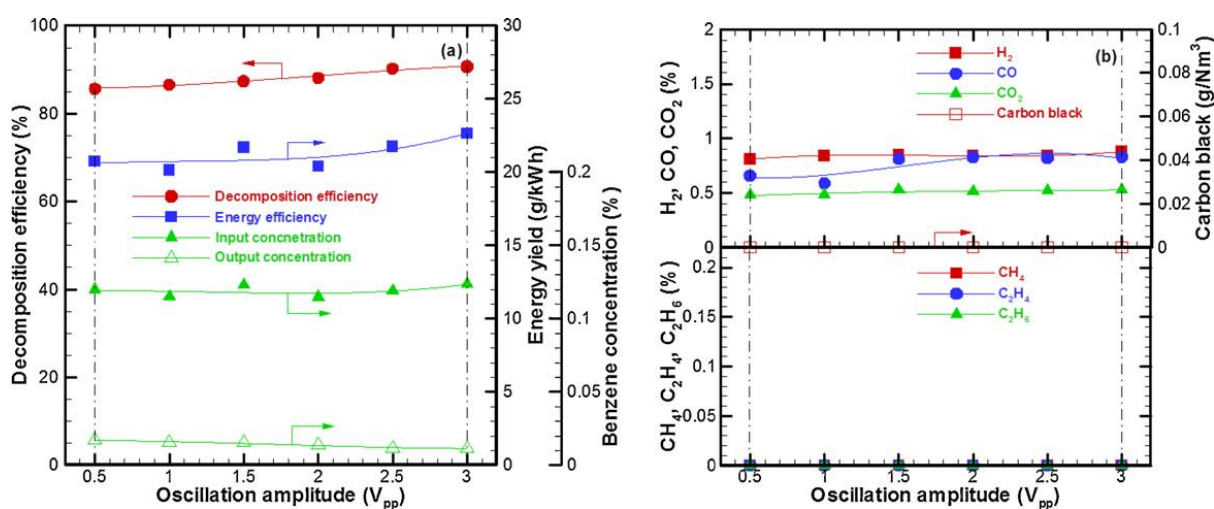


**Figure 2.19. Effect of the oscillation amplitude (Chun *et al.*, 2012)**

It has been reported that cracking efficiency of tar compounds can be increased by addition of steam (Chun *et al.*, 2012; Chun *et al.*, 2013; Liu *et al.*, 2017a; Sun *et al.*, 2017; Jamróz *et al.*, 2018). The steam cracking of toluene was explored in a gliding arc discharge reactor using N<sub>2</sub> carrier gas. It was reported that the formation of OH radicals through plasma produced new reaction pathways to oxidize the toluene and its intermediates, which significantly increased the decomposition efficiency and energy efficiency.

### *Microwave discharge*

Microwave discharges are mostly used for production of non-equilibrium and quasi equilibrium plasmas, for various applications. They can be produced at incident powers from several Watts to 100s of kW, at pressures as low as  $10^{-5}$  Torr, to ambient pressure. The electromagnetic waves of frequency above 300 MHz produce microwave discharges. 2.5 GHz is usually used in industrial and scientific applications (Lebedev, 1998; Lebedev, 2010; Ferreira and Moisan, 2013). The one of the main advantage of this plasma system is the electrodeless setup (Jamróz *et al.*, 2018). The presence of particles or oxidizers can limit the application of many plasma systems, due to erosion of electrodes. Hence, the microwave plasma system has a distinct advantage.

Plasma type	Current A	Voltage V	Frequency Hz	Pressure drop	Efficiency %
Dielectric barrier discharge	$10^{-3}$ to 10	$5 \times 10^3$ - $2 \times 10^4$	10 to $10^5$	large	30 to 80
Microwave discharge	$10^{-3}$ to 1	100 to 500	$>10^9$	small	30 to 60
Arc discharge	10-100	100-500	dc	middle	70-90
Pulsed corona	$10^{-2}$ to 1	$3 \times 10^4$ - $2 \times 10^5$	10-1000	middle	20-70

**Table 2.5; Properties of different plasma discharges (flow rate/channel) (Urashima and Chang, 2000)**

The removal of toluene has been investigated in microwave discharges. The removal efficiency of toluene was more than 90% and the products included gases ( $H_2$ ,  $CH_4$ , and  $C_2H_2$ ) and solid carbon. The solid carbon could be removed by adding steam into the discharge reactions (Sun *et al.*, 2017). The microwave plasma has also been employed to decompose toluene, benzene and 1-methyl naphthalene in  $N_2$  carrier gas. The reactor was able to remove 98% of the tar compounds (Jamróz *et al.*, 2018). However, the conversion efficiency decreased with increasing concentration and flow rate (Jamróz *et al.*, 2018). In another study, microwave plasma was used to investigate the decomposition of tar from pine pyrolysis. Commercial grade ethanol was used to decrease the viscosity of the tar compounds. It was noted that tar completely decomposed into  $CO$ , solid carbon,  $H_2$  and

O<sub>2</sub>. The formation of CO increased as residence time decreased, whereas O<sub>2</sub> formation increased at high residence time (Elliott *et al.*, 2013). However, the formation of solid carbon produced operational problems. The formation of problematic deposits has been widely reported (Demidiouk *et al.*, 2003; Magureanu *et al.*, 2006; Chen *et al.*, 2009; Magureanu *et al.*, 2011; Gandhi *et al.*, 2013; Karatum and Deshusses, 2016). Jamroz *et al.* (2018) stated that the addition of steam increased the conversion of tar compounds and decreased the formation of benzene derivatives and soot (Jamróz *et al.*, 2018). Osman and Marc (2016) measured the time required to produce significant blocking in the reactor by measuring the pressure drop (Fig. 2.20) (Karatum and Deshusses, 2016). It was stated that formation of these deposits increased with decreasing residence time.

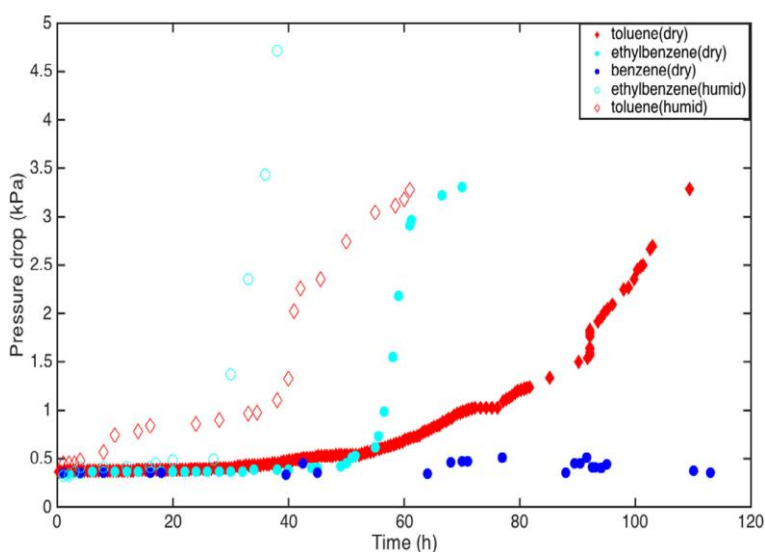


**Figure 2.20. Pressure drop measured with respect to time. SIE, 360J/L; Gas flow rate, 6.6 L/min; conc., 100 ppm<sub>v</sub> (Karatum and Deshusses, 2016).**

Many researchers reported the formation of solid residue and heavy hydrocarbons during the treatment of tar compounds and their formation inhibited either by adding the steam or by using the catalyst which may increase the operational cost of the process. Therefore, it is necessary to investigate the suitable conditions to convert the tar compounds to lower hydrocarbons.



## Chapter 3. Materials and methods

### 3.1 Chemicals and gases

Toluene and benzene (sigma Aldrich, 99.8%), CO<sub>2</sub> (99.8%), H<sub>2</sub> (99.99%), N<sub>2</sub> (99.99%), CO and CH<sub>4</sub> (100%) (BOC, UK).

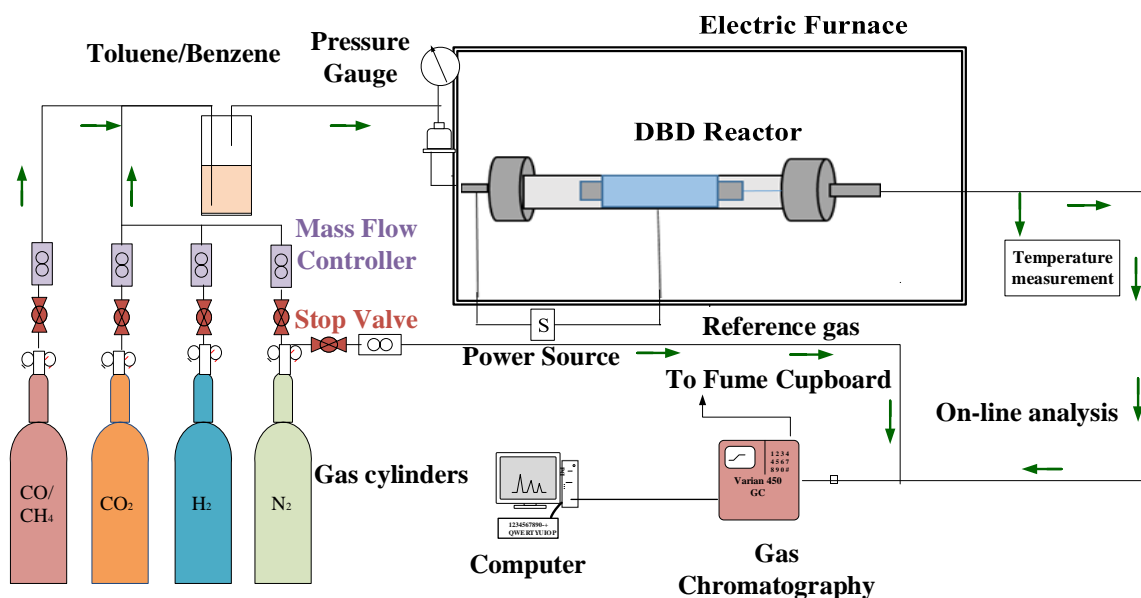
### 3.2 Experimental setup

Fig.1 shows a schematic of the experimental setup. The coaxial dielectric barrier discharge (DBD) reactor consisted of two coaxial quartz tubes one inside the other. The two metal electrodes, one outside the external cylindrical quartz tube (330 mm length, 18 mm outer diameter, 15 mm inner diameter) and the other inside the inner tube (outer diameter 12 mm, inner diameter 10 mm). The inner and the outer metal mesh electrodes were made from 316 stainless steel. The length of the external mesh was 45 mm resulting in a discharge region of about 2.86 cm<sup>3</sup>. The plasma was produced in the annular space between the coaxial cylindrical tubes. A variac was used to control the input voltage of the plasma generator which delivers power to DBD reactor. The power supplied to the reactor was measured before the plasma generator using power meter. This is also known as input power. In this study, the power supplied/delivered to the DBD reactor was varied from 5 to 40 W. Power can also be measured after the plasma generator which is known as deposited power. The voltage time dependence was sinusoidal.

Computer-controlled mass flow controllers regulated the flow rate of different gases. The carrier gas was saturated with toluene by passing through a bubbler (see Fig.3.1). The bubbler was placed in an ice bath to minimize the effect of diurnal fluctuations in ambient temperature on the rate of evaporation of toluene. For benzene, bubbler was placed inside water bath. The gas flow rate was varied from 40.6 ml/min to 120 ml/min. To monitor the change of flow rate as a consequence of plasma chemical reactions, a constant flow of nitrogen (6.0 mL/min) as reference gas was added to the exit of the reactor. All values are stated at STP. To study the effect of temperature on the performance of plasma chemical reactions, the plasma reactor was placed inside a furnace which can adjust the temperature between ambient and 400 °C.

The calibration of GC was performed to measure concentration of toluene /benzene. The known concentrations (82, 60, 41, 20 and 5 g/Nm<sup>3</sup>) of toluene/benzene were injected to GC to measure the corresponding area of peaks. Then, obtained area were plotted against known

concentrations to make calibration curve. The product compositions were monitored by a Varian 450-GC equipped with a TCD (Thermal conductivity detector) to measure CH<sub>4</sub> and H<sub>2</sub>, and a FID (Flame ionization detector) to measure lighter hydrocarbons (LHC) including C<sub>1</sub>, C<sub>2</sub> (C<sub>2</sub>H<sub>4</sub>, C<sub>2</sub>H<sub>6</sub>), C<sub>3</sub> (C<sub>3</sub>H<sub>6</sub>, C<sub>3</sub>H<sub>8</sub>), C<sub>4</sub> (C<sub>4</sub>H<sub>8</sub>, C<sub>4</sub>H<sub>10</sub>), C<sub>5</sub> (C<sub>5</sub>H<sub>10</sub>, C<sub>5</sub>H<sub>12</sub>), and C<sub>6</sub>H<sub>6</sub>.



**Figure 3.1. Schematic diagram of the experimental setup.**

### 3.3 Experimental procedure

1. First of all, plasma reactor was placed inside the fume cupboard. Then, clips of the power system were attached with the plasma system, one with the top end and other with the metallic mesh around the glass tube.
2. The appropriate gas cylinder for carrier gas (CO<sub>2</sub>, H<sub>2</sub>, N<sub>2</sub>, CO etc.) was opened, which connected with the bubbler through mass flow controller. The gas was bubbled through the toluene bottle at a specific flow which entrained the tar analogue before entering into the reactor. Online GC was connected with the outlet of plasma reactor to analyse the concentration of various compounds.
3. Another direct connection was made from nitrogen cylinder to GC through mass flow controller. It was used as nitrogen reference stream to calculate changes in total flow rate.
4. After establishing all connections, the DBD reactor was continuously purged (for 30 minutes) by the desired carrier gas (CO<sub>2</sub>, H<sub>2</sub>, N<sub>2</sub> or mixture) to remove air from the

- system (confirmed by GC analysis). After that flow rate of a specific gas was settled by a computer controlled mass flow controller. Flow was checked, after stabilizing, with the help of digital bubbler flowmeter to coincide with the settled value.
5. When the flow rate was stabilized, the blank run was completed to measure the initial peak area of toluene, CO<sub>2</sub> or H<sub>2</sub>, and nitrogen. The plasma power was off in the blank run to obtain the initial toluene's concentration in the absence of any reaction. The blank run can also help to identify any noise within the GC interface. The blank run was completed at least twice after getting stable reading before each set of experiments.
  6. After getting the stable reading of toluene concentration. The power of the plasma system was turned on, and adjusted at a certain wattage with the help of variac at least 5-10 minutes to eliminate the variation in power. The power delivered to the reactor was continuously monitored by using energy meter. The sample was injected to GC when the reading of power was stable on the energy meter.
  7. Then the plasma power was turned off after four minutes of injection of the sample into GC. The analysis of the sample took 15 minutes to get GC chromatogram.
  8. When significant amount (visible) of solid residues appeared inside the reactor, then it was replaced by new reactor and steps 4-7 were repeated. The used reactor was placed inside the furnace for 4 hours for cleaning at 700 °C.
  9. To study the effect of concentration, output stream from bubbler was diluted with the same carrier gas to change the concentration of toluene in the DBD reactor. The changes in the concentration was monitored by GC chromatograms. The variation of the peak areas was less than 2 % in consecutive readings.
  10. The series of experiments were performed by changing the level of power as well as residence time, each experiment was performed two times to produce the consistency in data.
  11. After completing the experiments, plasma system was turned off, and flow reduced to zero from control system.
  12. Cylinders were closed and all the connection disassembled from GC as well as reactor.

### 3.4 Definitions

The decomposition efficiency of toluene and CO<sub>2</sub> were defined as:

$$d_T = \frac{\text{moles of toluene in input stream} - \text{moles of toluene in outlet stream}}{\text{moles of toluene in input stream}} \times 100$$

$$\text{CO}_2 \text{ decomposition} = \frac{\text{moles of CO}_2 \text{ converted}}{\text{moles of CO}_2 \text{ input}} \times 100$$

The selectivity of different products were defined as follows:

$$\text{H}_2 \text{ selectivity (\%)} = \frac{\text{moles of H}_2 \text{ produced}}{4 \times \text{Moles of C}_7\text{H}_8 \text{ converted}} \times 100$$

$$\text{CO selectivity (\%)} = \frac{\text{moles of CO produced}}{7 \times \text{Moles of C}_7\text{H}_8 \text{ converted} + \text{moles of CO}_2 \text{ converted}} \times 100$$

$$\text{LHC selectivity (\%)} = \frac{\sum (m \times \text{moles of C}_m\text{H}_y)}{7 \times \text{Moles of C}_7\text{H}_8 \text{ converted}} \times 100$$

The yield of products was defined as:

$$\text{H}_2 \text{ yield (\%)} = \frac{\text{moles of H}_2 \text{ produced}}{4 \times \text{total moles of C}_7\text{H}_8 \text{ inlet stream}} \times 100$$

$$\text{CO yield (\%)} = \frac{\text{moles of CO produced}}{7 \times \text{moles of C}_7\text{H}_8 \text{ input} + \text{moles of CO}_2 \text{ input}} \times 100$$

The energy efficiency was calculated using the following formula:

$$\text{Energy efficiency } \left( \frac{\text{g}}{\text{kWh}} \right) = \frac{\text{grams of toluene converted per min}}{P \text{ (W)} \times 60/3600000}$$

The carbon balance was defined as:

$$\text{Carbon balance} = \frac{\sum C_{\text{measured}}}{\sum C_{\text{feed}}} \times 100$$

Benzene conversion is defined as:

$$d_B = \frac{[C_6H_6]_{in} - [C_6H_6]_{out}}{[C_6H_6]_{in}} \times 100$$

The following formulae were used to calculate the selectivity of different products using benzene as tar analogue

$$\text{LHC selectivity (\%)} = \frac{\sum (m \times \text{moles of } C_mH_y)}{6 \times \text{Moles of } C_6H_6 \text{ converted}} \times 100$$

$$\text{H}_2 \text{ selectivity (\%)} = \frac{\text{moles of H}_2 \text{ produced}}{3 \times \text{Moles of } C_6H_6 \text{ converted}} \times 100$$

$$\text{CO yield (\%)} = \frac{[\text{moles of CO}]_{out}}{[6 \times C_6H_6 \text{ moles}]_{in} + [CO_2 \text{ moles}]_{in}} \times 100$$

$$\text{Specific input energy } \left( \frac{\text{kJ}}{\text{L}} \right) = \frac{P \text{ (W)} \times 60/1000}{\text{Flow rate total (L/min)}}$$



## Chapter 4. The role of CO<sub>2</sub> in the conversion of toluene as a tar surrogate

### 4.1 Introduction

Various plasma techniques have been used to crack biomass gasification tars, using toluene as a tar surrogate. The results obtained so far were generated by plasma-enhanced catalytic steam reforming, where it has been found that the removal efficiency of toluene can be increased from 37% to 57% using non-thermal plasma. The selectivity towards CO and H<sub>2</sub> has been shown to increase in the presence of Ni/SiO<sub>2</sub> (Tao *et al.*, 2013).

Nair used pulsed corona discharge plasma for the removal of tar from product gas (Nair *et al.*, 2003a). It was demonstrated that the cracking of naphthalene in nitrogen is more economical than cracking in product gas. It had been observed that the energy requirement for this process was very high, as 20% of the output energy of the biomass gasification was consumed to remove the tar from fuel gas (Nair *et al.*, 2003a). The efficiency, at 95%, was higher than thermal or catalytic cracking.

An atmospheric dielectric barrier discharge (DBD) reactor is a more attractive method for conversion of tar compounds. It has been widely studied for the removal of volatile organic compounds to address environmental problems (Karatum and Deshusses, 2016). It has been demonstrated that the removal efficiency increases with increasing residence time and specific input energy. In another study, a wire plate dielectric barrier discharge was used with alumina/nickel foam/manganese oxide catalyst to investigate the decomposition of toluene at ambient pressure and temperature (Guo *et al.*, 2006). The complete removal of toluene was shown to be possible. Manganese catalysts and a DBD reactor were used to decompose the toluene in air as carrier gas (Magureanu *et al.*, 2006).

In this study, a DBD was used to decompose the toluene in CO<sub>2</sub> carrier gas. The role of CO<sub>2</sub> in product selectivity and decomposition of tar analogues was investigated as it makes up a significant proportion (15%-25%) of the gasifier effluent (Parthasarathy and Narayanan, 2014). It can help to understand the mechanism of tar decomposition in actual product gas from gasifiers, which mainly consists of CO<sub>2</sub>, H<sub>2</sub>, CO and N<sub>2</sub> (Parthasarathy and Narayanan, 2014). The effects of power, residence time, concentration and temperature on the removal of toluene and towards the selectivity of various compounds.

## 4.2 Results and discussion

### 4.2.1 Effect of Power

Plasma power is an important factor affecting NTP reactions. Toluene decomposition products include CO, H<sub>2</sub>, lighter hydrocarbons (LHC) including C<sub>1</sub>-C<sub>5</sub>, and heavier hydrocarbons. Fig.4.1 (a) shows the effect of input plasma power on decomposition of toluene. It was observed that toluene decomposition efficiency increased with increasing plasma power. The maximum removal of toluene was 99 %, achieved at 40 W and a residence time of 4.23 s. Previous experimental studies showed that increasing plasma power increased the electron density, electric field and gas temperature (Tu *et al.*, 2011), which could increase the conversion of toluene. Moreover, the formation of active species, such as ions, radicals, and excited molecules can also enhance the cracking of toluene.

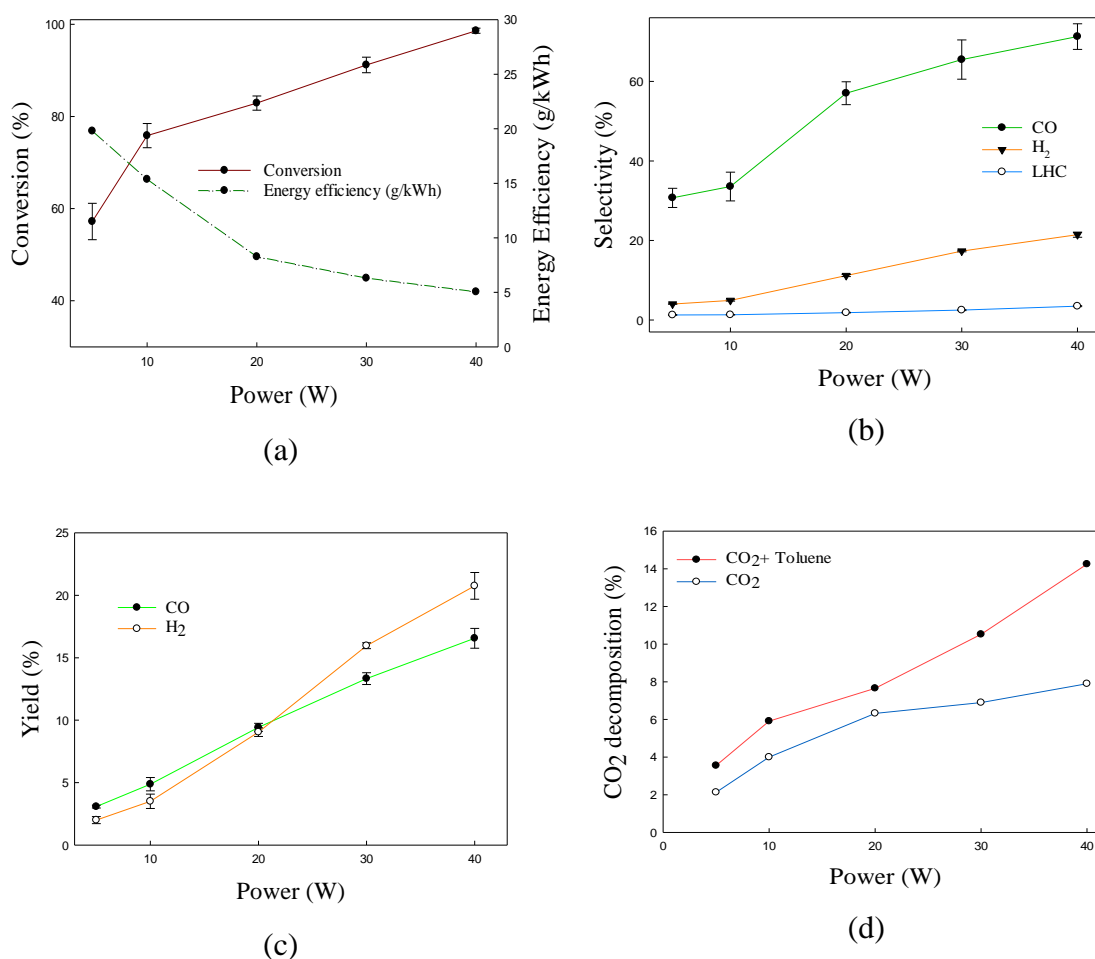


**Figure 4.1.** Effect of plasma power on the (a) conversion of toluene, (b) selectivity of CO, H<sub>2</sub> and LHC at residence time 4.23 s, (c) yield of CO and H<sub>2</sub> at 4.23 s, and (d) decomposition of CO<sub>2</sub>. Reaction conditions: gas flow rate, 40.6 ml/min; concentration, 82g/Nm<sup>3</sup>; temperature, ambient; and residence time, 4.23 s.

Fig. 4.1(a) also shows that the energy efficiency decreases from 22 g/kWh to 5 g/kWh with increasing plasma power from 5 W to 40 W. Similar results were reported for destruction of toluene in gliding arc discharge (Chun *et al.*, 2013).

Fig. 4.1(b) shows the selectivities of various gaseous products as a function of the discharge power at a residence time of 4.23 s. The selectivity to CO slightly increases from 5 to 10 W, after which it rises exponentially up to 30 W. This is because the dissociation of CO<sub>2</sub> also increases at high power, which increases the selectivity of CO exponentially. The selectivity to H<sub>2</sub> increases linearly with power, whereas the selectivity of lower hydrocarbons remains below 4 % at various levels of power.

Fig. 4.1(c) presents the relationship between yield of valuable gases and discharge power. The yield of both products (CO and H<sub>2</sub>) shows a linear relationship with power. The yields of CO and H<sub>2</sub> reach 17 and 21% respectively, at 40 W and 4.23 s. Clearly, increasing plasma power is beneficial for improving the yield of CO and H<sub>2</sub>.

The effect of power on the decomposition of CO<sub>2</sub> is shown in Fig. 4.1(d). The graph shows that decomposition of CO<sub>2</sub> increases with the rise of plasma power, and the maximum decomposition of CO<sub>2</sub> (14%) is obtained at 40 W and 4.23 s. This is consistent with previous experimental results regarding CO<sub>2</sub> decomposition (Yu *et al.*, 2012).

In NTP, the cracking of CO<sub>2</sub> may take place through electroionization dissociation channels and electron impact dissociation:



The threshold energy requirement for electron impact dissociation (Reaction (4.1)) is 5.5 eV (Zhang *et al.*, 2017), whereas the other three channels (Reactions 4.2-4.4) require electron energies from 19 to 40 eV (Locht and Davister, 1995). The electron energy is in the range of 1-10 eV in DBD plasma. Therefore, the main reaction for CO<sub>2</sub> decomposition is likely to be the electron impact dissociation. The dissociated O and CO can combine to produce CO<sub>2</sub> or O<sub>2</sub> (Cenian *et al.*, 1995), as follows:



### 4.2.2 Effect of concentration

The decomposition of toluene was studied at various concentrations (20 g/Nm<sup>3</sup>, 32 g/Nm<sup>3</sup>, 60 g/Nm<sup>3</sup> and 82 g/Nm<sup>3</sup>), to observe the effect on the conversion of toluene. Fig. 4.2(a) shows that the removal efficiency of toluene decreased from 94% to 77% when increasing the concentration to 82 g/Nm<sup>3</sup>. The decomposition efficiency of toluene decreased as the concentration increased. This has also been observed in rotating gliding arc discharges (Zhu *et al.*, 2016).

Fig. 4.2(b) presents the selectivity of different gaseous compounds, it can be seen that the selectivity of CO decreases from 78% to 36% as the concentration increases. The selectivities to hydrogen and LHC also decrease with increasing the concentration of toluene

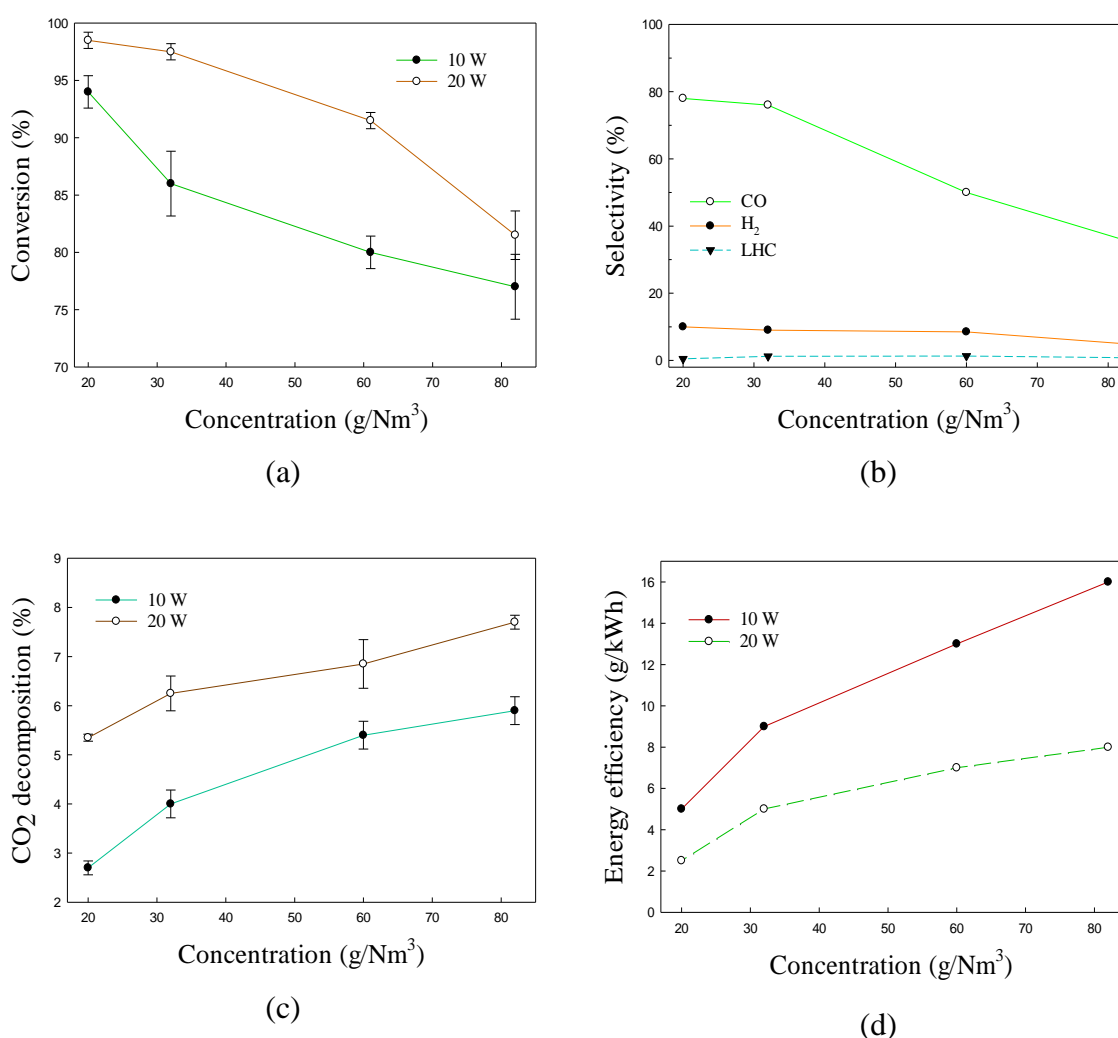


**Figure 4.2. Effect of concentration on the (a) conversion of toluene, (b) selectivity of CO, H<sub>2</sub> and LHC at 10 W, (c) decomposition of CO<sub>2</sub>, and (d) energy efficiency. Reaction conditions: gas flow rate, 40.6 ml/min; residence time, 4.23 s; concentration, 82g/Nm<sup>3</sup>; and Temperature, ambient.**

Fig. 4.2(c) represents that, at 20 W, the percentage decomposition of CO<sub>2</sub> increases from 5.4% to 7.8 % with changing the concentration from 20 g/Nm<sup>3</sup> to 82 g/Nm<sup>3</sup>. This may be due to increasing collisions between O radicals and toluene radicals rather than CO, which increases the consumption of O, thereby shifting the CO<sub>2</sub> decomposition equilibrium to the product side.

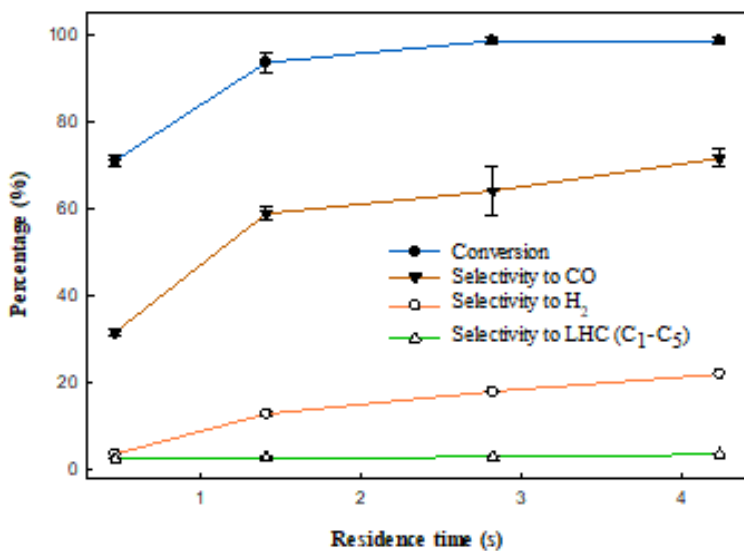
Fig. 4.2(d) shows the effect of concentration of toluene on the energy efficiency of plasma. The energy efficiency increases from 5 g/kWh to 16 g/kWh by changing the concentration from 20 g/Nm<sup>3</sup> to 82 g/Nm<sup>3</sup>. This is because the quantity of cracked toluene increased, whereas the plasma input energy and flow rate were kept constant. This agrees with previous work in which GAD (Gliding arc plasma) plasma (Chun *et al.*, 2013) and RGD (Rotating gliding arc discharge) plasma (Zhu *et al.*, 2016) were used. However, the efficiencies are higher: GAD plasma (3.6g/kWh) (Yu *et al.*, 2009a) and microwave plasma (4.52 g/kWh) (Elliott *et al.*, 2013).

### 4.2.3 Effect of residence time

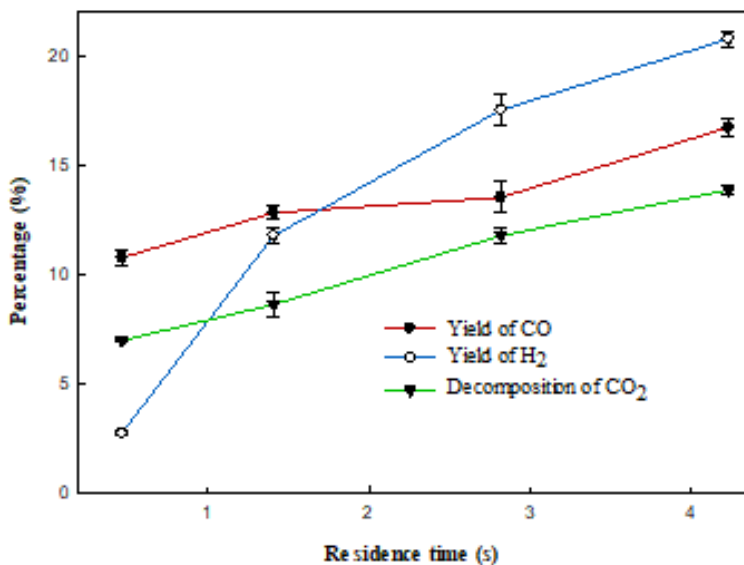
Tar decomposition is strongly influenced by residence time. Figure 4.3(a), below, shows that the decomposition of toluene increases with increasing residence time. At 40 W, decomposition of toluene increases continuously from 71% to 99%, as the residence time increases from 0.47 s to 4.23 s. Similar results were reported for the decomposition of toluene by GAD (Chun *et al.*, 2013).

The selectivities toward the various gaseous products are shown in Fig. 4.3(a). H<sub>2</sub> and CO are two major gaseous products that form during the decomposition of toluene. The selectivity of both products increased with increasing residence time, and the maximum selectivity reached 73.5% for CO and 21.9% for H<sub>2</sub>, at 4.23 s and 40 W of power. This may be due to the increase in the residence time in the plasma discharge, which increases collision frequency between toluene molecules, electrons and reactive radicals (O). It has previously been observed that O radicals are produced from the dissociation of CO<sub>2</sub> in plasma reactor (Yu *et al.*, 2012). They react with toluene fragments to produce CO and hydrogen (Guo *et al.*, 2006). The hydrogen is probably formed from toluene by H-extraction, because initially, hydrogen atoms come from the methyl group, as the C-H bonds in CH<sub>3</sub> are the weakest bonds in the C<sub>7</sub>H<sub>8</sub> molecule (Szwarc, 1948). As for CO and LHC, they are probably formed by the decomposition of C-C bond, as it has been suggested that toluene is decomposed in plasma by two types of reaction: (1) abstraction of methyl group (2) cracking of benzene ring

(Urashima *et al.*, 1997). LHC could be produced by decomposition of C-C bond with reaction energy values less than 8 eV (Blin-Simiand *et al.*, 2008). The selectivity to lower hydrocarbons, which slightly increases with increasing residence time. However, it remains lower than 4 % at all tested conditions, which is consistent with previous experimental results (Zhu *et al.*, 2016).



(a)



(b)

**Figure 4.3** Effect of residence time on the (a) conversion of toluene and towards selectivity of CO, H<sub>2</sub> and LHC (C<sub>1</sub>-C<sub>5</sub>), (b) decomposition of CO<sub>2</sub> and towards yield of CO and H<sub>2</sub>. Reaction conditions; temperature, ambient; gas flow rate, 40.6-120 ml/min; concentration, 82g/Nm<sup>3</sup>; and Power, 40 W.

Fig. 4.3(b) shows that the yield of CO and H<sub>2</sub> also increased with residence time, which would ultimately increase the production of valuable syngas. It was reported that decomposition of toluene could be achieved via three routes: (a) dissociation through electron impact, (b) radical reactions, and, (c) ion-molecule reactions (Blin-Simiand *et al.*, 2008). It was noted that the most important channel for the initial reactions in toluene cracking was electron impact. The 2<sup>nd</sup> important mechanism for toluene decomposition was radical attack. However, the direct ion process does not have a significant effect on destruction of toluene (Lee and Chang, 2003). Fig.4.3 (b) also shows the effect of residence time on the decomposition of CO<sub>2</sub>. The trend of the graph shows that the decomposition of CO<sub>2</sub> increased linearly with residence time from 7% to 14%, with increasing residence time, from 0.47 to 4.23 s, at 40 W. It is similar to Yu *et al* (2012), who reported CO<sub>2</sub> decomposition in a DBD reactor. The expected toluene destruction process is represented in Fig. 4.4. Decomposition of toluene can take place via impact of high energy electrons. It is probably initiated through hydrogen abstraction from the methyl group (because it has the minimum bond dissociation energy, 3.7 eV), producing hydrogen and benzyl radicals (Urashima and Chang, 2000). A second electron impact can remove hydrogen from the aromatic ring. The aromatic intermediates can react with each other to produce oligomers/polymers (Wang *et al.*, 2017a). High energy electrons and excited species can also attack the aromatic ring to produce ring-opening products (C<sub>1</sub>-C<sub>6</sub>) (Zhu *et al.*, 2011). Decomposition of CO<sub>2</sub> produces oxygen atoms, which oxidize the intermediates to CO<sub>2</sub> and H<sub>2</sub>O ultimately (Wang *et al.*, 2017a).

During the treatment of toluene, formation of a solid, black deposit was observed inside the plasma zone. It was noted that the solid residue showed agglomerating tendencies. The formation of solid deposits decreases with increasing the residence time. The mass of the residue was determined by measuring the weight of the reactor before and after the reaction. It was more than 35wt. % of the decomposed toluene. This value is not accurate, because some amount of solid carbon was also carried out into the downstream equipment's and pipes, which was difficult to measure. It was observed that, at 40 W and 4.23 s, the formation of solid residue increased with decreasing residence time. Guo *et al.* (2006) reported that the formation of solid residue increased in limited supply of oxygen (Guo *et al.*, 2006). The deposits were dark brown and tarry. Similar deposits have been described as polymeric substances, or carbonaceous deposits (Magureanu *et al.*, 2011). It was difficult to perform carbon balance due to presence of CO<sub>2</sub> carrier gas. The CO may be produced either by decomposition of CO<sub>2</sub> or via oxidation reactions of toluene. Therefore, it was hard to predict that how much amount of toluene converted to CO. Secondly, significant amount of solid

residues also formed inside the reactor. These solid residues are complex mixture of heavy hydrocarbons and difficult to quantify each of compound.

These solid residues can clog the reactor if not managed properly. These deposits can be removed from the surfaces of the DBD reactor by converting them into CO, CO<sub>2</sub> and lower hydrocarbons. It was reported that in the presence of excess oxygen, almost all decomposed toluene were transformed to CO<sub>2</sub> and CO (Guo *et al.*, 2006). Moreover, the presence of other gases like CO<sub>2</sub>, CO, N<sub>2</sub> and H<sub>2</sub> in the product gas from gasifier can contribute towards the removal of solid residues (Parthasarathy and Narayanan, 2014). It has previously been demonstrated that the solid deposition problem could also be resolved by increasing the plasma volume and placing additional dielectric tubes (Zhang *et al.*, 2014b).

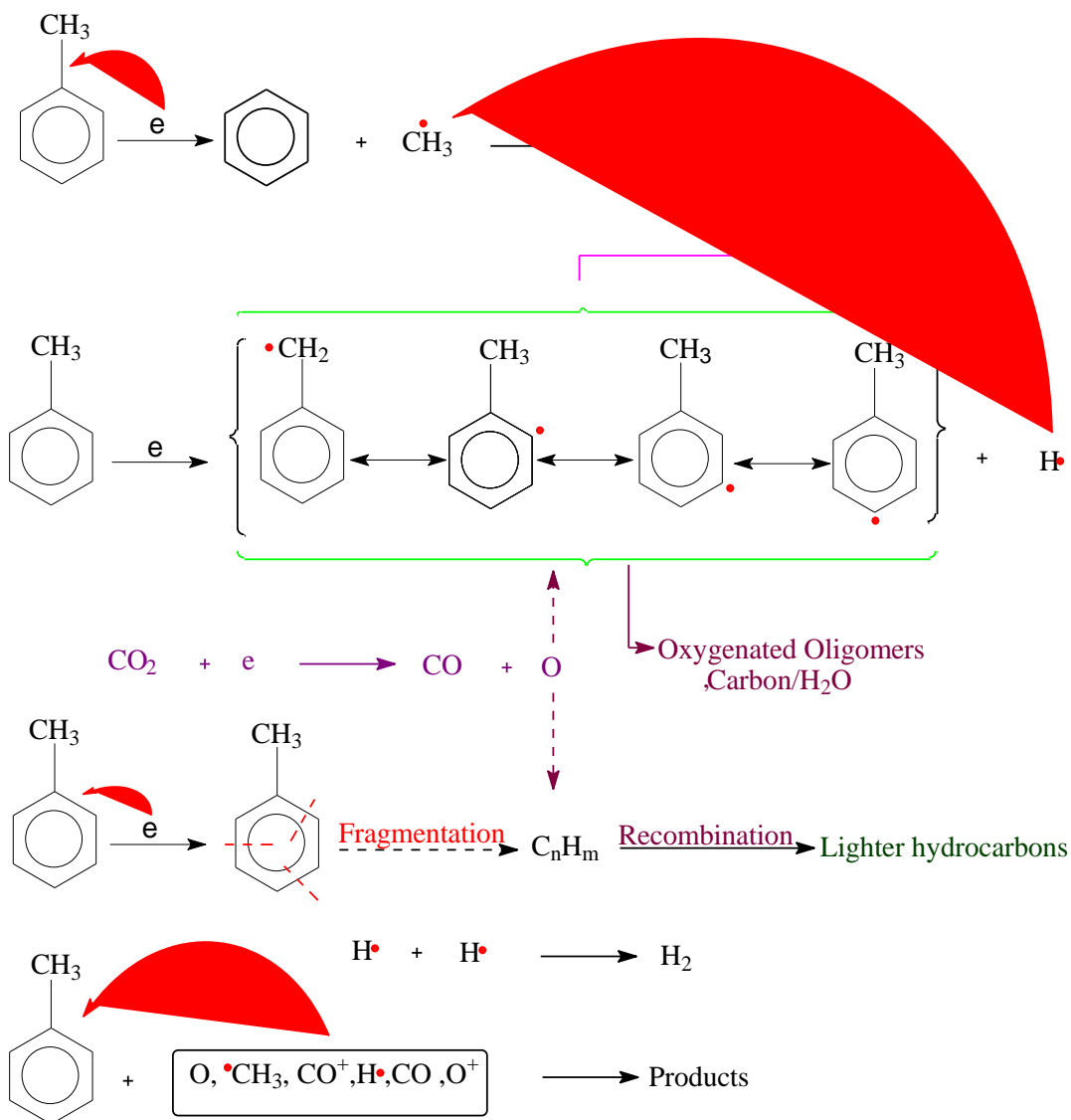
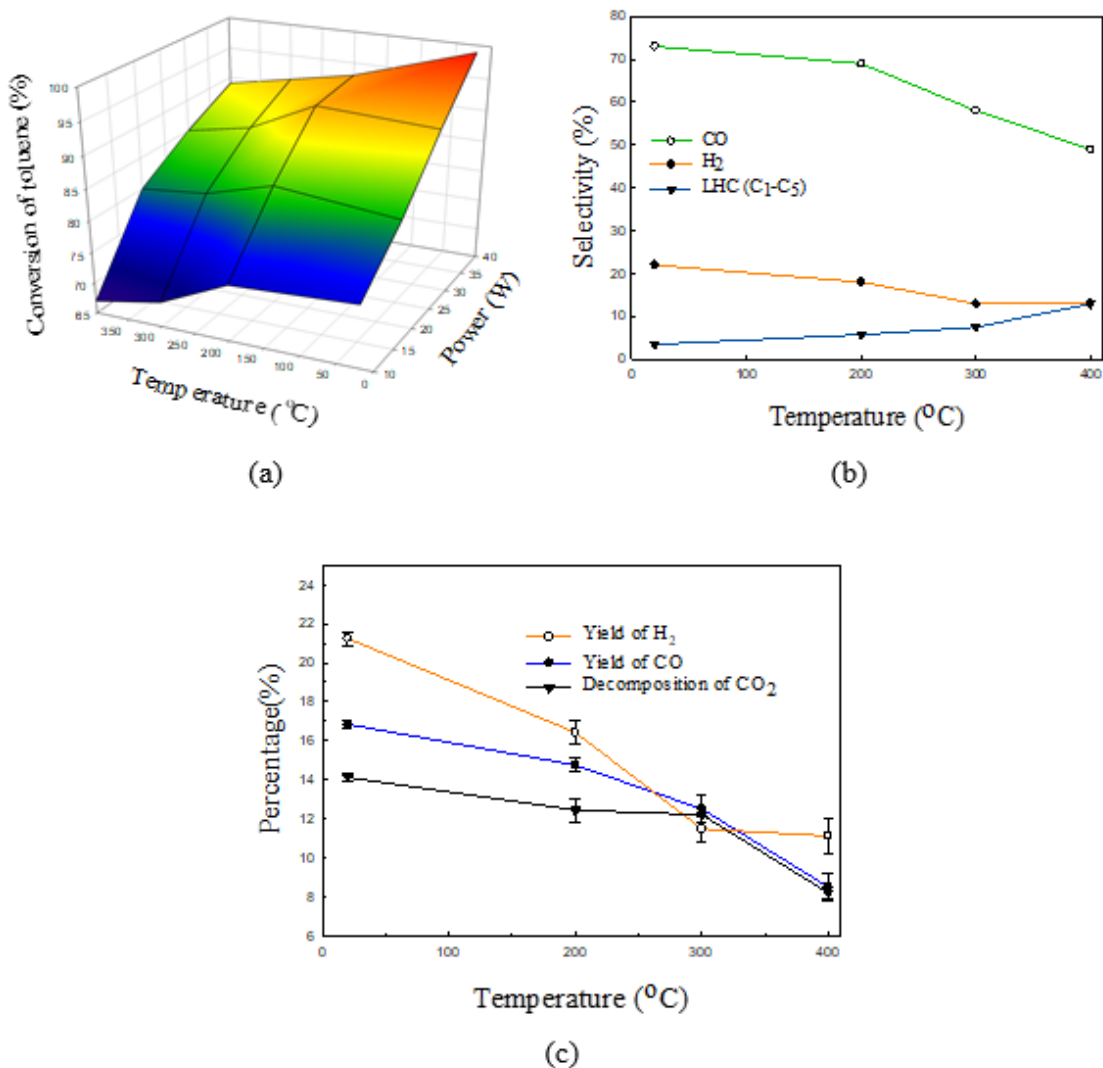


Figure 4.4. Reaction mechanism

#### 4.2.4 Effect of Temperature

Experiments were performed to determine the dependence of decomposition efficiency of toluene and product distribution, on temperature and plasma power, at a specific residence time (4.23 s). Fig. 4.5(a) shows that conversion of toluene slightly decreases with increasing temperature, from 200 °C to 400 °C, due to the increasing rate of the recombination reaction of the CO and O radicals, which reduces the amount of reactive species (Cenian *et al.*, 1995). Consequently, the conversion decreases from 99% to 88%, at 40 W. This contrasts with Song *et al.*, who reported high removal rates of toluene from air at elevated temperature (Song *et al.*, 2002).



**Figure 4.5.** Effect of temperature on (a) the conversion of toluene, (b) selectivity of CO, H<sub>2</sub> and LHC (C<sub>1</sub>-C<sub>5</sub>), and (c) the yield of CO, H<sub>2</sub> and decomposition of CO<sub>2</sub>. Reaction conditions: input power, 40 W; gas flow rate, 40.6 ml/min; concentration, 82g/Nm<sup>3</sup>; and residence time, 4.23 s

Elsewhere, it was shown that elevated temperature increased the removal efficiency of VOC. This was explained by the increased kinetic reaction of O radicals with tar compounds (Hsiao *et al.*, 1997). However, in those experiments air was used as a carrier gas instead of CO<sub>2</sub> to decompose VOC. It was found that decomposed O and CO radicals could be combined to form CO<sub>2</sub> and O<sub>2</sub> and reduced the concentration of reactive species in the plasma zone (Cenian *et al.*, 1995). Elevated temperature favours recombination reactions. Fig. 4.5(c) shows that the decomposition of CO<sub>2</sub> decreases with increasing temperature (due to recombination reactions of dissociative radicals).

A possible reason for decreasing the conversion of toluene at elevated temperature in CO<sub>2</sub>, is the re-association of O and CO radicals rather than O radicals reacting with toluene. In this way, the overall conversion of toluene is reduced in CO<sub>2</sub> carrier gas at elevated temperature.

Fig. 4.5, (b) and (c) shows the selectivity and yield of CO, H<sub>2</sub> and LHC. The selectivities of CO and H<sub>2</sub> decrease from 73.5% to 49% for CO, and from 21.9% to 12.6% for H<sub>2</sub>, by increasing the temperature to 400°C. However, selectivity to LHC increases gradually from 3.5 to 12.8% with the increase of temperature. A possible reason is the hydrocracking of toluene at elevated temperature, leading to a higher concentration of lower hydrocarbons (C<sub>1</sub>-C<sub>5</sub>) (Amano *et al.*, 1972; Castaño *et al.*, 2008).

### 4.3 Conclusions

The cracking of toluene in non-thermal plasmas was studied in a CO<sub>2</sub> carrier gas (15% - 25% of the gasifier effluent) (Parthasarathy and Narayanan, 2014) of the gasifier, to study the effects of this component of gasifier producer gas in isolation. The effects of plasma power and residence time on the selectivities of various gaseous products, at room temperature and elevated temperature, were investigated. The major findings can be summarized as follows:

- i. Toluene conversion increases with power and residence time. The maximum conversion (99%) was obtained at 40 W and 4.23 s of residence time (the highest levels used). The major products are H<sub>2</sub>, CO and solid residue.
- ii. Lower hydrocarbons (C<sub>1</sub>-C<sub>4</sub>) are also produced during the cracking of toluene. They remain below 3.5% at ambient temperature, but increased up to 12.8% as the temperature was increased to 400 °C.
- iii. At elevated temperature toluene conversion decreases due to reactions of O and CO radicals, selectivity. The yields of H<sub>2</sub> and CO also decrease.
- iv. Solid deposits were observed inside the reactor.

Toluene can be decomposed completely in CO<sub>2</sub> carrier gas using a DBD reactor, but the formation of solid residue is a negative outcome and needs to be resolved. However, other gases in the typical mixture from gasifier may have a role in removing/converting the residues.



## Chapter 5. Decomposition of toluene as a tar analogue in H<sub>2</sub> carrier gas

### 5.1 Introduction

Non-thermal plasma (NTP) is an attractive method for decomposing biomass gasification tars. In this chapter, the removal of toluene (as a gasification tar analogue) was investigated in a dielectric barrier discharge (DBD) reactor at ambient and elevated temperatures with hydrogen as the carrier gas. In previous studies, it has been observed that removal and energy efficacy of tar compound increases by adding the steam (Chun *et al.*, 2012; Chun *et al.*, 2013; Liu *et al.*, 2017a; Liu *et al.*, 2017b). The decomposition efficiency of toluene increased due to oxidation of toluene through OH radicals, which can provide new reaction routes for the direct and indirect removal of toluene (Liu *et al.*, 2017a). However, addition of steam increases the operational cost and process complexity.

In this study, a DBD reactor was used to remove toluene in H<sub>2</sub> carrier gas. In previous chapter (see 4.2.1) we reported almost complete conversion of tar (toluene) in CO<sub>2</sub> carrier gas, but with significant formation of problematic solid residue occurred. Toluene decomposition in H<sub>2</sub> has not been reported in the literature, even though the product gas from gasification contains significant amounts of H<sub>2</sub> (25.2-49.5%) (Luo *et al.*, 2009). Therefore, for a better understanding of tar removal from product gas, it is necessary to study the effect of H<sub>2</sub> on toluene conversion and product selectivity in the NTP. This study demonstrated that higher temperature in the presence of a DBD opens up new (thermal) reaction pathways to increase the selectivity to lower hydrocarbons via DBD promoted ring-opening reactions of toluene in H<sub>2</sub> carrier gas

The performance of the DBD reactor was also studied by varying power, toluene concentration, temperature, and residence time. The present study reveals that the operation temperature plays an important role in toluene conversion to lower hydrocarbons in H<sub>2</sub> carrier gas under NTP conditions.

### 5.2 Results and Discussion

#### 5.2.1 Effect of Power

The effect of power on the removal efficiency of toluene is shown in Fig. 5.1. Plasma power was varied from 5 to 40 W (SIE =7.39-59.11 kJ/L). The initial concentration of toluene was 33 g/m<sup>3</sup>, and the residence time was 4.23 s. It was found that toluene decomposition

efficiency increased with increasing plasma power, and the maximum removal of toluene was 99.5% at 40 W and 4.23 s. The similar effect of power on the decomposition of toluene was reported in previous experimental study (Wang *et al.*, 2017a).

The energy efficiency and selectivity to LHCs are also shown in Fig. 5.1. The energy efficiency of the plasma decomposition clearly decreases with increasing plasma power. There are diminishing returns as the input power is increased. Similar trends have been reported for the decomposition of tar analogue (Chun *et al.*, 2013). However, the overall selectivity of LHC increases from 11.20 to 20% as the power was increased from 5 to 40 W, which suggested that the aromatic ring was broken down at higher plasma power. Fig. 5.2 demonstrated that the selectivity of LHCs (C<sub>1</sub>-C<sub>5</sub>) increased with increasing plasma power

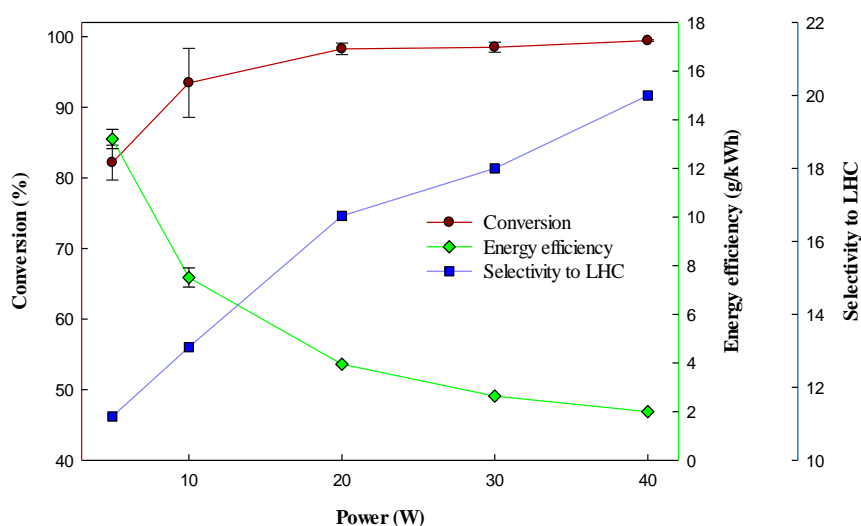


**Figure 5.1. Effect of plasma power on the conversion, energy efficiency and selectivity to LHC; bars represent standard deviation. Reaction conditions: concentration, 33 g/Nm<sup>3</sup>; Temperature, ambient; flow rate, 40.6 ml/min; residence time, 4.23 s; and SIE, 7.39-59.11 kJ/L.**

In a DBD plasma, the mean electron energy is in the range of 1-10 eV. The Maxwellian electron energy distribution function (EEDF) shows the higher the average electron energy is, the more electrons with higher energy will be produced (Michelmore *et al.*, 2013). These energetic electrons can generate active radicals, ionic and excited atomic and molecular species through electron-impact dissociation, ionization, and excitation of the source gases, i.e., H<sub>2</sub> and toluene, which can initiate plasma assisted toluene decomposition/hydrocracking in H<sub>2</sub> carrier gas. The bond dissociation energy of H<sub>2</sub> is 4.5 eV (Darwent, 1970). In a toluene molecule, the C-H bond dissociation energy (3.7 eV) of the methyl group is lower than the dissociation energy of the C-H bond, C-C and C=C of the aromatic ring (Darwent, 1970). The bond dissociation energy of the C-C bond between the aromatic ring and the methyl group is

also higher (4.4 eV) (Kohno *et al.*, 1998; Urashima and Chang, 2000). Therefore, initially, the toluene could be decomposed via H-abstraction from methyl group, because the C-H bond in the methyl group has lower bond dissociation energy. Moreover, the energetic electrons could break the C-C bond between benzene ring and methyl group, generating phenyl and methyl radicals (Liu *et al.*, 2017a).

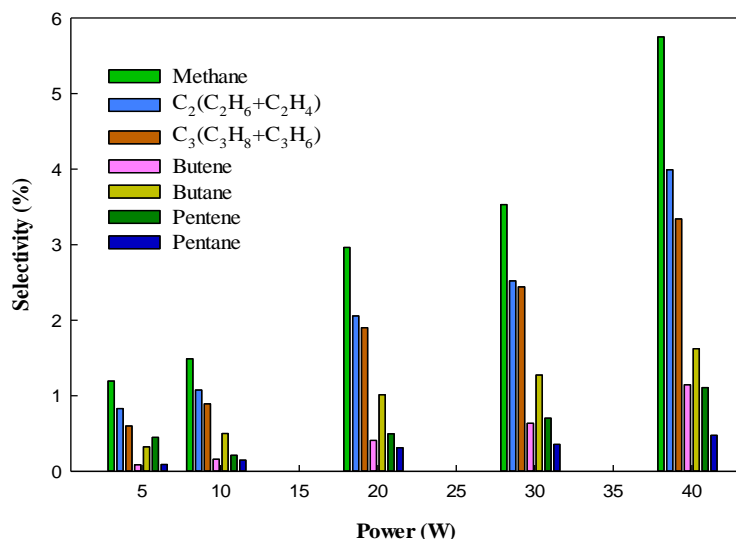


**Figure 5.2. Selectivity of different LHC at 4.23 s. Reaction conditions: concentration, 33 g/Nm<sup>3</sup>; Temperature, ambient; residence time, 4.23 s; and SIE, 7.39-59.11 kJ/L.**

The benzyl and phenyl radicals could agglomerate to form solid residue. Meanwhile, these radicals (phenyl, and methyl radicals) could combine with H radicals or react with H<sub>2</sub> to produce methane and benzene, respectively. The agglomeration of methyl radicals can form higher hydrocarbons (such as C<sub>2</sub>, C<sub>3</sub>, C<sub>4</sub>, C<sub>5</sub> hydrocarbons) (Zhang *et al.*, 2002; Zhang *et al.*, 2015). Another route for the decomposition of toluene is the cleavage of the aromatic ring, which can produce LHCs (<C<sub>6</sub>) directly by plasma assisted hydrocracking of aromatic ring in an NTP (Blin-Simiand *et al.*, 2008). Therefore, both H radicals and energetic electrons contribute to the decomposition of toluene in H<sub>2</sub> carrier gas. In an NTP, the formation of these chemically reactive species is necessary for the tar decomposition/hydrocracking reactions. In the cracking of a toluene molecule, the removal of methyl group, and the decomposition of aromatic ring are important (Blin-Simiand *et al.*, 2008). An increase in plasma power/voltage can increase the electric field strength and the electron energy, which increases the number of reactive species in a DBD plasma. The increased electric field strength, the electron density, and the higher energetic electrons at high power/voltage could all contribute to the enhanced toluene conversion and the increased selectivity of LHCs in an NTP.

It was observed that the NTP reactions strongly depended upon input energy. Hence, the specific input energy (SIE) is the main factor affecting the performance of the plasma process. It is reported that, even at 725 °C, the toluene conversion remains below 20%, although the complete decomposition occurs by 900 °C (Taralas *et al.*, 2003). It was observed that the most favourable required temperatures for toluene conversion was above 650 °C (Swierczynski *et al.*, 2008).

The decomposition of toluene with respect to SIE can be written as

$$r = -1/n \times d[C_7H_8]/dSIE = k_{SIE}[C_7H_8]^n \quad (5.1)$$

Here n shows the reaction order and  $k_{SIE}$  is the energy constant in the given reaction. The natural log of remaining fraction of the toluene with respect to SIE in H<sub>2</sub> carrier gas is shown in Fig. 5.3. It can be observed that the cracking of toluene in H<sub>2</sub> carrier gas can be represented by the following equation.

$$\ln \frac{[C_7H_8]}{[C_7H_8]_0} = -k_{SIE} \times SIE \quad (5.2)$$

The values of the R<sup>2</sup> here is 0.96. Therefore, the cracking of toluene in dielectric barrier discharge reactor as a function of SIE exhibits first order behaviour and the value of the energy constant ( $k_{SIE}$ ) is 0.16 (L/kJ). It was reported that electron impact plays a key role in NTPs in similar reactions (Urashima *et al.*, 1997; Kohno *et al.*, 1998). The rates for radical reactions were very low, in the range of 10<sup>-22</sup>-10<sup>-12</sup> cm<sup>3</sup>/s (Miziolek *et al.*, 1994). However, charge transfer reactions of toluene with ions and recombination of electrons and toluene's were significant (10<sup>-10</sup>-10<sup>-7</sup>), but densities of ions were much lower (4-5 orders of magnitude) as compared to radical densities (Miziolek *et al.*, 1994; Kohno *et al.*, 1998). The electron density is significantly high (10<sup>12</sup> cm<sup>-3</sup>) in the discharge channel (Uraahima *et al.*, 1995), whereas the rate of reactions is about 10<sup>-6</sup> cm<sup>3</sup>/s and a function mean energy of electrons (Miziolek *et al.*, 1994). Therefore, energetic electrons played a significant role in the decomposition of toluene due to high density and reaction rate. The equation 5.2 can be used to obtain the value of energy constant which can be used to compare systems and to determine the removal of tar compounds in NTPs reactors. However, scale up study is necessary to validate this equation because of complex nature of chemical reactions involved in non-thermal plasmas.

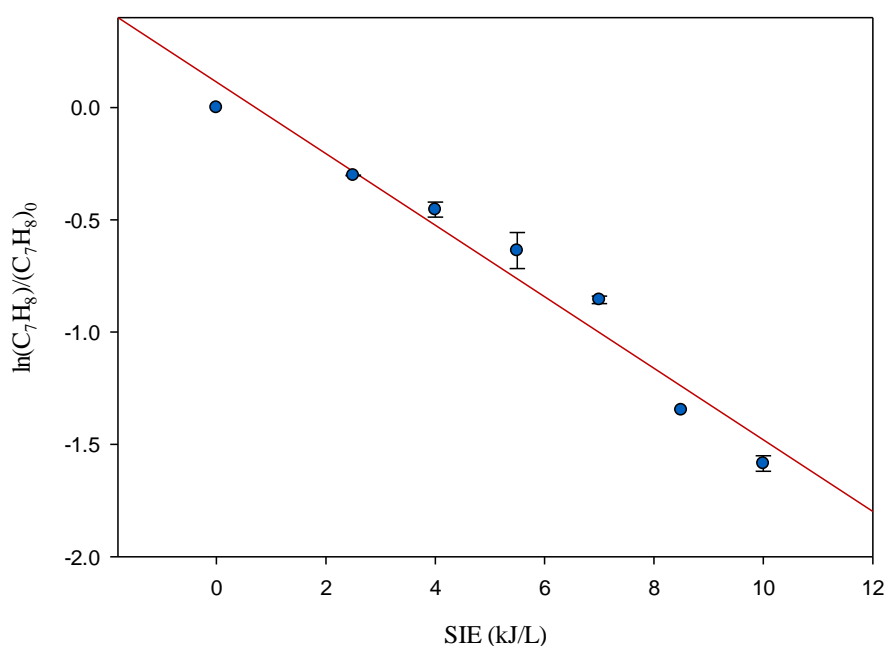


**Figure 5.3. Effect of specific input energy (SIE) on the remaining fraction of toluene (Reaction conditions: concentration, 33 g/Nm<sup>3</sup>; Temperature, ambient; and residence time, 1.43 s).**

### 5.2.2 Effect of concentration

The toluene concentration was varied between 20 and 82 g/Nm<sup>3</sup>, to observe the effect on the conversion of toluene. Fig. 5.4 shows that the removal of toluene decreased from 98.5% to 78% by increasing the concentration from 20 to 82 g/Nm<sup>3</sup>. The trend is consistent with previous experimental results in which decomposition efficiency of toluene decreased with increasing the concentration in a DBD plasma (see 4.2.2), and that for benzene in a gliding arc plasma (Chun *et al.*, 2013).

At constant power, the plasma-generated reactive species react with the toluene to decompose it. However, when the concentration is increased whilst keeping the others parameters constant, the relative amount of toluene molecules increases with respect to reactive species. Therefore, as the concentration of toluene increases, the ratio of plasma-activated reactive species to toluene molecules will decrease, which will reduce the toluene conversion. Due to this reason, the selectivity to LHCs also decreases with increasing the concentration of toluene (Fig. 5.4). Fig. 5.4 also shows the effect of the concentration of toluene on the energy efficiency of plasma. The energy efficiency increases from 4.79 g/kWh to 15.6 g/kWh by changing the concentration from 20 g/m<sup>3</sup> to 82 g/Nm<sup>3</sup>. As the concentration is increased, it also increases the total amount of decomposed toluene, and so the energy efficiency of the plasma process.

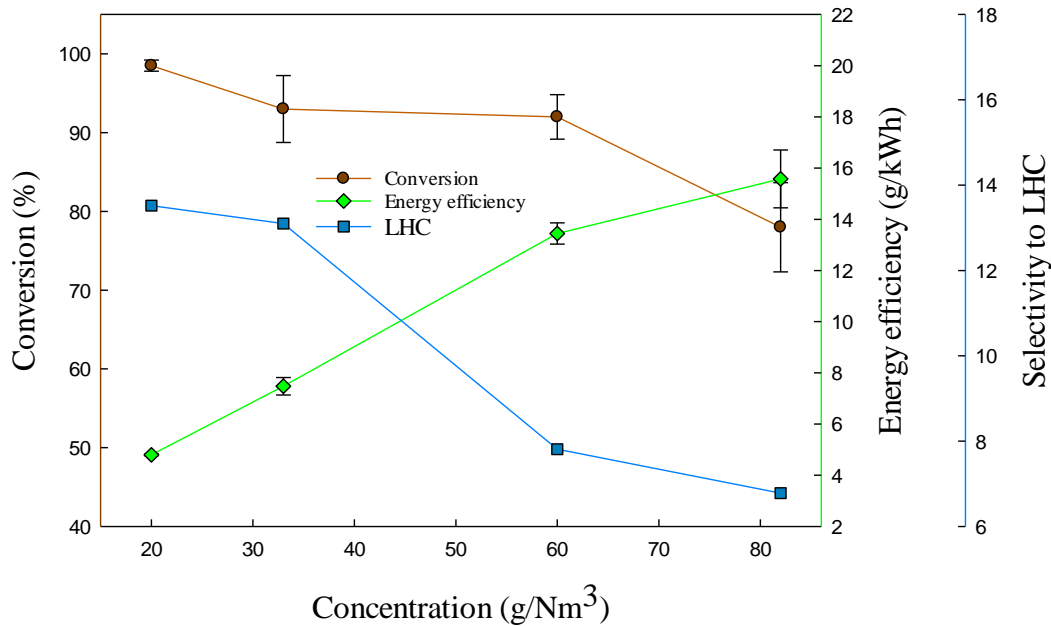
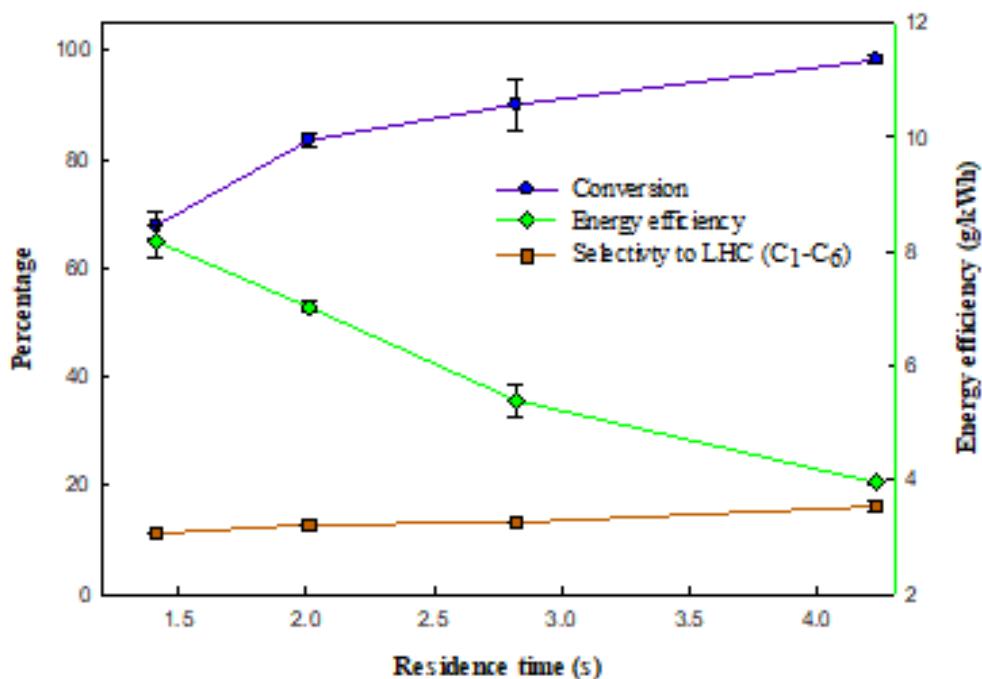


**Figure 5.4.** Effect of concentration on the conversion of toluene and energy efficiency of the plasma process; bars represent standard deviation. Reaction conditions: input power, 10 W; residence time, 4.23 s; flow rate, 40.6 ml/min; ambient temperature; and SIE, 14.77 kJ/L.

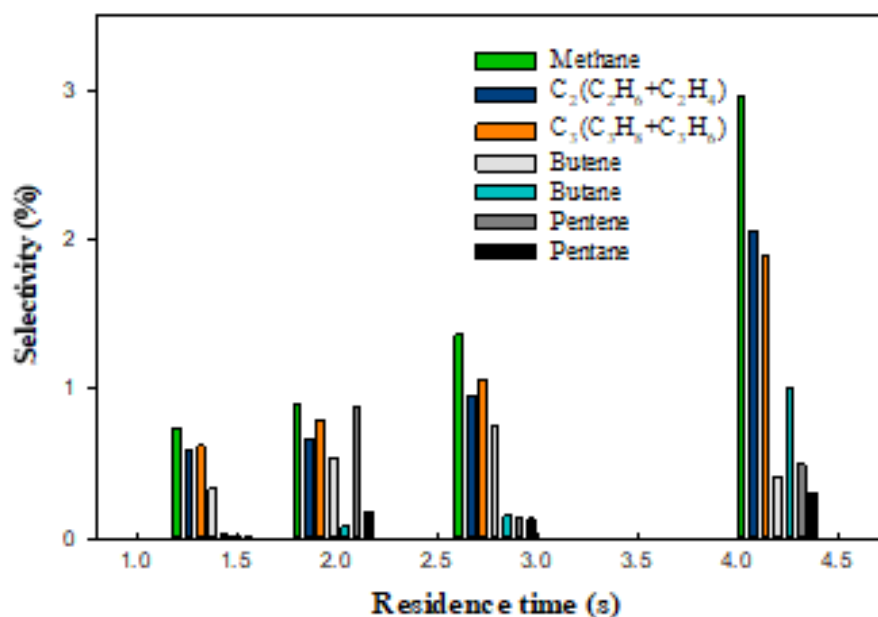
### 5.2.3 Effect of residence time

The removal efficiency of toluene is also influenced by residence time. Fig. 5.5(a) shows the effect of residence time on the conversion of toluene at 20 W. It can be observed that decomposition of toluene increases with increasing residence time. The removal of toluene continuously increases from 67 % to 98 % as the residence time increases from 1.43 s to 4.23 s at 20 W (SIE: 10-29.6 kJ/L).

At high residence time, the tar compound and carrier gas are subjected to plasma discharge zone for longer time, which can increase the collision between reactive species and tar compound. Therefore, increasing residence time promotes the conversion of toluene due to high number of collision between tar compounds and reactive species (Zhu *et al.*, 2016). The maximum conversion attained was 98% at the highest residence time used here (4.23 s).



(a)



(b)

**Figure 5.5. Effect of residence time (a) on the conversion of toluene, energy efficiency and selectivity to LHC; bars represent standard deviation, and (b) selectivity to individual lower hydrocarbons. Reaction conditions: concentration, 33 g/Nm<sup>3</sup>; flow rate, 40.6-120 ml/min; Temperature, ambient; and Power, 20 W; and SIE, 10-29.6 kJ/L.**

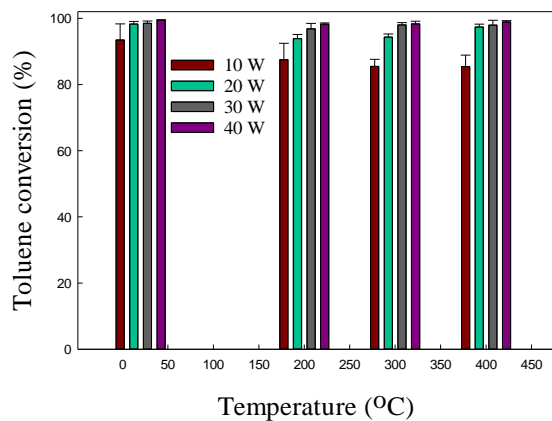
The energy efficiency and selectivity towards the lower hydrocarbons (C<sub>1</sub>-C<sub>5</sub>) are shown in Fig. 5.5(a). The energy efficiency of the process decreases with increasing residence time. It

can be seen that energy efficiency decreases from 7.9 g/kWh to 3.9 g/kWh with increasing residence time from 1.43 s to 4.23 s. A similar trend of decreasing flow rate has been reported on the conversion of benzene (Chun *et al.*, 2013). The residence time is associated with the flow rate, and for high residence time flow rate needs to be reduced. At low flow rate, the amount of tar compound subjected to plasma reactor also decreases, which decreases the total amount of decomposed toluene. Therefore, at high residence time, energy efficiency of the system decreases due to reduction in the total amount of decomposed toluene. Fig. 5.5(b) shows that selectivity of LHC (C<sub>1</sub>–C<sub>5</sub>) increases with residence time. The H<sub>2</sub> carrier gas spends more time in the plasma discharge with increasing residence time, which produces more H reactive radicals. These H radicals may contribute to increases the selectivity of lower hydrocarbons by reacting with toluene and its fragments.

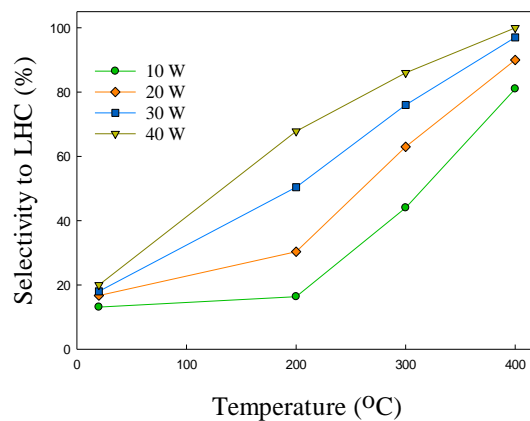
During the decomposition of toluene, a solid yellow residue was found inside the plasma zone. Guo *et al.* (2006) studied the decomposition of toluene in catalytic wire plate dielectric barrier discharge reactor with N<sub>2</sub> and O<sub>2</sub> as a carrier gas (Guo *et al.*, 2006). They found that the formation of solid residue increased at lower oxygen concentrations. In some reports, these deposits were described as polymeric substances, or carbonaceous deposits (Magureanu *et al.*, 2011; Karatum and Deshusses, 2016). It was also reported that solid particles formed during the cracking of toluene in air, leading to the formation of solid deposits on the surface of the catalyst, thereby decreasing catalytic activity (Demidiouk *et al.*, 2003). Moreover, formation of these solid residues can also clog the reactor. Therefore, it is very important to avoid the deposition of solid residue. However, in current study we have observed that the formation of solid residue completely disappeared at elevated temperature in the presence of H<sub>2</sub> carrier gas.

#### **5.2.4 Effect of temperature**

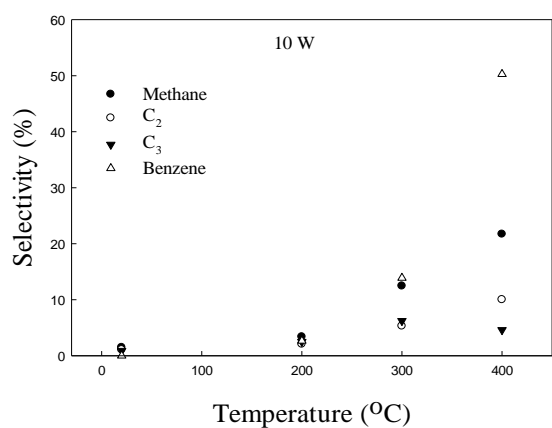
Experiments were conducted to investigate the effect of temperature on product distribution and solid residue formation, at various powers (5-40 W) and a specific residence time (4.23 s). Fig. 5.6(a), below, shows that removal of toluene is not affected by increasing the temperature. However, Song *et al.*, reported that decomposition of toluene increased at elevated temperatures (Song *et al.*, 2002). In other research, it was demonstrated that elevated temperature increased the removal efficiency of VOC in a non-thermal plasma reactor, and it was explained on the basis of increased kinetic reaction rate of O radicals (Hsiao *et al.*, 1997).



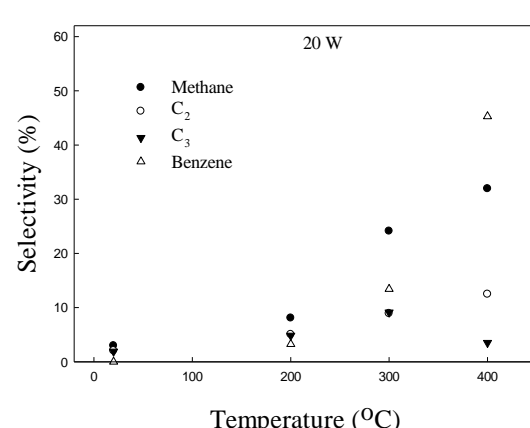
(a)



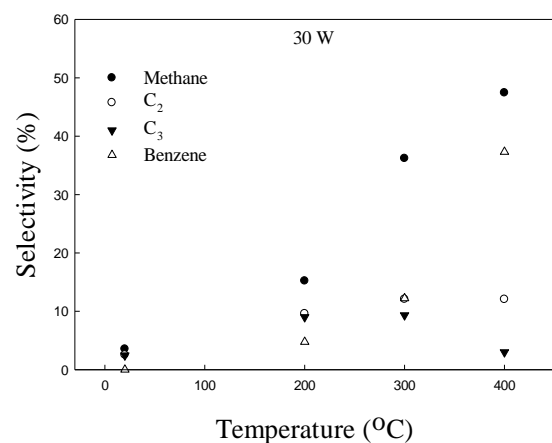
(b)



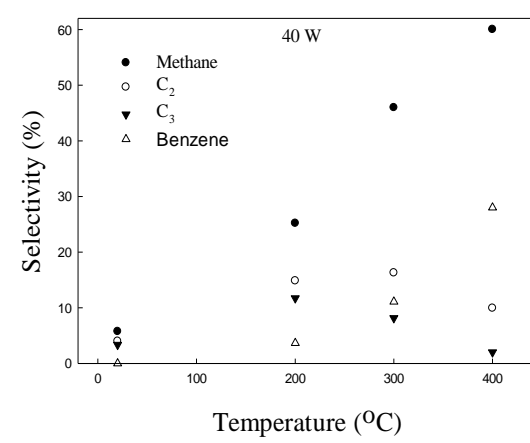
(c)



(d)



(e)



(f)

**Figure 5.6.** Effect of temperature on (a) the conversion of toluene, (b) total selectivity LHC; (c) selectivity to various LHCs at 10 W, (d) selectivity to various LHCs at 20 W, (e) selectivity to various LHCs at 30 W, and (f) selectivity to various LHCs at 40 W. Reaction conditions: concentration, 33 g/Nm<sup>3</sup>; flow rate, 40.6 ml/min; residence time, 4.23 s; and SIE, 14.77-59.11 kJ/L.

However, in those experiments air was used as the carrier gas instead of H<sub>2</sub>. In this research, at 40 W, almost complete removal of toluene was obtained at all temperatures.

Fig. 5.6(b) shows the effect of temperature on the total selectivity to lower hydrocarbons at various levels of power and 4.23 s, it can be seen that total selectivity significantly increases with increasing temperature at each level of power. At 400°C and 40 W, the selectivity rises from 20 % to 99.97 %, without the formation of solid residue. At 400 °C and 4.23 s, the minimum selectivity towards LHC reaches to 81 % even at 10 W, which shows the high conversion of toluene to LHC, at high temperature, in the presence of H<sub>2</sub> carrier gas. There are three different types of reaction involve in hydrocracking of aromatics: (a) hydrogenation-dehydrogenation (b) isomerization and (c) cracking.

The cracking reaction can be categorized as primary (ring-opening), secondary and tertiary (Arribas and Martinez, 2002). Hydrogenation and isomerization take place at lower temperature because of lower activation energy, whereas the rate of cracking (ring-opening) increases with increasing temperature (Castaño *et al.*, 2008).

Fig. 5.6 (c), (d), (e), and (f) show the effect of temperature on the selectivity of individual LHCs at 10, 20, 30 and 40 W, respectively. Fig. 5.6 (c) shows that, at 10 W, selectivity of benzene and methane reaches 50 % and 21 % respectively, with increasing temperature up to 400 °C. However, the selectivity of C<sub>2</sub> (C<sub>2</sub>H<sub>6</sub> + C<sub>2</sub>H<sub>4</sub>) and C<sub>3</sub> (C<sub>3</sub>H<sub>8</sub>+C<sub>3</sub>H<sub>6</sub>) remains below 11%. It has been reported that formation of benzene increases rapidly when increasing the temperature to 400°C (Amano *et al.*, 1972). The high selectivity to the aromatic compounds may be due to a radical exchange reactions during the hydrocracking of toluene at high temperature (Amano *et al.*, 1965). It can be observed from Fig. 5.6 (f) that the selectivity of methane increases to 60%, whereas selectivity of benzene reduces to 28%, at 40 W and 400°C. This happened due to the high population of energetic electrons at high power. In the absence of plasma, the selectivity of methane was reported to be nearly 10% at 450 °C by hydrocracking of toluene (Castaño *et al.*, 2008). It was reported that higher temperatures (>850 °C) are required to produce CH<sub>4</sub> and C<sub>2</sub>H<sub>4</sub> as the major gaseous products (Jess, 1996; Gai *et al.*, 2015). However, in this study, selectivity to methane reaches 60% at 400 °C, due to the additional effect of non-thermal plasma.

The selectivity of C<sub>2</sub> (C<sub>2</sub>H<sub>6</sub> + C<sub>2</sub>H<sub>4</sub>) increases to 16.3% by increasing the temperature up to 300°C, afterwards it decreases to 9.93 % at 400 °C. Similarly, the selectivity to C<sub>3</sub> (C<sub>3</sub>H<sub>8</sub>+C<sub>3</sub>H<sub>6</sub>) increased when increasing the temperature from ambient to 200 °C, after which it decreased, from 200 to 400 °C. This occurred because of formation of methane in the

presence of excess H<sub>2</sub> at high temperature (Freel and Galwey, 1968). Hence, the synergetic effect of plasma and temperature enhance the selectivity to lower hydrocarbons rather than solid residue. Plasma causes the production of reactive H radicals which hydrocrack toluene into lower hydrocarbons, when operating at elevated temperatures. It has been reported that adding steam reduces the formation of solid carbon and heavy hydrocarbons (Jamróz *et al.*, 2018), which increase the operational cost and process complexity. However in this study, it was noted that problem can instead be resolved using hydrogen gas, which is already present (27-53%) (He *et al.*, 2009) in fuel product gas.

### 5.3 Conclusions

In this study, the decomposition of toluene was studied in a dielectric barrier discharge (DBD) reactor using H<sub>2</sub> as carrier gas, as a proxy for biomass gasification tars. For the first time, this study investigated that elevated temperature in the presence of a DBD opens up new (thermal) reaction pathways to raise the selectivity to lower hydrocarbons via DBD promoted ring-opening reactions of toluene. H<sub>2</sub> was selected as a carrier gas because it is the major component in most steam gasifier effluents. Experiments were performed at various levels of power (5-40 W) and residence time (1.43-4.23 s), at ambient and elevated temperature (20-400 °C), to determine the conversion and selectivity towards valuable gaseous products.

The main findings are as follows:

- i. The removal efficiency of toluene can be as high as 99.5% in this design of DBD reactor. The toluene is converted to lower hydrocarbons (C<sub>1</sub>-C<sub>6</sub>) and solid residue.
- ii. The rate of decomposition of toluene increases with power input and residence time. At ambient temperature, solid residue was formed in the reactor, which would create various problems over time.
- iii. Toluene conversion is not a function of temperature, but the selectivity is under plasma conditions, which is different from conventional chemical process. The selectivity towards lower hydrocarbons increases with increasing temperature, reaching 99.9 % at 400°C, without formation of solid deposits and heavy hydrocarbons (>C<sub>6</sub>).
- iv. Formation of methane, C<sub>2</sub> (C<sub>2</sub>H<sub>6</sub> + C<sub>2</sub>H<sub>4</sub>) and benzene increases with increasing temperature. Here, the maximum selectivities observed were 60%, 9.93% and 28%, respectively, at 400 °C and 40 W (the highest values used).

Clearly, there are benefits of combining thermal and non-thermal effects in this particular application. Here, adding in thermal effects allowed high selectivity to LHCs, without solid residue formation: both desirable outcomes. It seems that, for this application at least, combinations of non-thermal plasma and thermal phenomena can have advantages.

## Chapter 6. Removal of toluene as a tar analogue in a N<sub>2</sub> carrier gas using a non-thermal plasma dielectric barrier discharge (DBD) reactor

### 6.1 Introduction

The main drawback of NTP technology is the formation of organic by-products and solid residues, and it has proven very difficult to eliminate the formation of these unwanted by-products (Guo *et al.*, 2018). These by-products may be toxic and/or environmentally malign, and they may create operational problems (Zhu *et al.*, 2016). Therefore, the complete conversion of targeted compounds to non-toxic and valuable products is desirable. Guo *et al.* (2018) studied the decomposition of toluene in a DBD reactor to investigate by-product formation. They reported that a spectrum of organic compounds were formed, including formaldehyde, acetaldehyde, methanol, benzene, acetic acid, benzaldehyde, formic acid, benzoic acid. However, the risks associated with these organic products were sometimes higher than that of the parent VOC (Guo *et al.*, 2018). The formation of solid deposits is widely reported and can cause an array of problems. For the long-term stable operation of plasma discharges, solid carbon must be removed (Sun *et al.*, 2017). Jamroz *et al.* (2018) stated that during decomposition of benzene, soot presented in significant amounts (Jamróz *et al.*, 2018). Osman and Marc (2016) measured the time required to produce significant blocking in a reactor by measuring the pressure drop (Karatum and Deshusses, 2016). The increase in pressure drop due to such deposits could produce leakages or cracks in dielectric tubes, and eventually cause blockage of the pipes.

N<sub>2</sub> is the most significant component of typical biomass gasifier product gas (around 50%) (Narvaez *et al.*, 1996). Many researchers investigated the decomposition of tar analogue compounds in N<sub>2</sub> carrier gas. However, formation of soot and heavy hydrocarbons was observed (Zhu *et al.*, 2016). Therefore, in this study N<sub>2</sub> was used as a carrier gas to investigate the decomposition of toluene (as a tar analogue) in a DBD reactor, and H<sub>2</sub> was also added into N<sub>2</sub> carrier gas at elevated temperature to evaluate its role in reducing solid residue formation.

## 6.2 Results and discussion

### 6.2.1 Effect of power and residence time

Plasma power plays a key role in the reactions in non-thermal plasmas. A range of products are produced when toluene is cracked, including H<sub>2</sub>, lighter hydrocarbons (C<sub>1</sub>-C<sub>6</sub>), and heavier hydrocarbons (>C<sub>7</sub>). The effect of input power on the conversion of toluene is shown in Fig. 6.1 below. Initially, the concentration of toluene was maintained at 33 g/Nm<sup>3</sup>. The results show that high input power favours the cracking of toluene, and nearly complete removal of toluene is obtained at 40 W and residence time of 4.23 s.

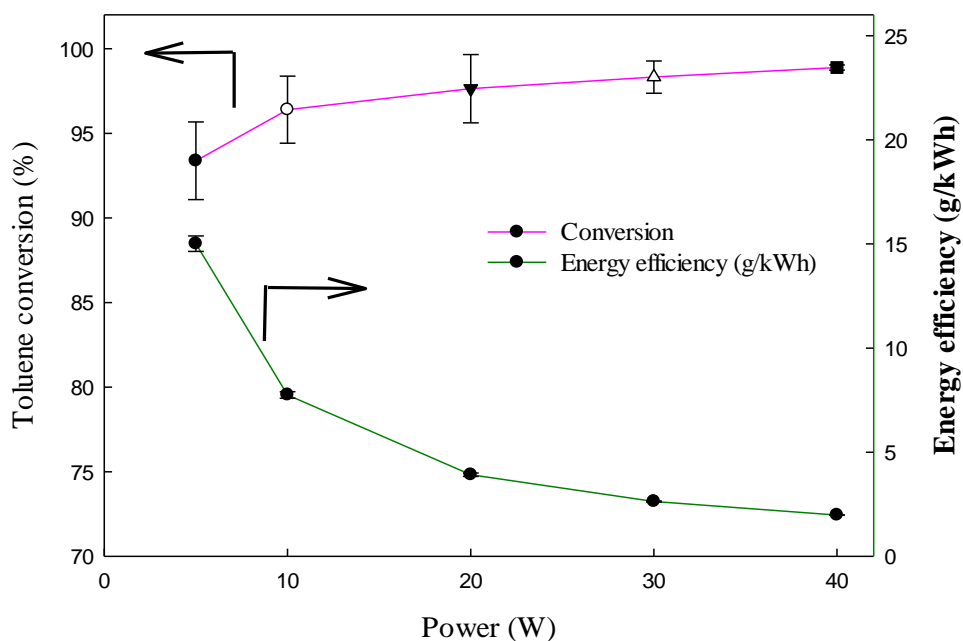


**Figure 6.1.** Effect of plasma power on the conversion of toluene. Reaction conditions: ambient temperature; Concentration, 33 g/Nm<sup>3</sup>; flow rate, 40.6 ml/min; residence time, 4.23 s; carrier gas, N<sub>2</sub>; and SIE, 7.39-59.11 kJ/L.

The conversion of toluene increased because at high power electron density, the electric field is stronger, producing more reactive species, such as radicals, ions, and excited molecules. In a non-thermal plasma, the mean electron energy is in the range of 1-10 eV (Petitpas *et al.*, 2007). The Maxwellian electron energy distribution function (EEDF) shows the higher the average electron energy is, the more electrons with higher energy will be produced (Michelmore *et al.*, 2013). These energetic electrons are the hottest species and play a key role for the decomposition of tar compounds.

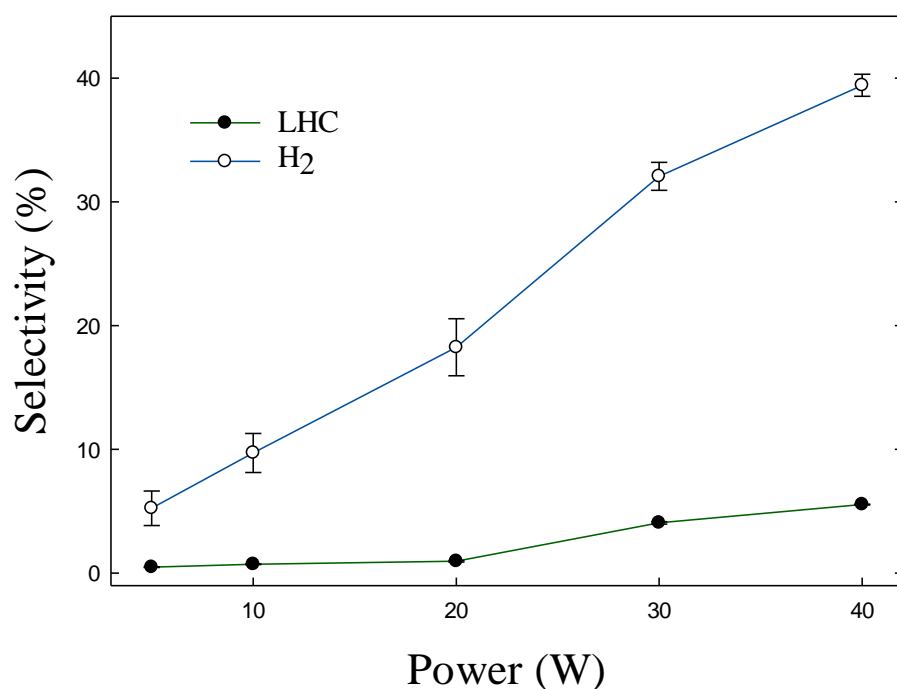


**Figure 6.2. Effect of plasma power on selectivity of gaseous products. Reaction conditions: ambient temperature; toluene concentration, 33 g/Nm<sup>3</sup>; flow rate, 40.6 ml/min; residence time, 4.23 s; carrier gas, N<sub>2</sub>; and SIE, 7.39-59.11 kJ/L.**

Fig. 6.2 presents the effect of power on the selectivity to gaseous products and the energy efficiency. The selectivity of H<sub>2</sub> gradually increases from 5% to 39% with increasing power from 5 W to 40 W. At lower power the average energy of an electron is not high enough to abstract the hydrogen from the aromatic ring, so the hydrogen originates in the methyl group (Szwarc, 1948). However, at higher powers, H<sub>2</sub> increases due to the breakage of the aromatic ring. This also increases the selectivity to lower hydrocarbons, which reach 5.5% at 40 W. However, the energy efficiency decreases with increasing the power, and decreases from 15 g/kWh to 2 g/kWh as the power increases from 5 W to 40 W. A similar trend was reported for the removal of tar analogue (see 5.2.1).

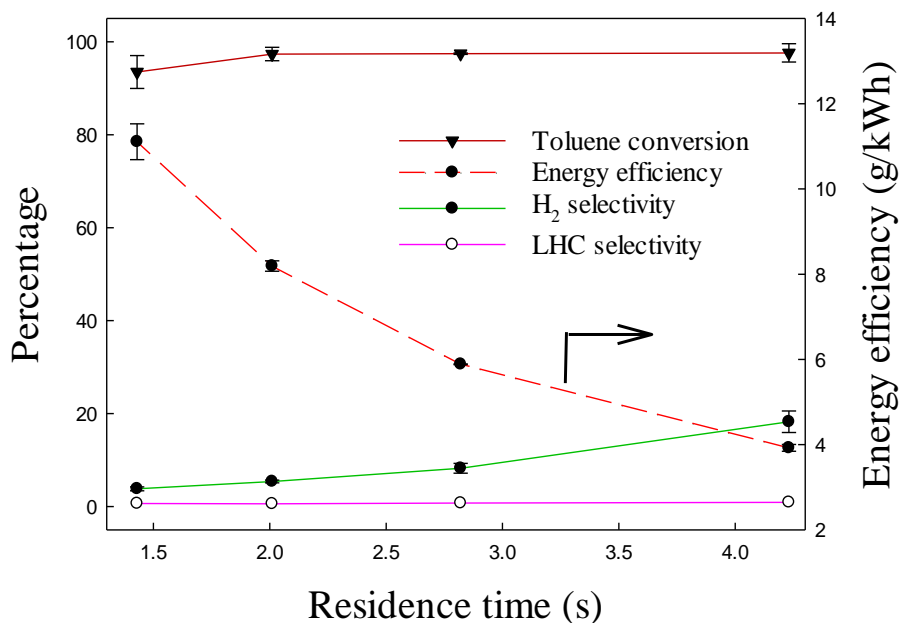


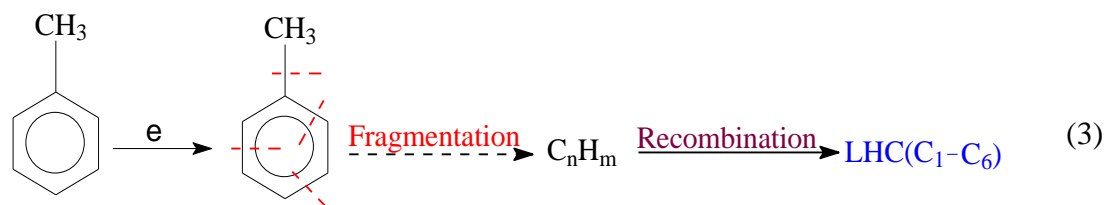
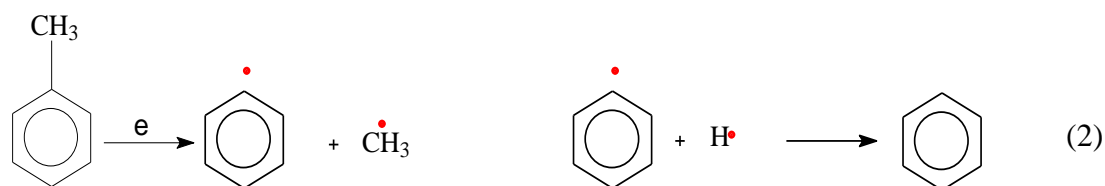
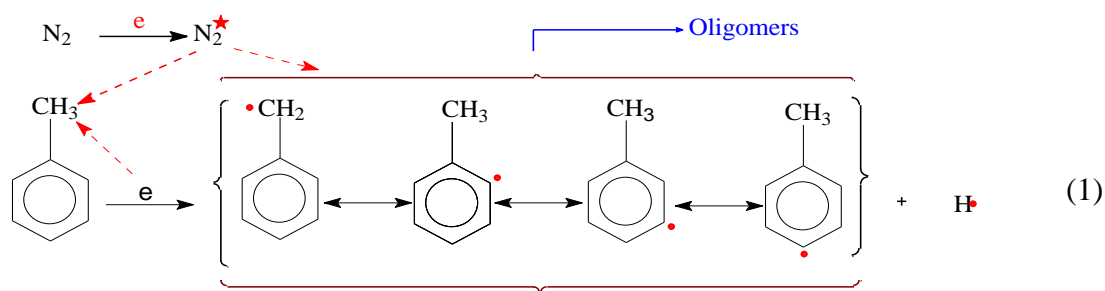
**Figure 6.3. Effect of residence time on the conversion and towards the selectivity of gaseous products. Reaction conditions: input power, 20 W; ambient temperature; concentration, 33 g/Nm<sup>3</sup>; carrier gas, N<sub>2</sub>; and flow rate, 40.6-120 ml/min.**

The effect of residence time on the product selectivity is shown in Fig. 6.3. With an increase in residence time, the removal efficiency of toluene increased from 93% to 99% at 20 W. This was simply because the toluene molecules spent more time in the plasma discharge zone, so the number of collisions with reactive species (ions, radicals and electrons) and toluene molecules increased (Bo *et al.*, 2008). The energy efficiency of the system decreases with increasing residence time. This is possible because at high residence time flow rate decreases, which also reduces the molar flow rate of toluene into the system. Therefore, the amounts of decomposed toluene decrease. Moreover, the toluene conversion for residence times of more than 2 s was almost 100%. Therefore, in this area, additional energy input reduced the apparent energy efficiency.

The selectivity of H<sub>2</sub> increased from 4% to 18% as the residence time increased from 1.43 s to 4.23 s. The decomposition of aromatic rings increased with increasing residence time due to the increase in the collision frequency of reactive species. However, the selectivity to lower hydrocarbons remained below 1% at different residence times. Figures 6.2 and 6.3 show that without any hydrogen in the initial carrier gas, the H<sub>2</sub> selectivity increases with increasing power and residence time. However the content of LHC remains very low. Hence, under these conditions the formation of oligomer/polymer compounds seems to be the main process. From a stoichiometric point of view, the formation of lower hydrocarbons from toluene is

probably due to hydrogen consumption. However the formation of simple alkanes such as methane, ethane, propane, butane etc. is a hydrogen-consuming process. Therefore, the formation of larger amounts of hydrogen is only possible by the deposition of solid residues.

The reaction scheme below shows the steps involved during the formation of various products. It shows that the decomposition of toluene can take place via high energy electrons or excited species (Step 1). It is probably initiated through hydrogen abstraction from the methyl group (as it has the minimum bond dissociation energy), producing benzyl and hydrogen radicals. The aromatic intermediates can react with each other to produce oligomer/polymer compounds (Zhu *et al.*, 2011). Step 2 shows that benzene can be produced through radical substitution reactions. Meanwhile high energy electrons and excited species can also attack the aromatic ring (Step 3) to produce ring-opening products (C<sub>1</sub>-C<sub>6</sub>) (Zhu *et al.*, 2011). H<sub>2</sub> and methane are produced by the combination of radicals (Step 4 and 5). N<sub>2</sub>\* shows the excited states of N<sub>2</sub> due to impact of electrons.



### 6.2.2 Effect of toluene concentration

The concentration of toluene affects the conversion as well as the selectivity (see Figure 6.4, below). Clearly, cracking decreases with increasing toluene concentration. The maximum toluene conversion (97%) was obtained at the minimum toluene concentration: 20 g/Nm<sup>3</sup>. Conversion then decreased monotonically up to 82 g/Nm<sup>3</sup>, where it was 91%. All conditions except toluene concentration were fixed, meaning that a constant number of reactive species were produced (Chun *et al.*, 2013). Therefore, with increasing the concentration of toluene, the relative amount of reactive species decreased. The energy efficiency of the process, however, increased with concentration, from 4.7 g/kWh to 18 g/kWh. This was because the production rate of decomposed toluene increased with concentration, whereas the input power and other parameters were kept constant (Szwarc, 1948). Similar behaviour was reported before in which toluene decomposition studied using N<sub>2</sub> and steam (Liu *et al.*, 2017a; Jamróz *et al.*, 2018).

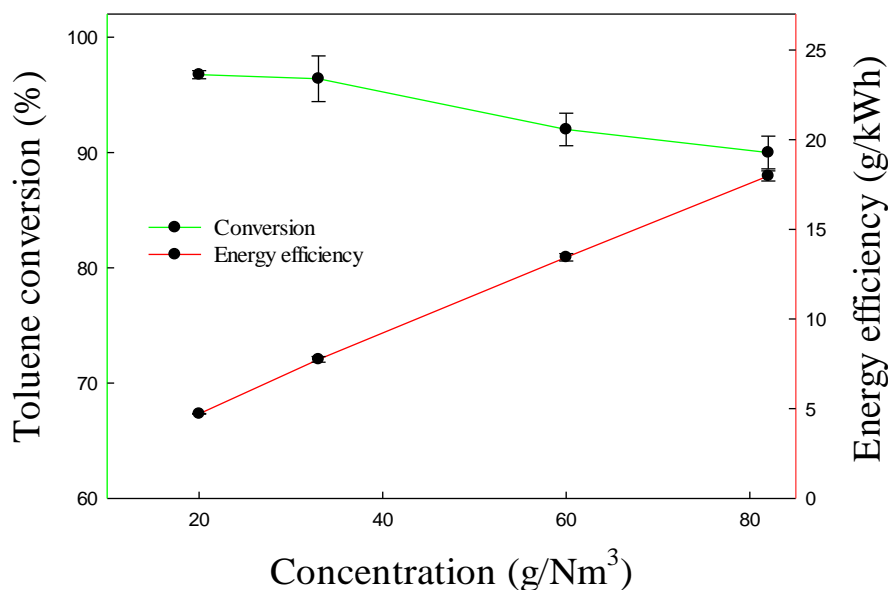


**Figure 6.4. Effect of concentration on the conversion and energy efficiency. Reaction conditions: input power, 10 W; ambient temperature; flow rate, 40.6 ml/min; residence time, 4.23 s; carrier gas, N<sub>2</sub>; and SIE, 14.77 kJ/L.**

Fig. 6.5, below, shows the changes in selectivity to gaseous products with respect to concentration. It can be observed that the selectivity of hydrogen decreases from 10.5% to 6.3% with increasing concentration. Note that the selectivity to lower hydrocarbons remains below 1% at all tested concentrations. This is due to low input power (10W).

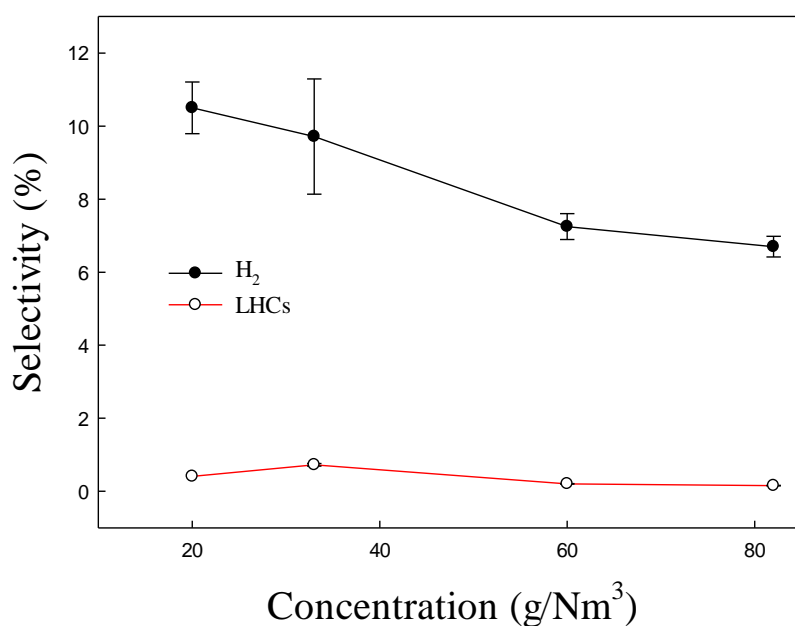


**Figure 6.5. Effect of concentration on the selectivity of gaseous products. Reaction conditions: input power, 10 W; ambient temperature; flow rate, 40.6 ml/min; carrier gas, N<sub>2</sub>; and residence time, 4.23 s.**

In current study, the significant amount of solid residue (67-78 wt. % of the input toluene) was formed inside the discharge zone during the plasma cracking of toluene. In fact, some solid residue was swept into the downstream pipes, the yield of solid residue should be high, and implying the yield of hydrocarbons should be very low. These solids were referred to as polymeric substances, or carbonaceous deposits (Magureanu *et al.*, 2011). In previous study, it was reported that solid carbon formation occurred and constituted 85 to 90% of the toluene input (Sun *et al.*, 2017).

In another study, formation of solid particles was reported during the removal of the tar analogue in air that deposited on the catalyst, reducing its efficiency (Demidiouk *et al.*, 2003). In addition, the production of these residues can block the reactor. Therefore, it is very important to avoid the formation of unwanted solid residue. They can often be controlled by improving operating procedures. For instance, it was reported that production of solid residue could be minimized by increasing the plasma discharge volume and using additional dielectric tubes (Zhang *et al.*, 2014b).

### 6.2.3 Effect of temperature

Fig. 6.6(a) presents the effect of temperature on the conversion of toluene and energy efficiency. It can be seen from fig. 6.6 (a) that the conversion and efficiency are not affected when increasing the temperature from 20 °C to 300 °C . This was partially because nearly complete removal of tar took place at 40 W .However, the decomposition of toluene started to decrease after 300 °C and reduced to 87 % at 400 °C. It has been reported that the decomposition of toluene decreases due to decrease in quartz electric insulativity which affected the plasma characteristics and formation, and reduced the intensity of the discharge (Liu *et al.*, 2018). Similarly, the decrease in conversion of toluene was observed in CO<sub>2</sub> carrier gas at elevated temperatures (see 4.2.4). On the contrary, the decomposition of toluene did not decrease at elevated temperatures in H<sub>2</sub> carrier gas and solid formation completely disappeared due to conversion into lower hydrocarbons. Therefore, the decrease in the conversion of toluene in other carrier gases may be possible due to presence of solid residue/soot which influences the plasma properties.

The elevated temperature had a significant influence on the chemistry of the products. Fig. 6.6(b) presents the effect of temperature towards the selectivity of lower hydrocarbons at different H<sub>2</sub> concentrations and it shows that selectivity to lower hydrocarbons increased from 5.5% to 10% in the pure N<sub>2</sub>.

The different concentrations (15-35%) of hydrogen were added to eliminate the problematic solid formation. It can be seen that selectivity of LHC increases from 14.5% to 45% using 15% hydrogen at 400 °C, and it reaches 57 % by increasing the hydrogen concentration to 35%. At high temperatures, hydrocracking of aromatics is responsible for the increase in selectivity of lower hydrocarbons (Castaño *et al.*, 2008). In the presence of hydrogen, hydrogenation and isomerization reactions occur at lower temperatures at the lower activation energies, whereas cracking requires high temperatures (Arribas and Martinez, 2002).The following reactions take place at elevated temperature in the presence of hydrogen.

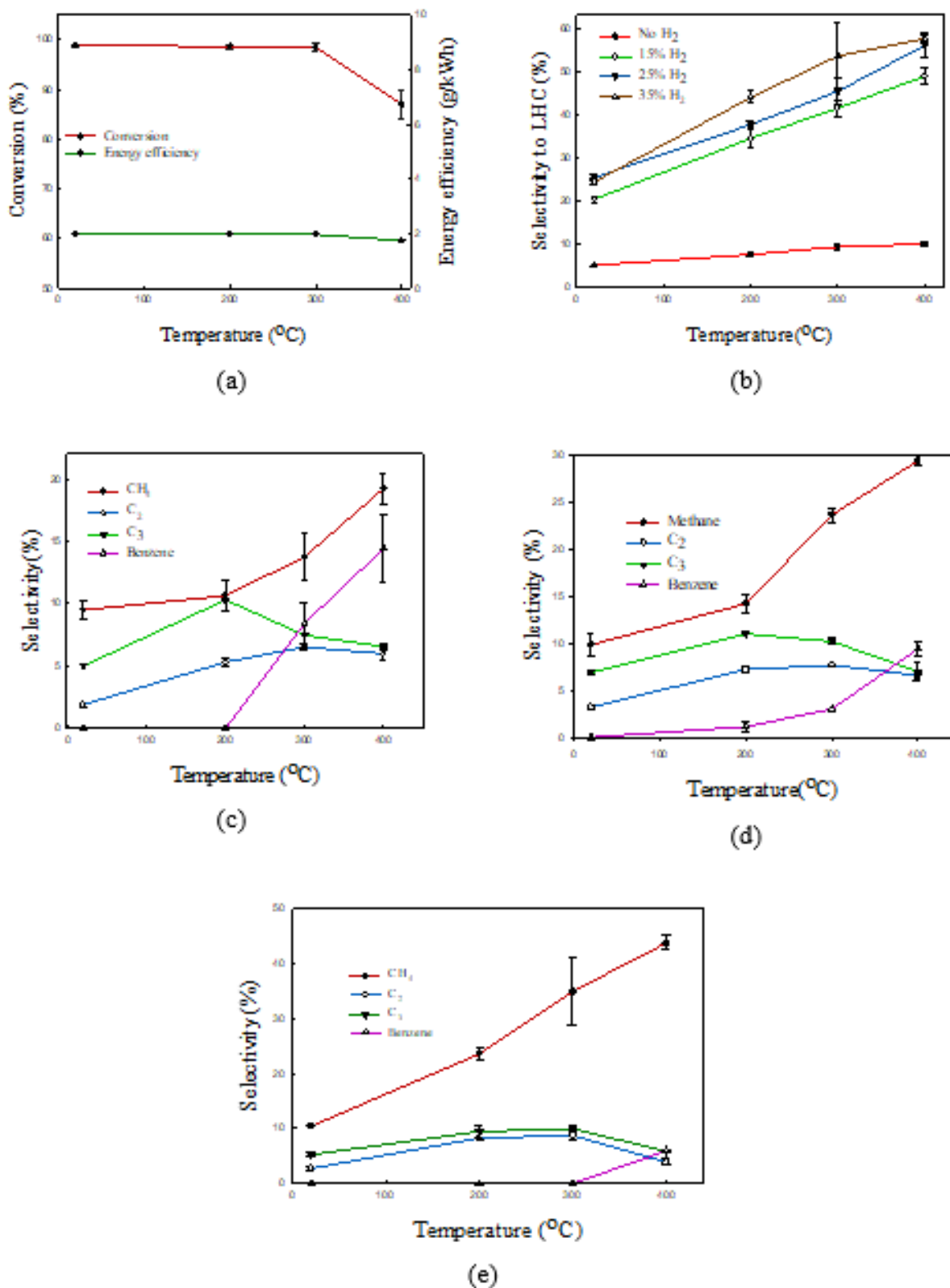
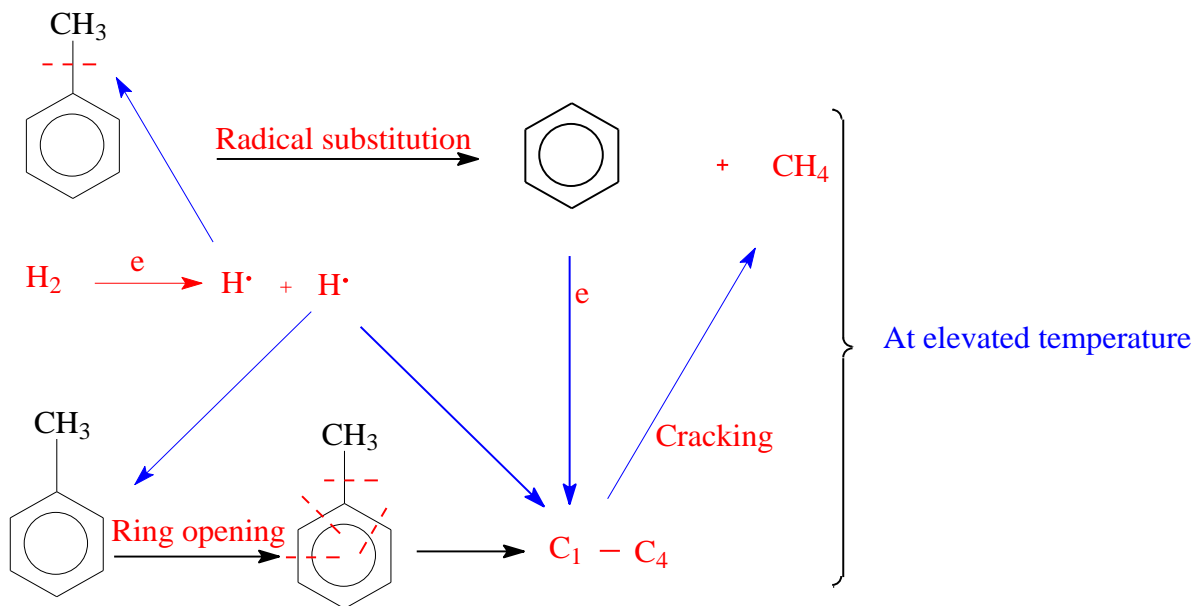


Figure 6.6. Effect of temperature on (a) the conversion of toluene, (b) total selectivity to LHCs formation (C<sub>1</sub>-C<sub>6</sub>), (c) selectivity to individual LHCs, 15% H<sub>2</sub>, (d) selectivity to individual LHCs, 25% H<sub>2</sub>, and (e) selectivity to individual LHCs, 35% H<sub>2</sub>. Reaction conditions: input power, 40 W; and concentration, 33g/Nm<sup>3</sup>; and residence time, 4.23 s; and SIE, 14.77-59.11 kJ/L.

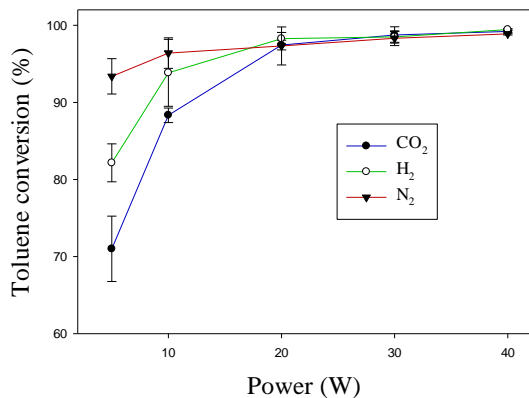


**Figure 6.7 Reaction mechanism at high temperature**

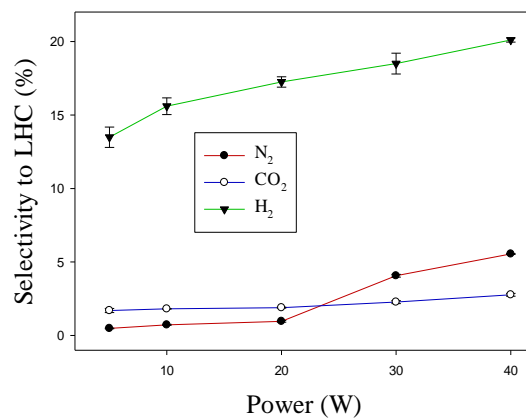
Fig. 6.6(c) presents the selectivity of individual lower hydrocarbons. It can be seen that the selectivity of methane gradually increases from 10% to 20% with increasing the temperature from ambient to 400°C. The selectivity to  $C_2$ - $C_3$  decreased at higher temperatures due to cracking to  $CH_4$ . The production of methane increased due to cleavage of aromatic and aliphatic compounds in the presence of plasma at elevated temperatures (see 5.2.4). However, the formation of benzene occurred at high temperature and its selectivity reached 14 % at 400°C. This was because radical exchange reactions took place at high temperature in the presence of hydrogen (Arribas and Martinez, 2002). Fig. 6.6(e) shows that selectivity to methane increased to 44 % by raising the  $H_2$  concentration to 35% at elevated temperature (400 °C). This occurred due to plasma assisted hydrocracking conversion of hydrocarbons in the presence of excess  $H_2$  at elevated temperatures (see 5.2.4).

### 6.3 Comparative decomposition of toluene in different carrier gases

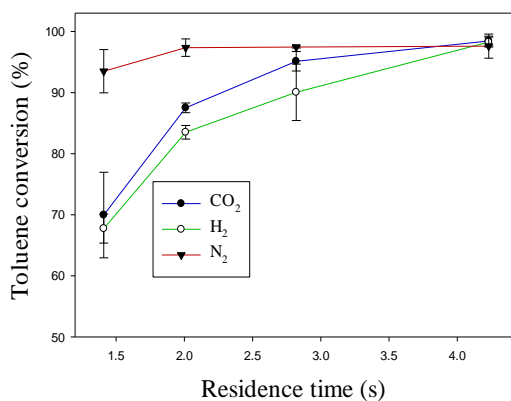
Figure 6.8 compares the effect of different parameters on the conversion of toluene and selectivity to lower hydrocarbons in individual carrier gases. It shows that the conversion of toluene increases in the following order,  $CO_2 < H_2 < N_2$ . The maximum conversion was obtained in  $N_2$  carrier gas. It was noted that the decomposition of toluene in  $N_2$  occurred due to energetic electrons and excited molecular states of nitrogen, ( $N_2 (A^3\Sigma_u^+)$ ,  $N_2 (B^3\Pi_g)$  and  $N_2 (C^3\Pi_u)$ ) (Zhang *et al.*, 2014a; Zhu *et al.*, 2016). It was reported that reactions of  $N_2 (A^3\Sigma_u^+)$  (metastable nitrogen) with tar molecules played an important role for decomposition of tar molecules (Bityurin *et al.*, 2009).



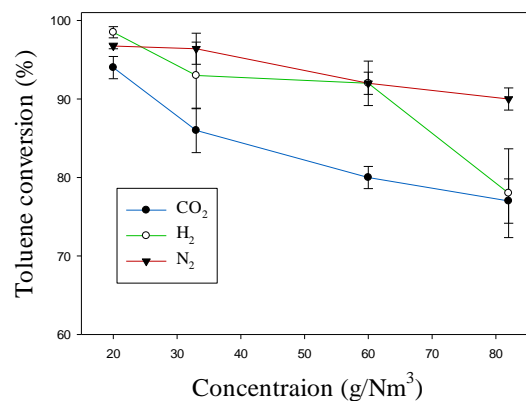
(a)



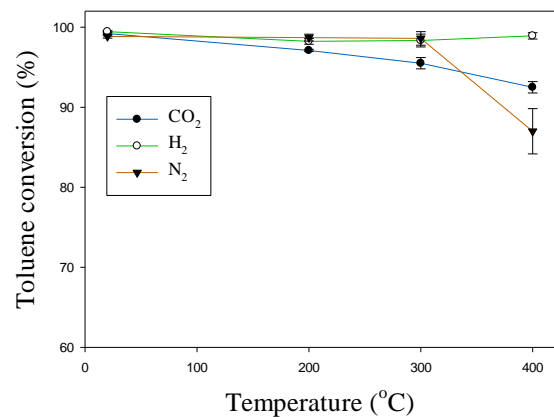
(b)



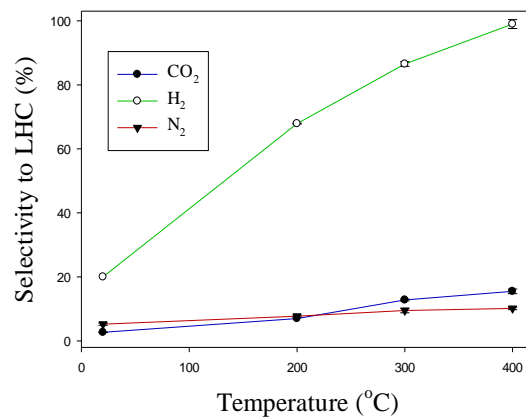
(c)



(d)



(e)



(f)

**Figure 6.8.** Effect of (a) power on the conversion of toluene, (b) power on the total selectivity to LHC; (c) RT on the toluene conversion, (d) concentration on toluene conversion, (e) temperature on toluene conversion, and (f) temperature on the selectivity to LHCs at 40 W. Reaction conditions: concentration, 33 g/Nm<sup>3</sup>.

It was further revealed that the decomposition of naphthalene initiated with nitrogen excited states, whereas the effect of energetic electrons was not significant (Yu *et al.*, 2009a; Yu *et al.*, 2010; Abdelaziz *et al.*, 2013). Therefore, all other carrier gases gave lower conversion than N<sub>2</sub> carrier gas.

The voltage required to initiate the plasma discharge is known as breakdown voltage. It has been reported that number of electrons increases per unit discharge length at a lower value of breakdown voltage (Fridman, 2008). Hence, electron energy distribution function may vary with changing the carrier gas, because each gas has different breakdown voltage. It was reported that the minimum breakdown voltage for N<sub>2</sub> and H<sub>2</sub> was 251 and 273 respectively (Chen, 2016). Therefore, N<sub>2</sub> gave maximum conversion than H<sub>2</sub> and CO<sub>2</sub>. The value of minimum breakdown voltage for CO<sub>2</sub> was 420 (Chen, 2016), due to this reason CO<sub>2</sub> shows less conversion among all carrier gases.

It can be seen (Fig. 6.8 b) that the selectivity of LHC is maximum in hydrogen carrier gas and it increases with increasing power. It was reported that thermal cracking of toluene produced methane and benzene in H<sub>2</sub> carrier gas at 750 °C (Burr *et al.*, 1964). It was suggested that hydrogen reacted with benzyl, methyl and phenyl radicals and acted as a scavenger for these radicals. However, in current study, reactive species produce H radicals at ambient conditions, which react with intermediates to produce lower hydrocarbons. The formation of reactive species also increases with increasing power. For N<sub>2</sub> and CO<sub>2</sub> carrier gases, the selectivity to lighter hydrocarbons does not increase above 6 % due to polymerisation of the fragments of toluene. It can be observed that significant amount of carbon is missing in all carrier gases. It is possible due to substantial amount of solid residues formation in all carrier gases. The colour of the solid residues was black in N<sub>2</sub> carrier gas, light yellow in hydrogen carrier gas, brown in CO, and black and brown in CO<sub>2</sub>. The destruction of toluene was investigated in non-oxidative atmosphere, which ultimately enhanced the deposition of solid carbon (Zhu *et al.*, 2016).

It can be observed (Fig. 6.8 e) that conversion of toluene decreases in CO<sub>2</sub> and N<sub>2</sub> carrier gases when increasing temperature up to 400 °C. It was reported that conversion of toluene decrease because local thermal runaway of quartz tube take place and impurities present in the quartz become moveable at high temperature, which ultimately reduce the electric insulativity of quartz. This phenomena affects the formation of plasma and characteristics, and reduces the intensity of discharge (Liu *et al.*, 2018). High temperature can also affect the breakdown voltage.

The Paschen's law tells that the breakdown voltage of a gas changes (non-linear) with respect to product of pressure and discharge gap. The higher temperature affects the pressure and density of gases which ultimately influences the breakdown voltage. However, in current study, conversion is not affected by temperature in H<sub>2</sub> carrier gas. Therefore, it may be possible due to presence of solid residues which affect the discharge properties.

Fig. 10.1(f) shows that with increasing temperature the selectivity to lower hydrocarbons increases. For CO<sub>2</sub>, and N<sub>2</sub> it remains below 18%, but in H<sub>2</sub> carrier gas selectivity to LHC reaches to nearly 100%. At high temperature, movement of excited species and free radicals and their collisions frequency are accelerated, which increases selectivity to lower hydrocarbons. H<sub>2</sub> carrier gas showed nearly complete conversion of toluene to lower hydrocarbons. From a stoichiometric point of view, the formation of lower hydrocarbons from toluene is likely due to hydrogen consumption. Exceptions would be the formation of hydrocarbons such as acetylene, cyclopropene, propyne, propadiene etc. which formation process is very energy consuming or less likely. However the formation of simple alkanes as methane, ethane, propane, butane etc. is a hydrogen consuming process. Therefore, nearly complete conversion of toluene to C<sub>1</sub>-C<sub>5</sub> was observed at elevated temperature due to presence of H radicals in H<sub>2</sub> carrier gas.

## 6.4 Conclusions

In this study a DBD reactor was used to decompose a biomass gasification tar analogue (toluene). The performance of the reactor was studied as a function of process conditions: power (5-40 W), residence time (1.43-4.23 s), concentration (20-82 g/Nm<sup>3</sup>), and temperature (ambient-400 °C).

The key findings from the experimental results can be summarized as follows:

1. Almost complete removal of tar was achieved, at 20 W and 4.23 s. The main products were hydrogen, lower hydrocarbons and solid residue.
2. The decomposition efficiency of toluene depends upon power, residence time and concentration. It increases with power and residence time. The maximum conversion here was obtained at 40 W and 4.23 s (the highest level used). The conversion decreased slightly with increasing toluene concentration.
3. At ambient conditions, the selectivity to lower hydrocarbons remained below 6%. However, it increased to 10% by increasing the temperature to 400°C.

4. Solid deposition took place inside the reactor. This is generally an undesirable effect, but it can be substantially reduced by introducing H<sub>2</sub>.
5. At elevated temperatures in the presence of H<sub>2</sub>, the selectivity to lower hydrocarbons increased with increasing hydrogen concentration. It reached 57 % at a concentration of 35% of H<sub>2</sub> at 400 °C. The main product in these conditions was CH<sub>4</sub>, formed from decomposition of the aromatic ring. Its proportion increased with increasing temperature and power to as high as 44 %.

The addition of H<sub>2</sub> has been demonstrated to significantly reduce solid residue formation at elevated temperatures, which would allow longer operation and reduced maintenance of gasifiers, if this result could be extrapolated to “real world” systems. H<sub>2</sub> is present in significant amounts in real fuel product gas streams. Therefore, the installation of a DBD reactor at a suitable location after the gasifier exit, where the temperature was high enough, could substantially reduce tar formation.

## **Chapter 7. Plasma-assisted decomposition of toluene in a mixture of gases**

### **7.1 Introduction**

In previous chapters (4-6), the performance of a DBD reactor was investigated in individual carrier gases. It has been observed that nearly complete removal of toluene is possible in each carrier gas. However, the product selectivity was strongly dependent on nature of gas. In all carrier gases, significant amount of solid residues formation occurred at ambient temperature. At elevated temperature, these residues successfully converted to lower hydrocarbons in H<sub>2</sub> carrier gas. The major products were methane and benzene. However, these solid residues did not disappear in N<sub>2</sub> and CO<sub>2</sub> carrier gases even at elevated temperature. These residues create significant operational problems. These gases present in significant amount in actual product gas from gasifier. Therefore, it is very important to investigate the performance of DBD reactor in the mixture of carrier gases

The typical composition of product gas from gasifier depends upon gasifying medium (air, steam, and oxygen). The N<sub>2</sub> presents as major component if air is used as a gasifying agent, whereas H<sub>2</sub> constitutes high percentage in product gas in case of steam gasifying agent. In steam gasification, the gasifier product gas is a mixture of CO<sub>2</sub>, H<sub>2</sub>, CO, and various by-products (Luo *et al.*, 2009).

Hence, in this work, the performance of a DBD was investigated for cracking toluene in synthetic fuel gas (CO<sub>2</sub>: 30%; CO: 20 %; H<sub>2</sub>: 50%). The variables investigated were power, temperature, residence time and concentration. The length of the external electrode was 30 mm in this experiment.

### **7.2 Results and discussion**

#### ***7.2.1 Effect of Power***

Figure 7.1(a) clearly demonstrates that toluene removal increases with the power input to the DBD. This behaviour was expected: as power increases, the number of higher energy electrons increases, which increases the rate of activation of the reactant molecules by formation of free radicals and ions.

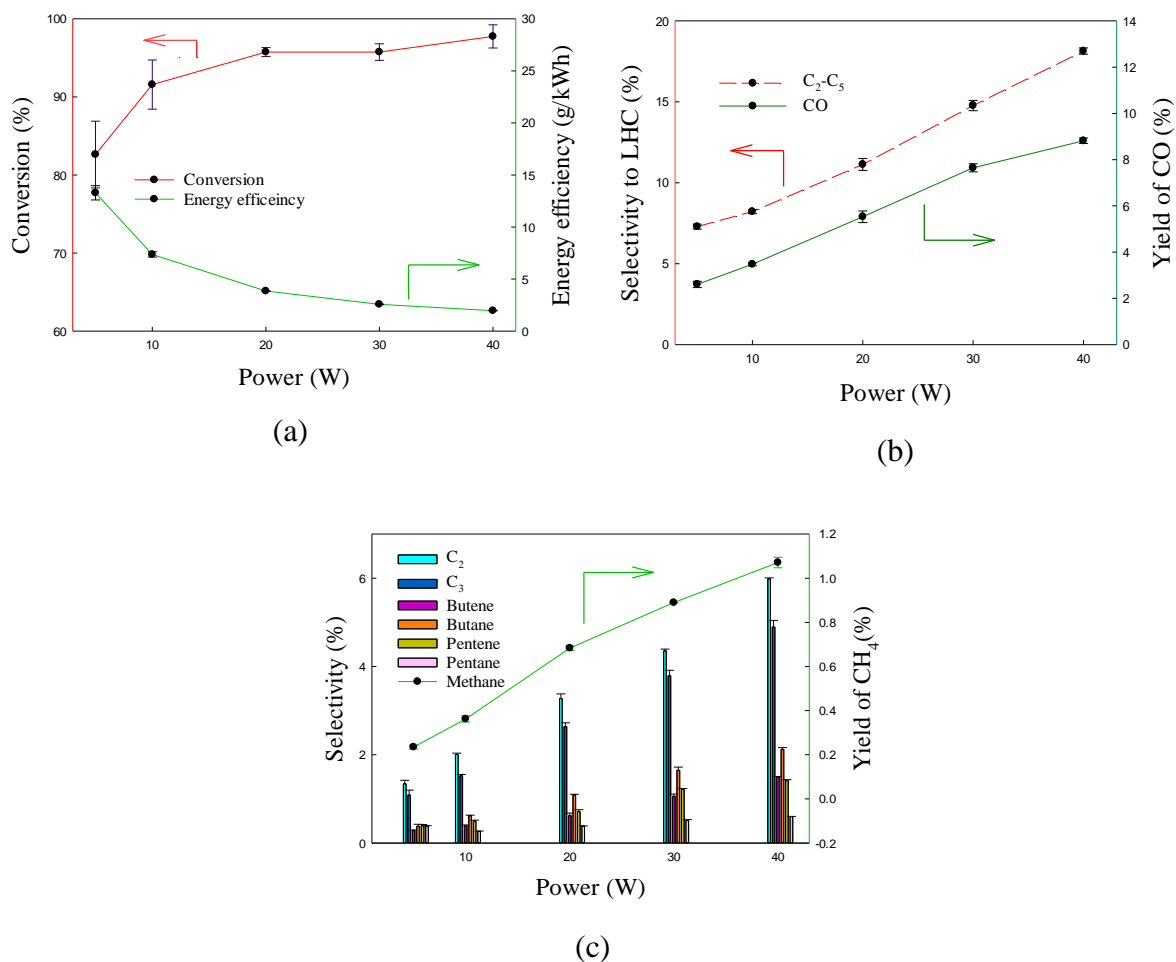


**Figure 7.1. Effect of plasma power on (a) the conversion and energy efficiency of toluene, (b) the selectivity and yield of different gaseous products, and (c) individual lower hydrocarbons.**

**Reaction conditions: Concentration, 33g/Nm<sup>3</sup>; residence time, 2.82 s; flow rate, 40.6 ml/min; SIE, 2.05-16.4 kWh/m<sup>3</sup>; and Temperature, ambient.**

The effect of power on the energy efficiency of the system is also shown in Fig. 7.1(a). The energy efficiency decreases with increasing power, from 13 g/kWh to 1.9 g/kWh as the power is increased from 5 to 40 W. Essentially, this is due to “diminishing returns” as the conversion approaches 100%. Similar trends have been reported for the removal of tar analogues (Chun *et al.*, 2013). It was observed that at 10 W more than 93% of the tar analogue is decomposed.

Fig. 7.1(b) shows that the yield of CO gradually increases from 2.6% to 8.8% as the power increases from 5 to 40 W, and the selectivity to C<sub>2</sub>-C<sub>6</sub> increases from 7.3 to 18%. It can be observed from Fig. 7.1(c) that the selectivity and yield of lower hydrocarbons increased with power. At lower powers, the average electron energy is not high enough to crack aromatic C-C bonds, hence a greater proportion of lower hydrocarbons is observed at higher powers. In addition, in this case it is clear that the formation of active species, such as radicals, ions, and

excited molecules can also increase selectivity to CO and LHCs. It has previously reported that dissociation by electron impact played a significant role in the decomposition of aromatic compounds (Kohno *et al.*, 1998; Urashima and Chang, 2000; Lee and Chang, 2003).

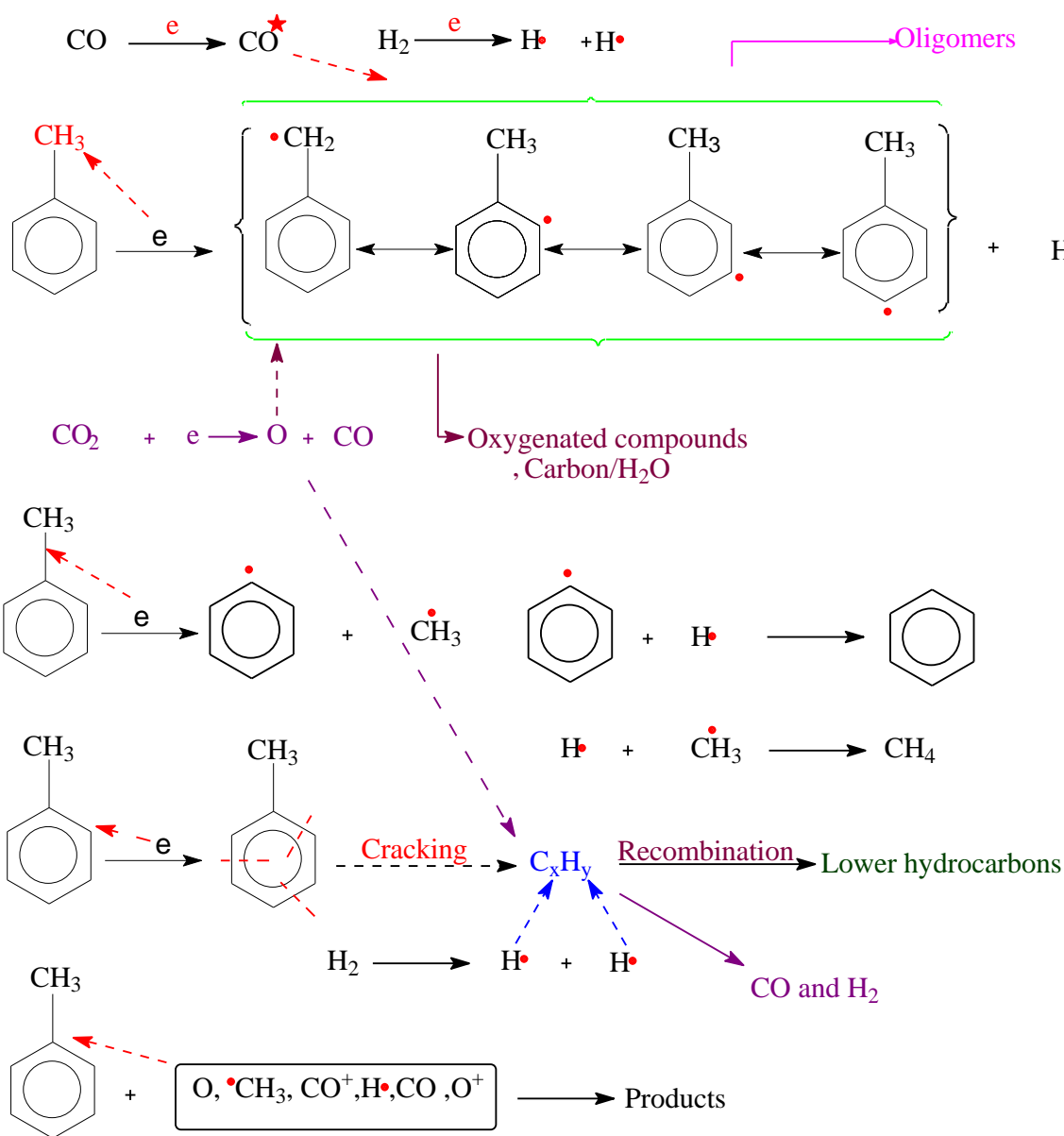


**Figure 7.2 Reaction mechanism**

It was reported that the bond dissociation energy of different bonds in toluene decreases in the following order: C=C and C-C in aromatic ring > C-H in aromatic ring (4.5 eV) > C-C between methyl and aromatic ring (4.4 eV) > C-H bond in methyl group (3.7 eV) (Darwent, 1970; Kohno *et al.*, 1998; Urashima and Chang, 2000). For this reason, decomposition of toluene could begin with abstraction of an H-atom from the methyl group, as the bond dissociation energies of these C-H bonds are the lowest (Huang *et al.*, 2011), via electron

impact, excited species or radicals and the reaction scheme is shown in Fig. 7.2. The abstraction of H atom produces H radicals and benzyl radicals. The aromatic ring containing intermediate compounds can self-polymerise. The reactive species can separate the methyl group from toluene to produce benzene and methyl radicals. These radicals can react with H radicals to produce methane. Meanwhile ring opening products (C<sub>1</sub>-C<sub>5</sub>) form due to impact of high energy electrons which directly start the cleavage of the aromatic ring

### 7.2.2 Effect of residence time

The effect of residence time is also clear (Fig. 7.3(a)) since decomposition increases with the residence time, as would be expected. Understanding the combined effects of these 2 variables (residence time and power) is part of the development of a design protocol for plasma reactors for this application, based on the relative costs of increasing residence time (thereby increasing the size of the reactor and therefore capital cost for a given duty) and increasing power (thereby increasing operating cost). As evident in Fig. 7.3(a), with increasing residence time, the conversion of toluene increased from 76% to 96% at 20 W, as the number of opportunities for collision between active species, energetic electrons and toluene's molecules increased (Chun *et al.*, 2013) However, the energy efficiency decreases with increasing residence time. To increase the residence time the flow rate needs to be reduced, which also decreases the flow rate of toluene. Therefore, the energy efficiency is reduced at high residence time due to a decrease in the total amount of decomposed toluene. These results are consistent with a previous experimental study in which decomposition of toluene was investigated in a DBD reactor (see 4.2.3). The selectivity and yield of different gaseous products are shown in fig. 7.3 (b) and (c). The yield of CO increases from 1.9 % to 5.7 %, and selectivity of C<sub>2</sub>-C<sub>5</sub> increases from 3 to 11% with the increasing residence time. Similarly, Fig. 7.3(c) shows that the yield of methane gas and selectivity of C<sub>2</sub>-C<sub>5</sub> also increase with residence time. This is possibly due to the cleavage of the aromatic ring due to high number of collisions between tar analogue and reactive species, or second phase reactions.

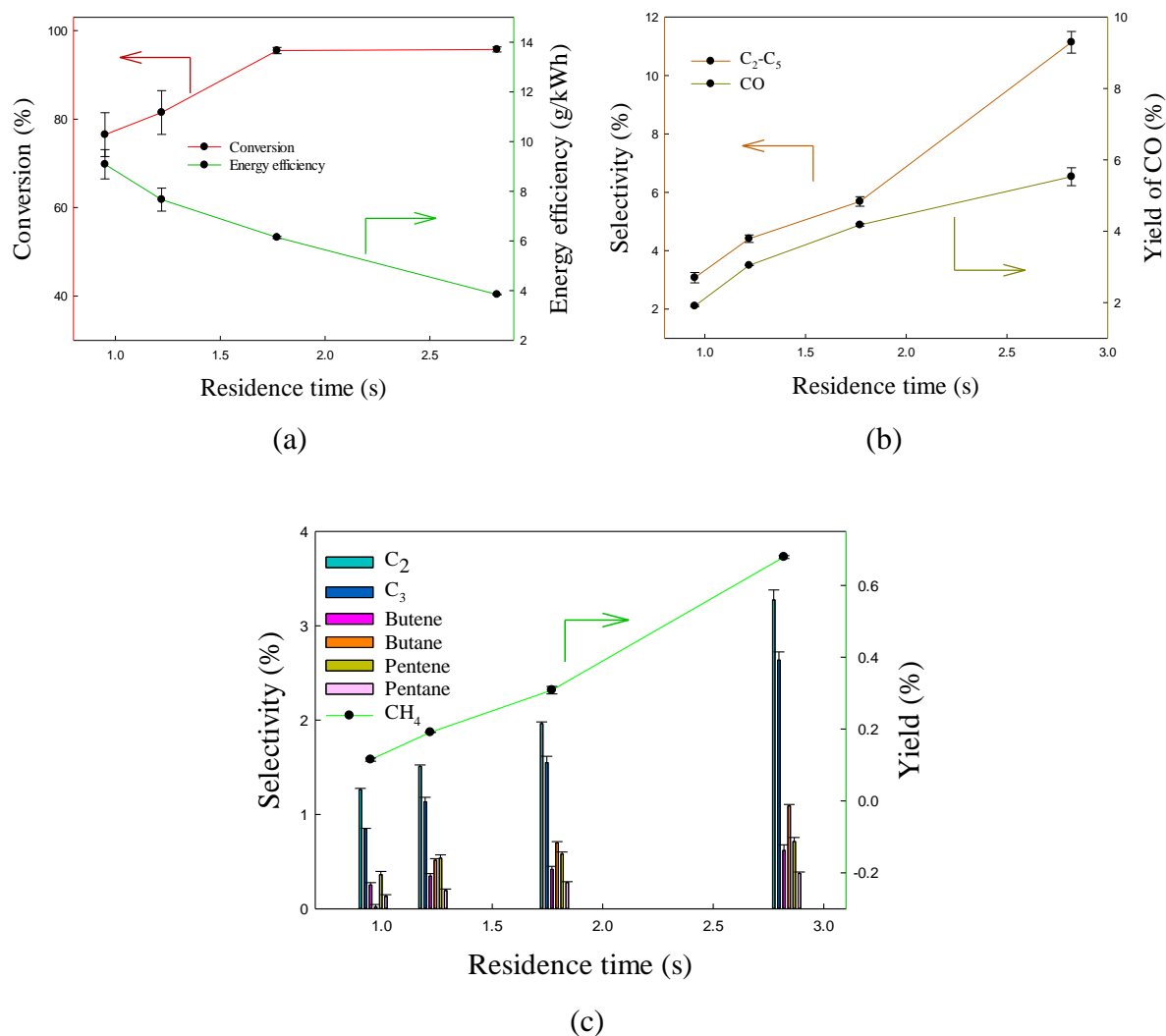


**Figure 7.3. Effect of residence time (a) on the conversion and energy efficiency of toluene, (b) on the selectivity and yield of different gaseous products, and (c) on individual lower hydrocarbons. Reaction conditions: concentration, 33g/Nm<sup>3</sup>; Power, 20 W; flow rate, 40.6-120 ml/min; and Temperature, ambient.**

### 7.2.3 Effect of concentration

The concentration of toluene was varied from 20 to 82 g/Nm<sup>3</sup>. Fig. 7.4(a) shows the effect of concentration on the conversion and energy efficiency. It can be observed that the conversion of toluene decreased with increasing toluene concentration. The maximum conversion was obtained at 20 g/Nm<sup>3</sup> (95.5%), then decreased monotonically when increasing the concentration up to 82 g/Nm<sup>3</sup> (68%). At constant power, the plasma-generated reactive species react with the toluene to decompose it. However, when the concentration is increased whilst keeping the others parameters constant, the relative amount of toluene molecules increases with respect to reactive species and the conversion is reduced. However, the energy

efficiency of the process increased with increasing concentration, as the number of molecules of toluene converted increased. Here, the value increased from 4.6 g/kWh to 13.5 g/kWh over the range studied here. The similar effect of concentration has been reported previously in gliding arc discharge (Zhu *et al.*, 2016). Fig.7.4, (b) and (c) shows the changes in selectivity and yield of gaseous products with respect to concentration. The yields of CO, LHC (C<sub>2</sub>-C<sub>6</sub>) and CH<sub>4</sub> decrease with increasing concentration.

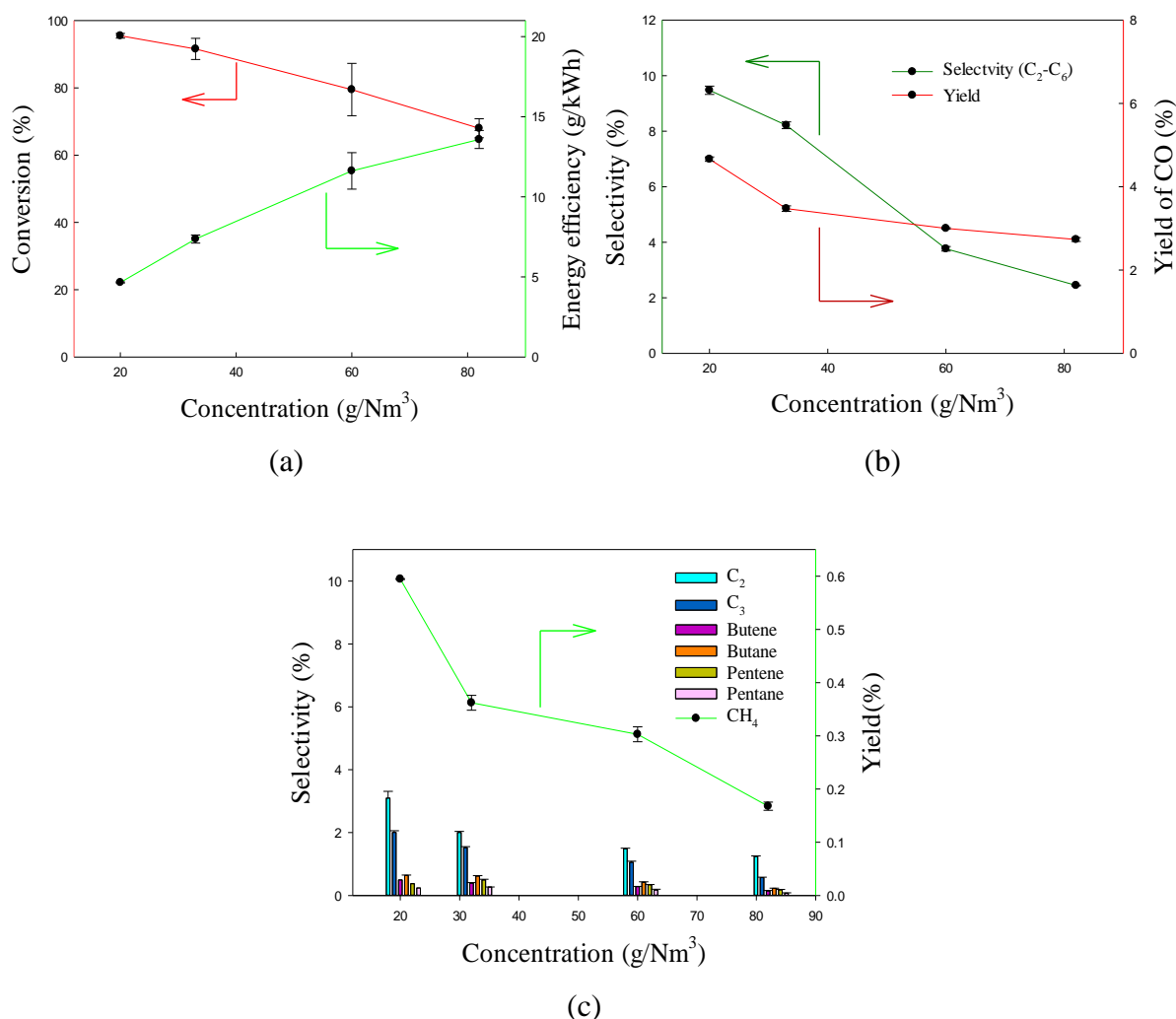


**Figure 7.4. Effect of concentration (a) on the conversion and energy efficiency of toluene, (b) on the selectivity and yield of different gaseous products, and (c) on individual lower hydrocarbons. Reaction conditions: residence time, 2.82 s; power, 10 W; flow rate, 40.6 ml/min; and temperature, ambient.**

This behaviour is consistent with previous experimental results in which the effect of concentration has been studied on the removal of tar analogue (Liu *et al.*, 2017a). It was also observed that solid residue was produced in the discharge zone during the cracking of tar analogue at ambient temperature. Yellowish deposits have been previously reported when

operating in limited oxygen (Guo *et al.*, 2006). Here, in an attempt to mitigate this effect, the synergetic effect of temperature and plasma was studied to avoid the formation of hazardous solid residue (see 7.2.4).

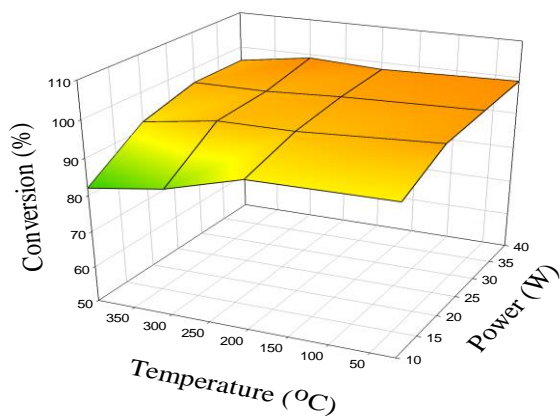
#### 7.2.4 *Effect of temperature*

The performance of DBD reactors was studied at elevated temperatures. The effect of temperature and power on the conversion of toluene is shown in Fig. 7.5(a). It can be noted that the decomposition of toluene does not change when increasing the temperature over the power range 20 to 40 W.

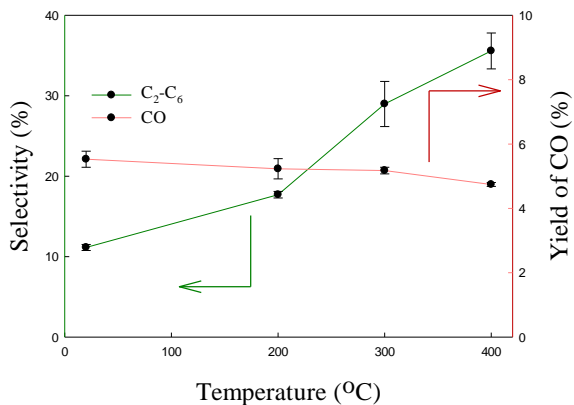
However, at 10 W, it varied from 82% to 91%. It may be decreased due to formation of solid deposits in the plasma zone. This is also possible due to the radical termination reaction of CO and O to form CO<sub>2</sub> (Cenian *et al.*, 1995).

It was reported that the decomposition of toluene in CO<sub>2</sub> carrier gas decreased with increasing temperature in DBD reactor (see 4.2.4). However, toluene conversion is not significantly affected by increasing the temperature at higher powers (20-40 W). This is because the reaction is mainly a function of the number of energetic electrons and excited species generated by the plasma. The influence of elevated temperature on the selectivity and yield of products is shown in Fig. 7.5(b) at 20 W. It shows that the selectivity to lower hydrocarbons (C<sub>2</sub>-C<sub>6</sub>) increased with increasing temperature up to 400 °C at 20 W. This is possibly due to hydrocracking of toluene into lower hydrocarbons (C<sub>1</sub>-C<sub>6</sub>) becoming significant at elevated temperatures (Amano *et al.*, 1965; Amano *et al.*, 1972). However, the yield of CO slightly decreases with increasing temperature, probably because of the recombination reactions of CO and O radicals. Hydrocracking of toluene could occur through three different routes: (a) isomerization, (b) hydrogenation-dehydrogenation, and (c) cracking reactions (Arribas and Martinez, 2002). The first two types of reactions can occur at lower temperatures because of their low activation energy, while cracking reactions of aromatics require higher temperatures (Castaño *et al.*, 2008). These cracking reaction can take place through primary (ring opening) secondary and tertiary cracking (Arribas and Martinez, 2002).

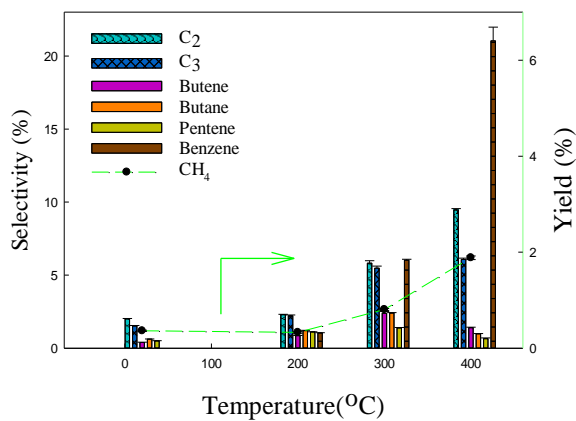
Fig. 7.5(c) shows the effect of temperature on the selectivity to lower hydrocarbons (C<sub>2</sub>-C<sub>6</sub>) and the yield of methane at 10 W. It can be observed that the selectivity of each individual lower hydrocarbons increases with increasing the temperature. The selectivities to C<sub>2</sub> and benzene reach 9.5 and 21.7 % at 400°C, respectively. However, the selectivity to C<sub>2+</sub> alkanes and alkenes remains below 10%.



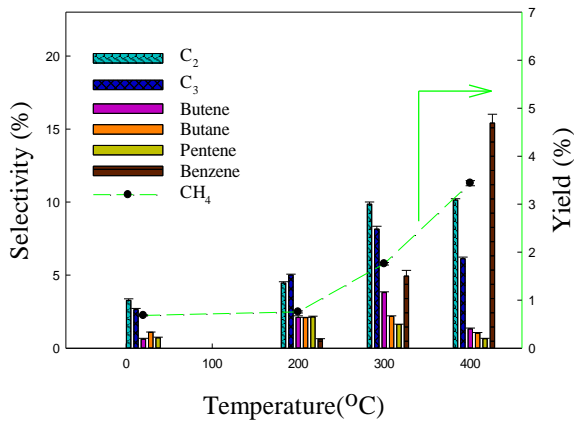
(a)



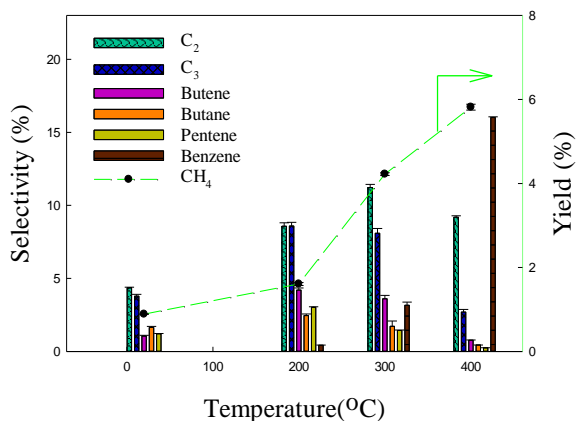
(b)



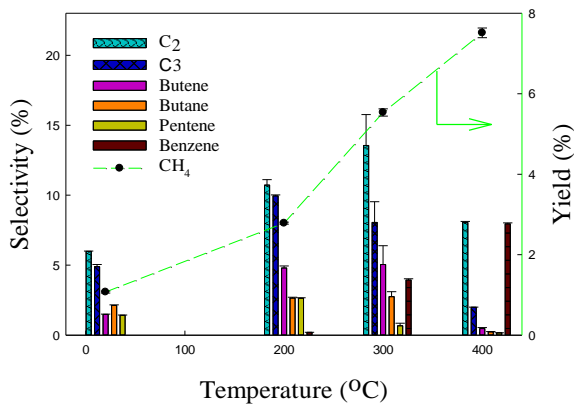
(c)



(d)



(e)



(f)

**Figure 7.5.** Effect of temperature on (a) the conversion of toluene, (b) total selectivity and yield of LHC and CO at 20 W; selectivity and yield of different LHC at (c) 10 W, (d) 20 W, (e) 30 W, and (f) 40 W. Reaction conditions: concentration, 33 g/Nm<sup>3</sup>; residence time, 2.82 s; flow rate, 40.6 ml/min.

The yield and selectivity of lower hydrocarbons increases with temperature because of cracking reactions at high temperatures, while for benzene this occurs via radical substitution reactions (Amano *et al.*, 1972). It has previously been reported that the production of methane and aromatics increases with increasing the temperature in the presence of H radicals (Amano *et al.*, 1972; Castaño *et al.*, 2008).

The effect of power on yield and selectivity of lower hydrocarbons at elevated temperature can be observed from Fig. 7.5(c to f). Clearly, the yield of methane increases with increasing power, whereas the selectivity to benzene exhibits a clear decrease due to impact of reactive species. The yield of methane increases from 1.04% to 7.5% with increasing the temperature at 40 W. This is because the presence of H radicals at elevated temperature promotes the formation of methane (Freel and Galwey, 1968). In addition, at high power, the fragmentation of the benzene ring because of energetic electron and excited species increase the yield of methane as well.

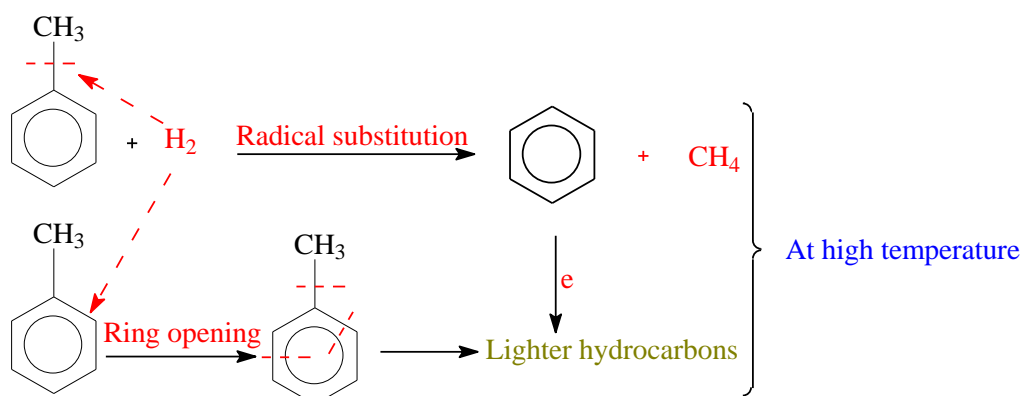


**Figure 7.6 Reaction mechanism at elevated temperature**

The selectivity to benzene decreases to 8% at 40 W. This occurs because the electrons produced at 40 W are energetic enough to decompose the aromatic carbon-carbon bonds. It was reported that the formation of methane increases to 10% when increasing the temperature up to 450 °C in the presence of a catalyst (Castaño *et al.*, 2008).

The effect of temperature on the production of C<sub>2</sub>-C<sub>5</sub> species at 40 W can be observed in Fig 7.5(f). The selectivity to C<sub>2</sub> hydrocarbons increases with increasing temperature up to 300 °C and after that decreases at 400°C, while for >C<sub>3</sub> it started to decrease at 200 °C. This was due to hydrocracking of these hydrocarbons into methane. It has previously been reported that cracking of C<sub>2</sub> to C<sub>4</sub> increased with increasing temperature and converted to methane (Freel and Galwey, 1968). It has been observed that cracking of ethane increases with increasing

temperature from 260 to 322 °C producing methane, while cracking of C<sub>3</sub> increased even at lower temperature range (206-240 °C) and produced methane (Freel and Galwey, 1968).

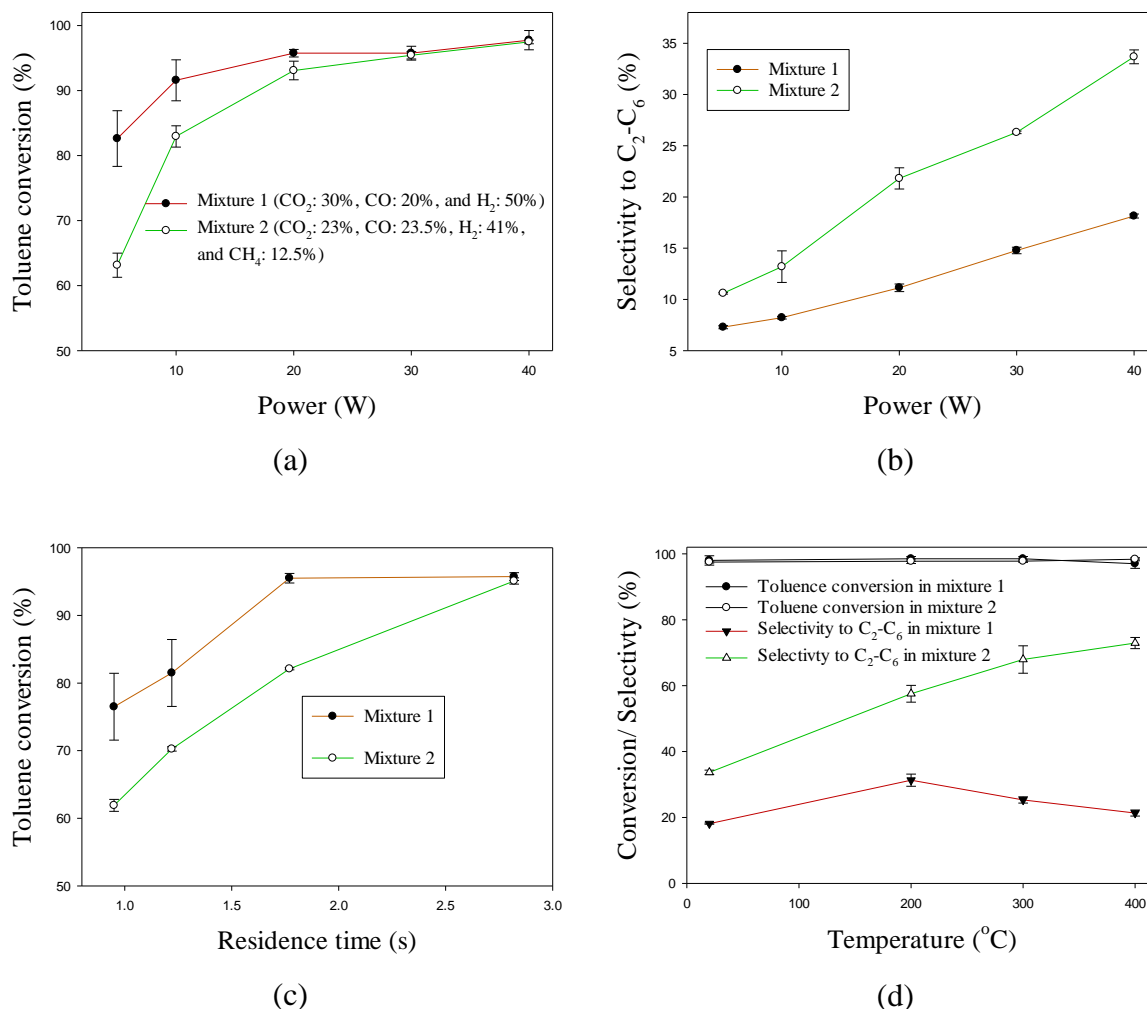


**Figure 7.7.** Effect of (a) power on the conversion of toluene (b) power on the total selectivity to C<sub>2</sub>-C<sub>5</sub>, (c) residence time on the conversion of toluene at 20 W, and (d) temperature on the conversion and selectivity at 40 W. Reaction conditions: concentration of toluene, 33 g/Nm<sup>3</sup>

Fig. 7.7 compares the conversion of toluene in two different mixture of gases. Mixture 2 shows lower conversion due to presence of CH<sub>4</sub>, which produces CH<sub>3</sub> radicals. These radicals terminate H radicals due to combination reactions of CH<sub>3</sub> and H radicals. However, mixture 2 shows higher selectivity to C<sub>2</sub>-C<sub>6</sub> than mixture 1. The presence of CH<sub>4</sub> in carrier gas mixture promoted formation of C<sub>2</sub>-C<sub>5</sub> hydrocarbons. It was reported that electron impact with methane in non-thermal plasma produces CH<sub>3</sub>, CH<sub>2</sub> and CH radicals, which can combine to form lower hydrocarbons (Xu and Tu, 2013; Chiremba *et al.*, 2017).

### 7.3 Conclusions

In this study, decomposition of toluene as a tar surrogate was evaluated in a dielectric barrier discharge (DBD) reactor using a synthetic fuel gas mixture (H<sub>2</sub>: 50%, CO<sub>2</sub>: 30% and CO: 20%). Power (5-40 W), temperature (20-400 °C), concentration of toluene (20-82 g/Nm<sup>3</sup>) and residence time (0.95-2.82 s) were varied to investigate the performance of the DBD reactor and its selectivity towards valuable gaseous products.

The main findings were:

1. The conversion of toluene can be as high as 99% and the latter was converted to CO, lower hydrocarbons (LHC) and solid residue.
2. The conversion increases with both power and residence time.
3. At ambient temperature, solids appeared inside the reactor, which would create problems due to fouling and blockages over time. However, here we demonstrated that this problem can be eliminated by increasing the wall temperature. A further benefit of increasing the temperature was that it increased both the selectivity and yield of the lower hydrocarbons.
4. Formation of methane increased with increasing the temperature and power. The highest yield of methane in this study was 7.5%, at 400 °C and 40 W of power.

Overall, this work demonstrates that toluene can be completely converted to smaller molecules by a DBD non-thermal plasma, and that a degree of control can be established by varying power, residence time and temperature, including eliminating the problem of solid residue formation.



## Chapter 8. Decomposition of benzene as a tar analogue in CO<sub>2</sub> and H<sub>2</sub> carrier gases, using a non-thermal plasma.

### 8.1 Introduction

Various types of non-thermal plasmas have been investigated to decompose tar compounds. Jamroz *et al.* (2018) investigated the steam reforming of tar representative compound in microwave plasma. Tar compounds were converted to CO, CO<sub>2</sub> and hydrogen in the presence of steam (Jamróz *et al.*, 2018). The performance of a gliding arc discharge reactor was studied by Zhu *et al.* (2016). They reported 95% conversion of the toluene, and the major products were acetylene and hydrogen (Zhu *et al.*, 2016). In another study, the decomposition of toluene as a biomass tar representative was studied in gliding arc discharge reactor. It was reported that conversion and energy efficiency of toluene increased by adding the steam (Liu *et al.*, 2017a). In many studies, the dielectric barrier discharge (DBD) reactor was used for cleaning gases (Lee and Chang, 2003; Blin-Simiand *et al.*, 2008; Karatum and Deshusses, 2016; Wang *et al.*, 2017a). It was observed that 74 % of the toluene is converted at specific input energy of 360 J/L (Karatum and Deshusses, 2016). However, the conversion decreased with increasing flow rate and concentration (see 5.2).

In this study, a DBD reactor was used to investigate the decomposition of benzene in CO<sub>2</sub> and H<sub>2</sub> carrier gases. Benzene was selected as a model compound due to its thermal stability and it has been reported as a tar representative in many experimental studies (Simell *et al.*, 1997a; Simell *et al.*, 1999; Zhang *et al.*, 2007; Park *et al.*, 2010; Chun *et al.*, 2012; Chun and Lim, 2012; Chun *et al.*, 2013). Therefore, this study was conducted to test the performance of DBD reactor for more stable compound. Moreover, the effect of each carrier gas on the product selectivity was also studied. CO<sub>2</sub> and H<sub>2</sub> are present in significant amounts (62-75%) in product gas (He *et al.*, 2009). Therefore, for a good understanding of tar removal in NTP to clean the product gas, it was very important to study the effect of both carrier gases individually. The effect of different parameters (SIE, residence time, concentration and temperature) was also investigated to study the performance of DBD reactor.

## 8.2 Results and discussion

### 8.2.1 Effect of carrier gas and SIE

Figure 8.1(a) shows the effect of changing the specific input energy (SIE) in CO<sub>2</sub> and H<sub>2</sub>. The conversion of benzene was similar for each type of carrier gas at high SIE (above 30 kJ/L). The SIE was increased by increasing the input power (5-40 W). It has been reported that the most of the energy supplied by providing electric fields is absorbed by electrons rather than heavy species (ions, molecules and gas atoms) (Kortshagen *et al.*, 2016).

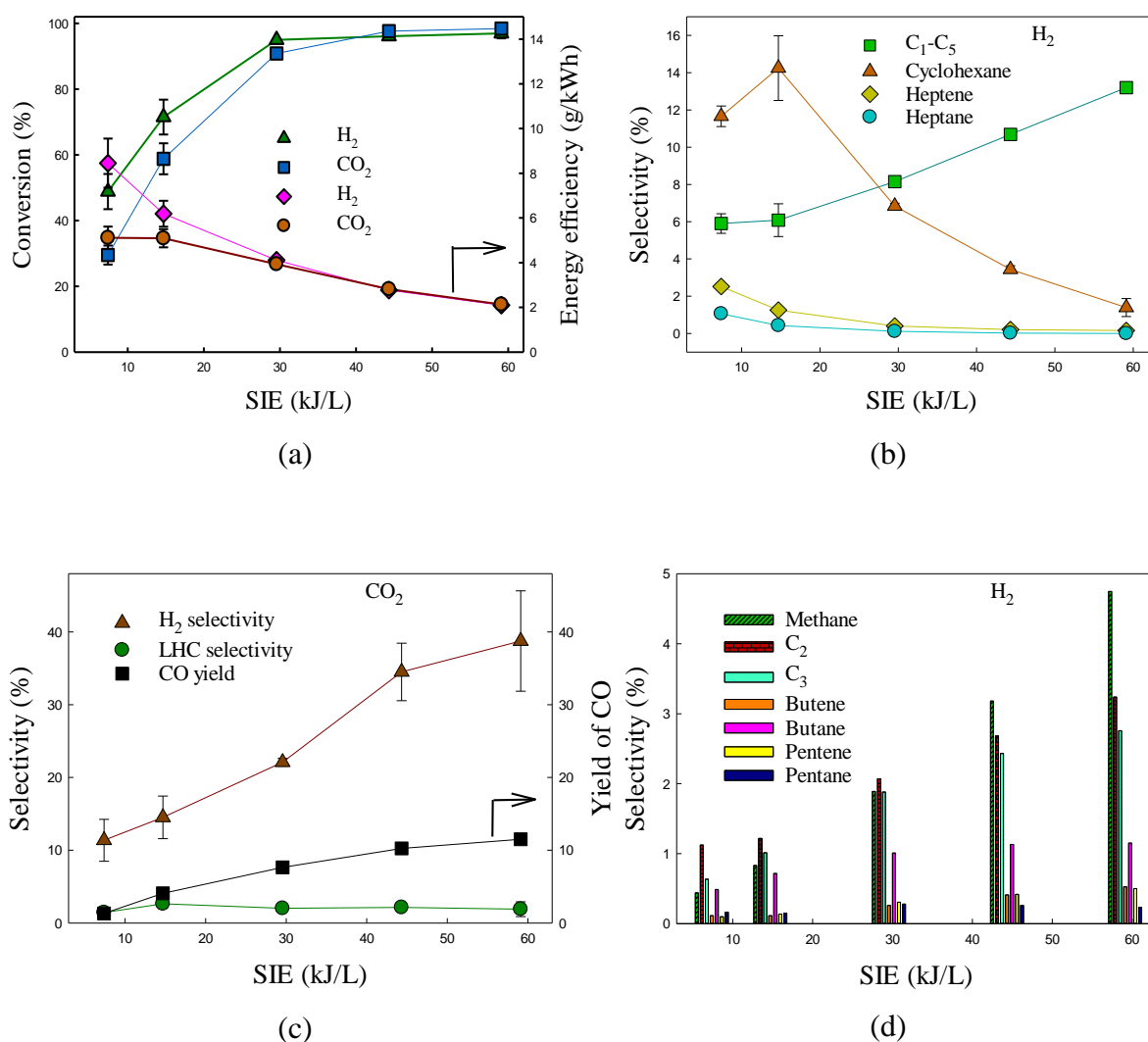


**Figure 8.1.** Effect of carrier gas and SIE on (a) the conversion and energy efficiency of benzene, (b) selectivity of products in H<sub>2</sub> carrier gas, (c) selectivity of products in CO<sub>2</sub> carrier gas, and (d) detailed selectivity to LHC. Reaction conditions: concentration, 36 g/Nm<sup>3</sup>; temperature, ambient; and residence time, 4.23 s.

At higher powers, the number of high energy electrons increases, so the probability of decomposing benzene (by electron impact) increases. Energy efficiency generally decreases with increasing SIE. Similar behaviour has been reported in previous experimental studies (see 4.2.1).

Below 35 kJ/L, the conversion in the H<sub>2</sub> carrier gas was higher than that for the CO<sub>2</sub>. This may be due to production of more reactive H radicals at lower powers, as the bond dissection energy of H<sub>2</sub> (4.53 eV) is lower than that of CO<sub>2</sub> (5.5 eV) (Darwent, 1970).



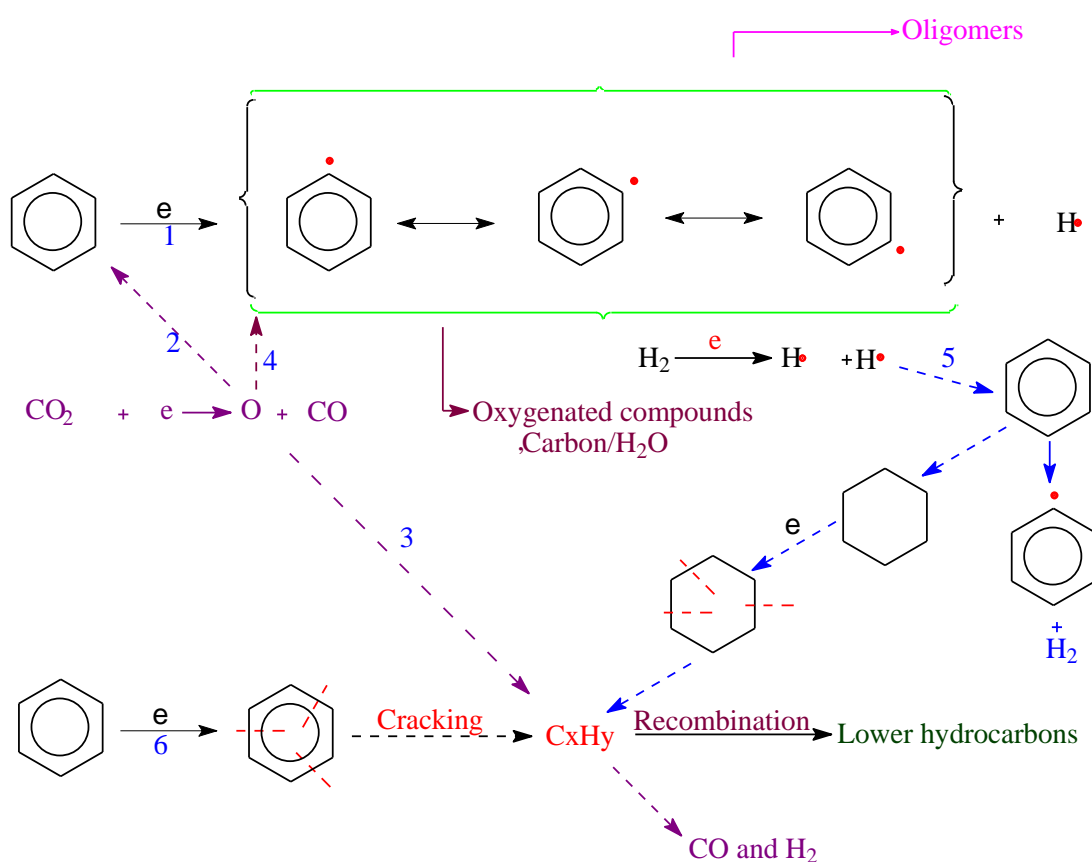
Fig. 8.1(a) also shows the energy efficiency of the process. It can be observed that, below 30 kJ/L, the higher energy efficiency is obtained in H<sub>2</sub> carrier gas. At higher SIE (>35 kJ/L), the energy efficiencies converge. In the absence of plasma, the decomposition of benzene was not observed even at 400 °C. It was reported that only 2-3 % conversion of benzene was observed in a sand bed at 650 °C. However, the complete conversion occurred at same temperature in the presence of H<sub>2</sub> and Fe<sub>2</sub>O<sub>3</sub> catalyst (Tamhankar *et al.*, 1985). However, in the absence of catalyst, only 40 % of benzene conversion was observed even above 1200 °C, and the reactivity of benzene was minimum as compared to toluene and naphthalene. The non-thermal plasma produces reactive species due to impact of electrons, which have mean energy in the range of 1-10 eV. The reactive atmosphere of active species play a vital role for the decomposition of aromatic compounds.

Fig. 8.1(b) shows the selectivity to hydrocarbons in H<sub>2</sub> carrier gas. It can be seen that the selectivity to LHC (C<sub>1</sub>-C<sub>5</sub>) increases with specific input energy, but heptane and heptane decrease. The selectivity to cyclohexane increased up to 14.7 kJ/L and then decreased. Equation 8.2 shows that H radicals (4.5 eV) produced in the plasma discharged due to the impact of energetic electrons (Darwent, 1970). These reactive H radicals are responsible for the hydrogenation reactions of benzene. However, with increasing SIE, due to the increased abundance of electrons, cyclic and long chain compounds began to be converted into lower hydrocarbons. Hence, it can be observed in Fig. 8.1 (d) that the selectivity to C<sub>1</sub>-C<sub>3</sub> significantly increased with increasing SIE.

In CO<sub>2</sub> carrier gas, the main products were, CO, H<sub>2</sub>, LHCs and solid residue. Fig. 8.1(c) shows the selectivity and yield of gaseous products. The selectivity to lower hydrocarbons

remained below 2% at all tested powers due to the presence of O radicals which promote CO and H<sub>2</sub> formation (see 4.2.1). It can be observed that the selectivity and yield of H<sub>2</sub> and CO also increased with SIE due to increase in the number of reactive species with power.

It was found that formation of solid residue occurred in both carrier gases. The colour of the solid residue was light yellow in hydrogen carrier gas, and black and brown in CO<sub>2</sub>. The solid residue formation occurred due to oxygen deficit environment. These solid residues will eventually foul the DBD reactor, and are not desired products. Conversion to these residues must be decreased for plasma processing to present a feasible solution to this problem (tar production). Fig. 8.2 shows the proposed mechanisms of benzene decomposition under plasma conditions:



**Figure 8.2 General Mechanism for benzene decomposition**

The first impact of the electron or excited species can abstract the H atom from benzene, as the C-H bond dissociation energy (4.5 eV) is the minimum in the benzene molecule (Darwent, 1970). Therefore, cracking of benzene could begin through this route and produce the phenyl radicals. These radicals react together to produce solid residue/benzene derivatives. The hydrogenation of benzene through H radicals can also produce cyclohexane. The second impact of high energy electrons may decompose the aromatic ring and cyclic compound to

produce straight chain hydrocarbons (path 6). Two mechanisms have been reported for the decomposition of aromatic compounds: direct impact of electrons, and due to collision of gas-phase radicals with aromatic compounds (Liang *et al.*, 2013). Reaction mechanism 1 is initiated by collisions between benzene molecules and energetic electrons in the plasma discharge zone in both carrier gases, resulting in the production of intermediate radicals (phenyl).

Reaction route 2 is initiated by collision of reactive radical (produced due to impact of electrons) and benzene molecules. In Fig. 8.2, route 2 and 5 shows that reactive radicals react with benzene directly to initiate the decomposition process. However, these reactive radicals also can react with intermediates to produce final stable product. Route 3 and 4 shows that O radicals can also react with intermediate to produce oxygenated compounds.

Therefore, in the CO<sub>2</sub> carrier gas, due to presence of oxygen atoms, the intermediates can oxidize to CO and H<sub>2</sub>.

### 8.2.2 Effect of residence time.

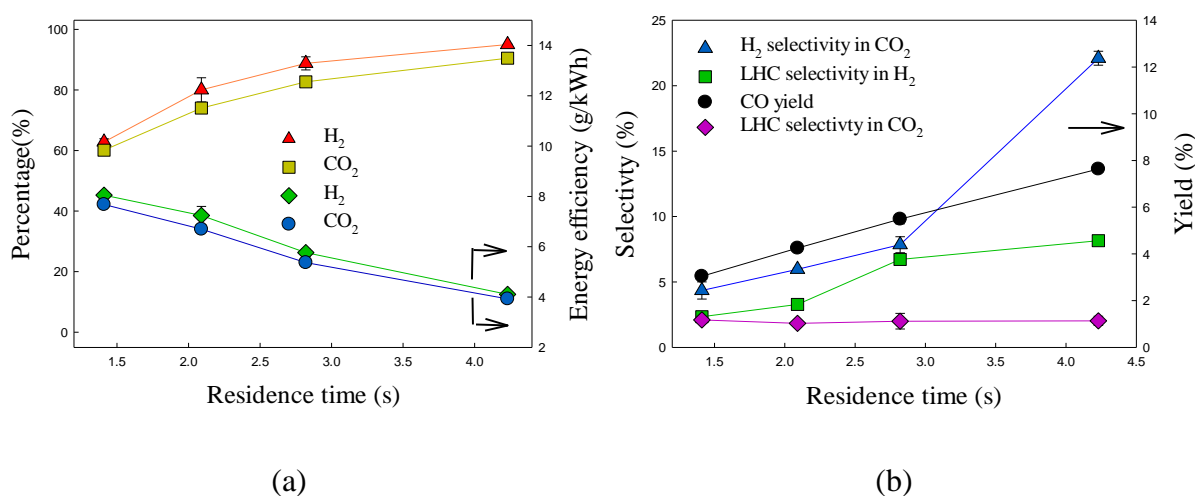


**Figure 8.3. Effect of residence time on (a) the conversion and energy efficiency of benzene, and (b) selectivity and yield of products, in H<sub>2</sub> and CO<sub>2</sub>. Reaction conditions: concentration, 36 g/Nm<sup>3</sup>; temperature, ambient; and plasma power, 20 W.**

The effect of residence time on the conversion of benzene in both carrier gases is shown in Fig. 8.3(a). The effect of changing the residence time on conversion in each carrier gas is the same: increasing with increasing residence time. At high residence time, the benzene molecules spend more time in discharge zone, which allow them to interact with the reactive

species for longer. In this way, higher residence time promotes the conversion of benzene due to the increased number of collision between tar analogue and discharge species (see 5.2.3).

Fig. 8.3(a) shows the effect of residence time on the energy efficiency of the plasma process. As Residence time and conversion increase, the energy efficiency decreases. To enhance the energy efficiency of the process, the residence time and power need to be optimized for the desired conversion of benzene.

Fig. 8.3(b) shows the selectivity of lower hydrocarbons (LHC). It can be noted that hydrogen gives maximum selectivity due to the rich environment of H radicals which combine with the fragments of benzene. The selectivity shows increasing trend with respect to residence time in H<sub>2</sub>. The reason may be that the number of collisions between H radicals and aromatic intermediate species increases when increasing residence time. Therefore, the selectivity of lower hydrocarbons increases due to high collision frequency of these species with H radicals.

However in CO<sub>2</sub> the selectivity of lower hydrocarbons does not increase above 2% due to presence of oxygen which oxidizes the intermediate compounds into CO and H<sub>2</sub>

The selectivity and yield of H<sub>2</sub> and CO are shown in Fig. 8.3(b). It can be observed that both the selectivity and yield of products increase with increasing residence time. The trend is consistent with previous experimental studies in which the decomposition of toluene was studied in a rotating gliding arc discharge reactor (Zhu *et al.*, 2016).

### 8.2.3 *Effect of Concentration*

Fig. 8.4(a) shows the effect of concentration on the conversion and energy efficacy of benzene in CO<sub>2</sub> and H<sub>2</sub> carrier gases. It can be observed from the figure that the removal efficiency of benzene decreases with increasing concentration. This is because the number of molecules in the discharge zone increases with concentration, while all the other parameters (power, residence time, discharge length) remain constant. Therefore, the chances of unconverted benzene molecules escaping the discharge zone increases. Fig. 8.4(a) shows that the energy efficiency of the process increases in both carrier gases with increasing concentration. This is because when the input concentration of benzene increases, it also raises the total no. of decomposed molecules.

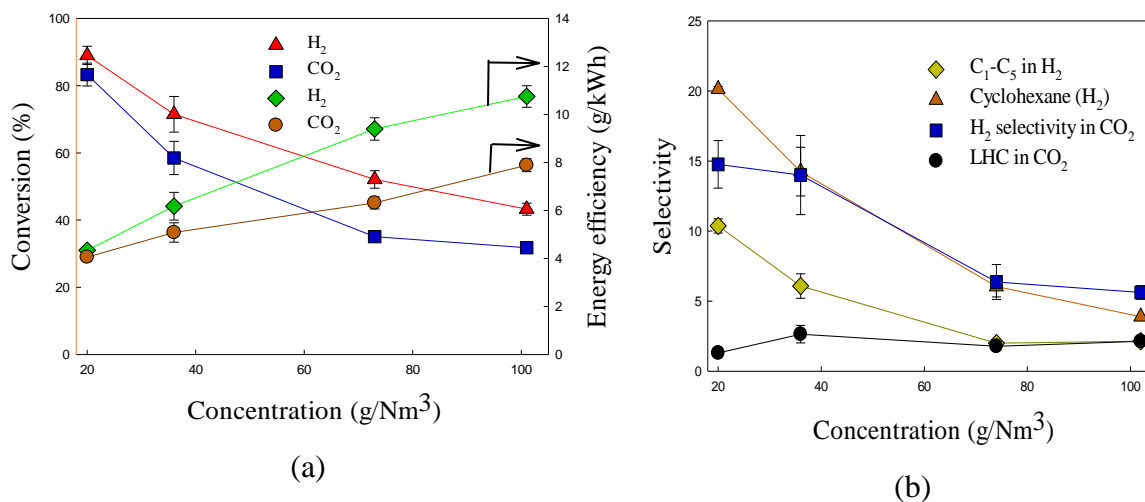


**Figure 8.4.** Effect of concentration in each carrier gas on (a) the conversion and energy efficiency of benzene, and (b) products selectivity and yield. Reaction conditions: SIE, 14.7 kJ/L; temperature, ambient; and power, 10 W.

Fig. 8.4(b) shows the selectivity of different products in each carrier gas. As concentration increases, selectivity to LHCs and cyclohexane decreases. This is probably due to decrease in the relative amount of reactive species with respect to benzene molecules. At higher concentration the relative amount of toluene molecules increases with respect to reactive species. Thereby, the selectivity to lower hydrocarbons decreases when increasing the concentration.

#### 8.2.4 Effect of temperature

The effect of temperature on the conversion of benzene can be observed in Fig. 8.5(a). It can be seen that the conversion of benzene is not influenced by temperature up to 300 °C, whereas after that it decreases with increasing temperature up to 400 °C in CO<sub>2</sub>. This may be due to radical termination reactions of CO and O, which reduce the reactive species in plasma discharge (Cenian *et al.*, 1995).

However, the decomposition of benzene gradually decreases with increasing temperature up to 400 °C. A possible route is that plasma produces phenyl radicals by abstracting H from benzene, as the C-H has the minimum bond dissociation energy. These benzyl radicals polymerize and produce solid residue at ambient temperature. However, as the temperature is increased, due to presence of excess reactive H radicals in H<sub>2</sub> carrier gas, it may react with H radicals and reproduce the benzene (Harding *et al.*, 2005).

Clearly, (fig. 8.5 a) the decomposition of benzene decreases with increasing temperatures. However, it previously been noted that the conversion of toluene did not change when increasing the temperature at 40 W. Fig. 8.5 (a) also shows that the energy efficiency of the process decreases due to the decrease in the conversion of benzene, which ultimately reduces amount of decomposed toluene.

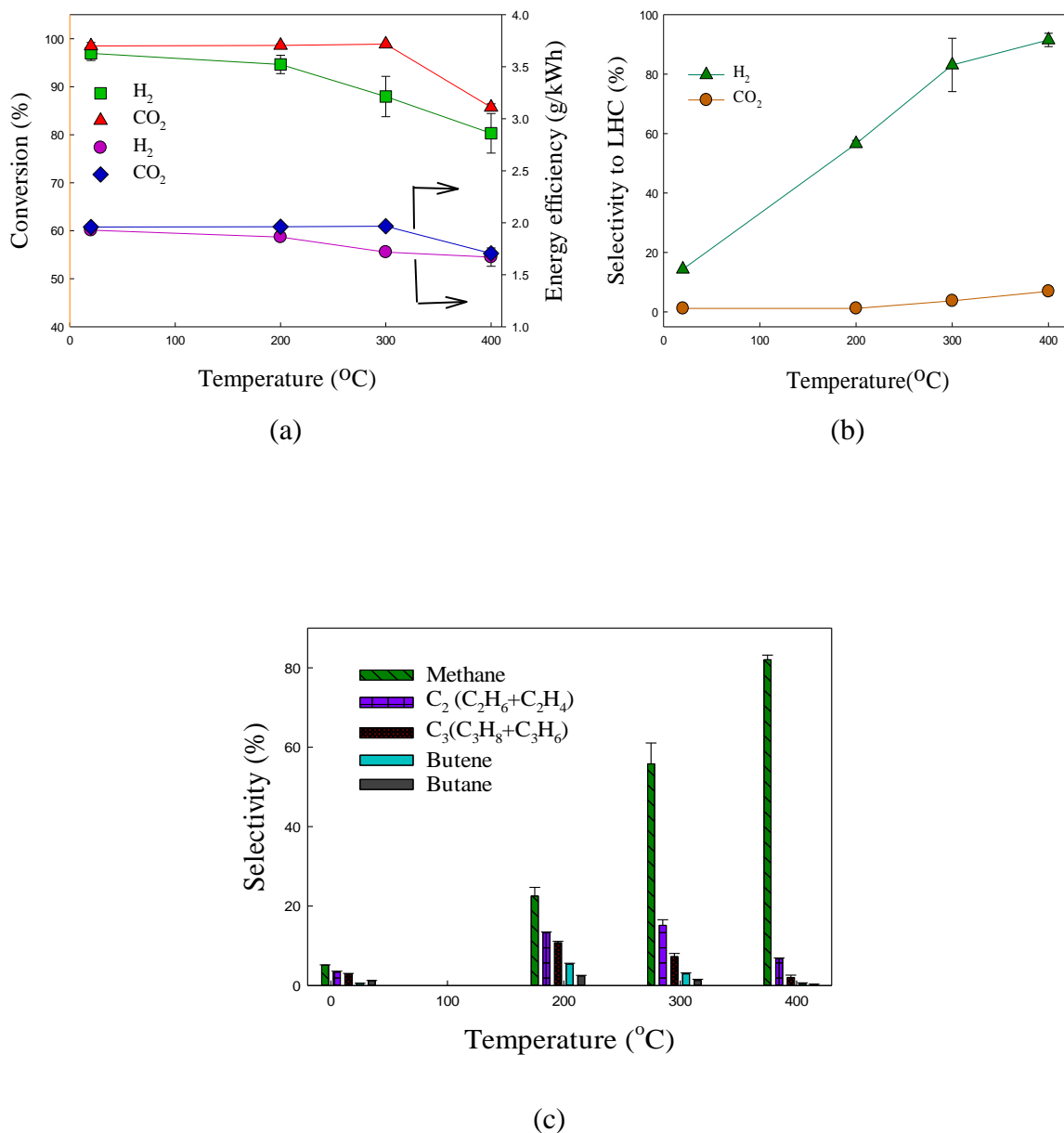


**Figure 8.5. Effect of temperature and carrier gas on (a) the conversion and energy efficiency of benzene, (b) selectivity to lower hydrocarbons, and (c) selectivity to individual LHC in H<sub>2</sub> carrier gas .Reaction conditions: concentration, 33 g/Nm<sup>3</sup>; residence time, 4.23 s; power, 40 W; and SIE, 59.1 kJ/L.**

Fig. 8.5(b) shows the selectivity to LHC (C<sub>1</sub>-C<sub>5</sub>) with respect to temperature. It can be observed that the selectivity in CO<sub>2</sub> carrier gas slightly increases with increasing the temperature, but in H<sub>2</sub> carrier gas, it increases significantly from 20% to 91% with increasing the temperature from ambient to 300 °C. Hence, it is clear that the H<sub>2</sub> carrier gas promotes the ring opening reactions and promotes the formation of lower hydrocarbons and eliminates the solid residue formation. This is possible because the plasma discharge produces reactive H radicals which react with benzene fragments and intermediates to produce lower hydrocarbons at elevated temperatures. In a previous study, the synergetic effect of plasma and temperature was studied on the hydrocracking of toluene using a dielectric barrier discharge reactor (see 5.2.4). It was observed that nearly complete conversion of toluene to lower hydrocarbons (C<sub>1</sub>-C<sub>6</sub>) occurred at elevated temperatures under plasma conditions. However, significant amounts of benzene (28%) were observed at elevated temperatures along with methane (60%) depending upon power. It was reported that hydrogen radicals promote the ring opening products at elevated temperatures in the presence of plasma (see 7.2.4).

Fig. 8.5(c) shows the detailed selectivity to lower hydrocarbons. It can be seen that the selectivity to methane increases from 14 to 80 % with increasing the temperature. For C<sub>2</sub>, selectivity increases up to 300 °C and after which it decreases, while for C<sub>3</sub>-C<sub>5</sub>, selectivity started to decrease even after 200 °C. Therefore, increasing the temperature under plasma conditions promotes the formation of methane from benzene at elevated temperature instead the production of >C<sub>2</sub>.

It has been reported that thermal decomposition of aromatic compounds requires temperatures in the range 500-1200 °C (Jess, 1996; Fagbemi *et al.*, 2001). It has been observed that the yield of methane doubles (11.7 to 23.8 wt. %) with increasing the temperature from 800 to 850 °C, whereas the yield of C<sub>2</sub>H<sub>4</sub> and C<sub>3</sub>H<sub>8</sub> decreases (Gai *et al.*, 2015). Therefore, it could be suggested that increasing temperature favours the conversion of C<sub>2</sub>H<sub>4</sub> and C<sub>3</sub>H<sub>8</sub> to CH<sub>4</sub>. However, in this study, these reactions took place at lower temperature ranges (20-400 °C).

It was noted that the input energy played a key role in the decomposition of the benzene. The rate equation for the cracking of benzene with respect to SIE can be written as

$$r = -d[C_6H_6]/dSIE = k_{SIE}[C_6H_6]^n \quad (8.3)$$

Here  $k_{SIE}$  is an energy constant and  $n$  is a reaction order. Fig. 8.6 a plot of  $\ln(C/C_0)$  exhibits a straight line in both carrier gases. Therefore, the benzene removal in both carrier gases can be written as

$$\ln \frac{[C_6H_6]}{[C_6H_6]_0} = -k_{SIE} \times SIE \quad (8.4)$$

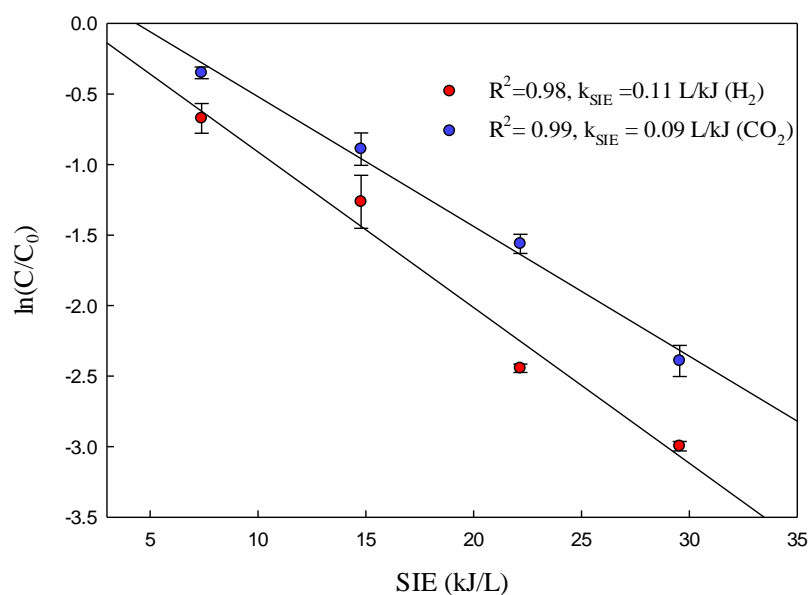


**Figure 8.6 Effect of specific input energy (SIE) on the remaining fraction of benzene. Reaction conditions: concentration, 36 g/Nm<sup>3</sup>; Temperature, ambient; and residence time, 4.23 s.**

In CO<sub>2</sub> and H<sub>2</sub>, the value of R<sup>2</sup> are 0.98 and 0.99 respectively. Hence, the decomposition of benzene in DBD reactor with respect to SIE shows first order kinetics. The equations can be used to determine the energy constant which is important to compare systems and to predict the decomposition of tar compounds in non-thermal plasma reactors.

### 8.3 Conclusions

In this study, a DBD reactor was used to investigate the conversion of benzene, acting as a tar analogue, in CO<sub>2</sub> and H<sub>2</sub> carrier gases. The parameters studied were SIE (7-59 kJ/L), residence time (1.41-4.23 s), concentration (20-102 g/Nm<sup>3</sup>) and temperature (ambient-400 °C).

The main findings were:

1. At high SIEs, the conversion of benzene was similar in both carrier gases, due to the high population of reactive species. However, at lower SIEs (<30 kJ/L), there was a clear difference, and the H<sub>2</sub> exhibited significantly higher conversions of benzene than the CO<sub>2</sub>. This is due to the higher reactivity of the H free radical.
2. The decomposition of benzene increased with increasing SIE and residence time in either carrier gas, and decreased with increasing concentration. The quantification of these effects should allow NTP DBD reactor design
3. The wall temperature of the reactor was identified as an important parameter in controlling the product distribution. Importantly, it was noted that solid formation completely disappeared in H<sub>2</sub> carrier gas at 400 °C, and the selectivity to LHC was as high as 91 %. The presence of H radicals at elevated temperatures in the presence of plasma promoted the new reaction route to crack the aromatic ring and intermediates to lower hydrocarbons. Therefore these reactors can be operated without solid residue formation in the presence of H<sub>2</sub> carrier gas at elevated temperatures along with NTP.
4. At higher powers and temperatures (40 W and 400 °C) selectivity to methane increased from 15 to 81% in H<sub>2</sub> carrier gas, whereas, the selectivity to C<sub>2</sub>-C<sub>4</sub> decreased from 38% to 12% with increasing temperature from 300 to 400 °C at 40 W. Clearly, hydrocarbon chain length can be controlled by judicious choice of wall temperature: chain length decreases as temperature increases.

These results illustrate the opportunities for combining thermal effects with non-thermal plasma effects for operation of gas phase reactors. In this case, judicious choice of temperature could be used to operate the reactor such that no solid residue was formed, and the “tar” was largely converted into methane.



## **Chapter 9. Role of methane in the product gas towards the formation of lower hydrocarbons during the decomposition of different tar analogues**

### **9.1 Introduction**

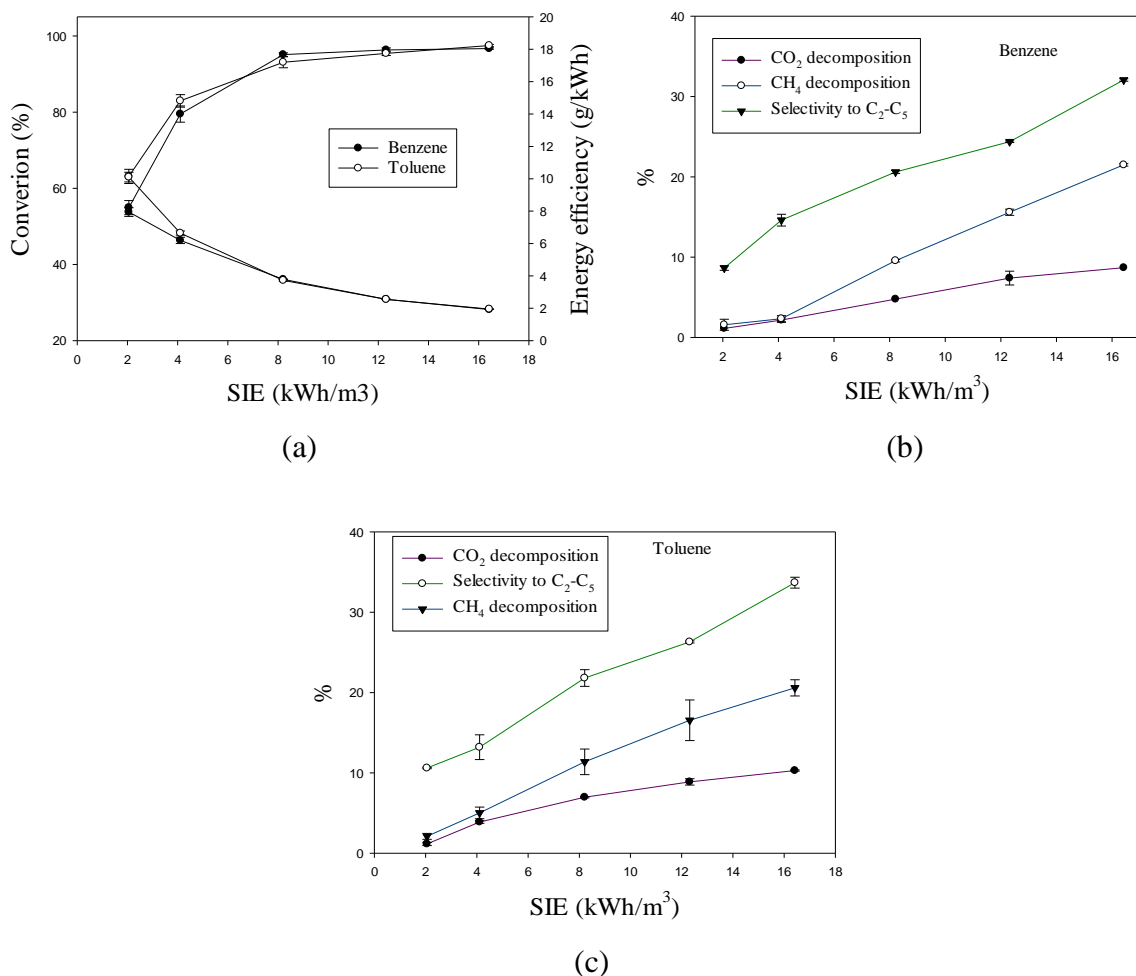
Chapter 7 reports the decomposition of toluene in a mixture of CO<sub>2</sub>, CO, and H<sub>2</sub>. Formation of solid residue was shown to be completely eradicated at elevated temperature. The major products were methane and C<sub>2</sub>-C<sub>6</sub>. Similarly, it was noted that methane showed maximum selectivity in both tar analogue compounds (toluene and benzene) at elevated temperature in H<sub>2</sub> carrier gas (see 5.2.4 and 8.2.4). Hence, most of the tar compounds were converted to methane instead of any other hydrocarbon. These studies were conducted in the absence of methane. However, real product gas from a gasifier, contains 4 to 14% methane, depending upon the gasification conditions.

Many studies have been conducted to investigate the conversion of methane to H<sub>2</sub> and C<sub>1</sub>-C<sub>5</sub> hydrocarbons. It was reported, for instance, that the methane converted predominantly to >C<sub>1</sub> hydrocarbons in a non-thermal plasma dielectric barrier discharge reactor (Tu and Whitehead, 2014). Hence, the presence of methane in a mixture of carrier gas can affect the product distribution. Therefore, this chapter concerns the addition of methane to model product gas (H<sub>2</sub>: 41%, CO: 23.5%, CO<sub>2</sub>: 23% and CH<sub>4</sub>: 12.5%), to study the effect on product selectivity. The effect of specific input energy (SIE) (2.05-16 kWh/m<sup>3</sup>), residence time (0.95-2.82 s), and temperature (20-400 °C) were studied.

### **9.2 Results and discussion**

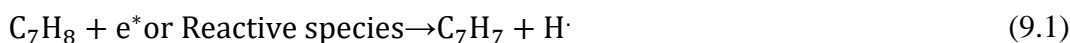
#### **9.2.1 Effect of SIE**

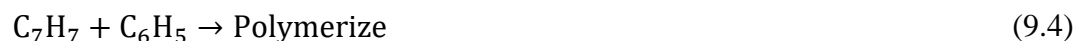
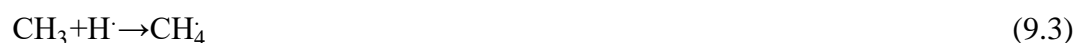
Figure 9.1(a) clearly shows that removal of both tar analogues increases when increasing the specific input energy (SIE). The number of electrons with higher energy increases as the input plasma power is increased, which increases the rate of cracking of the tar representative compounds at high power. Moreover, it can be observed that at high SIE (>7 kWh/m<sup>3</sup>) the two tar model compounds have very similar conversions.



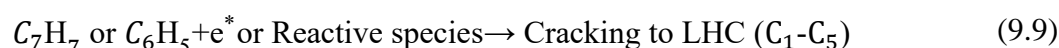
**Figure 9.1. Effect of SIE on (a) the conversion and energy efficiency of tar representatives, (b) the selectivity and decomposition of gaseous products (benzene), and (c) the selectivity and decomposition of gaseous products (toluene). Reaction conditions: concentration, 33g/Nm<sup>3</sup>; residence time, 2.82 s; flow rate, 40.6 ml/min; SIE, 2.05-16.4 kWh/m<sup>3</sup>; and temperature, ambient.**

At lower powers (< 7 kWh/m<sup>3</sup>) the conversion of toluene is higher than that of benzene. This is because the minimum bond dissociation energy of C-H in an aromatic ring is 4.5 eV, whereas the bond dissociation energy of methyl group in toluene is 3.7 eV (Darwent, 1970). Hence, the decomposition of toluene can proceed via the abstraction of H from the methyl group at lower input SIE. However, at high power the differential in bond dissociation energies makes little difference as there is a plentiful supply of electrons with sufficient energy to break aromatic bonds. Equations 9.1-9.5 show the reactions involved during the decomposition of toluene:





Similarly, the conversion of benzene can occur via the following reactions



The energetic electrons also produce reactive species from the background gas, which can play important roles in determining the product distribution:



The SIE effect on the energy efficiency is also shown in Fig. 9.1(a). The energy efficiency decreases with increasing SIE. Essentially, this is due to “diminishing returns” as the conversion approaches 100%. Similar trends have been reported for the removal of tar analogues in which decomposition of toluene was studied in H<sub>2</sub> carrier gas (see 5.2.1). Figure 9.2 shows how the LHC product distribution and the conversion of the product gas species varies as a function of SIE.

Fig. 9.2, (a) and (b) show that the product distribution (selectivity) of the lower hydrocarbons is influenced by the SIE. It has previously been observed that the selectivity to lower hydrocarbons was 18% at 40 W (see 7.2.1). In this study, the selectivity of LHC reaches 32% under same condition. This is probably due to the presence of CH<sub>4</sub> additive in the product gas: some of the lower hydrocarbons will be produced via cracking of aromatic ring, but some will be produced via reactions of CH<sub>3</sub> radicals produced in the decomposition of CH<sub>4</sub>.

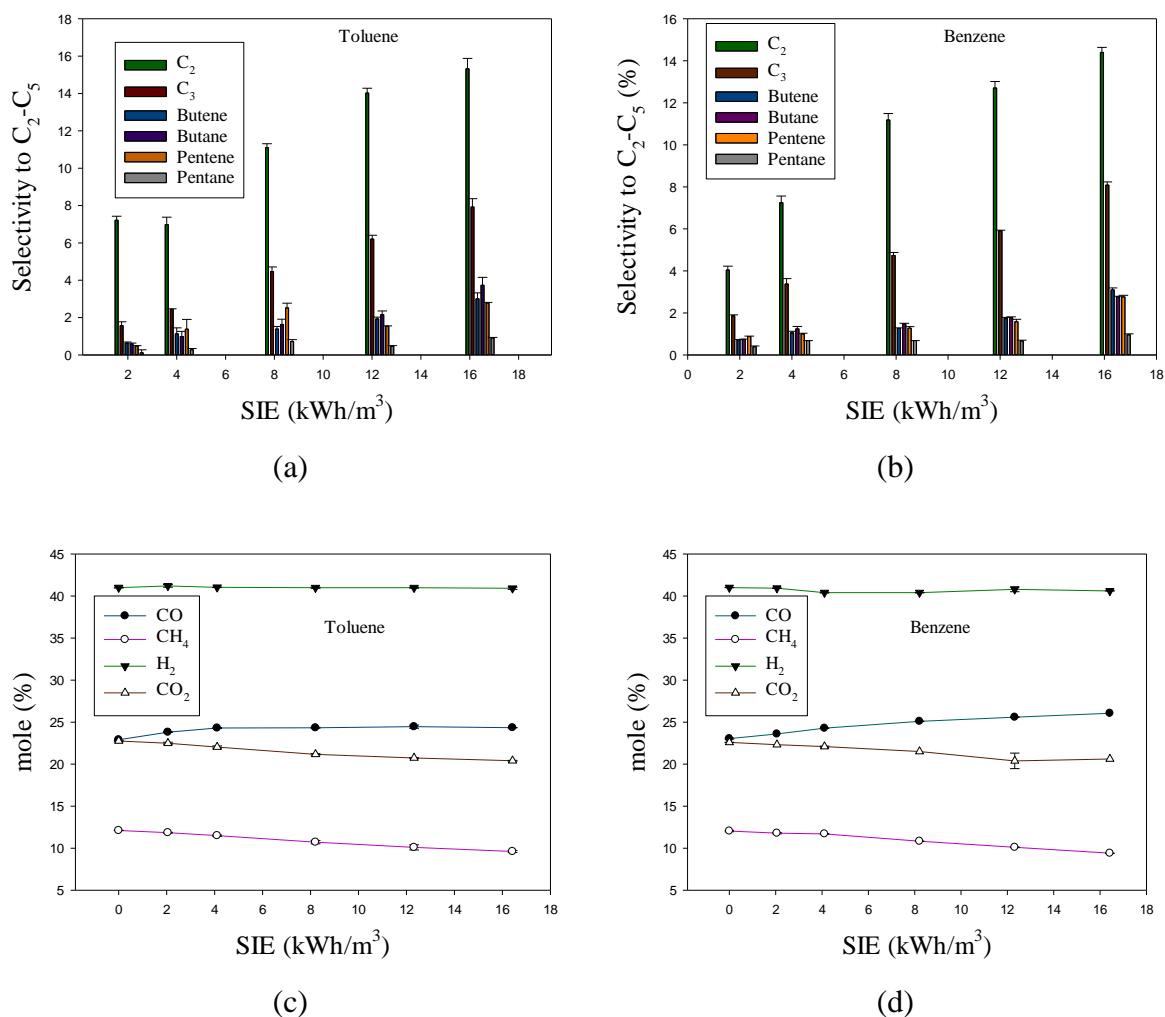


**Figure 9.2. Effect of SIE on (a) the individual selectivity to C<sub>2</sub>-C<sub>5</sub> (toluene), (b) the individual selectivity to C<sub>2</sub>-C<sub>5</sub> (benzene), (c) composition of permanent gas (toluene), and (d) the composition of permanent gases (benzene). Reaction conditions: concentration of benzene and toluene, 33 g/Nm<sup>3</sup>; residence time, 2.82 s; flow rate, 40.6 ml/min; SIE, 2.05-16.4 kWh/m<sup>3</sup>; and temperature, ambient.**

It has been reported that electron impact produces CH<sub>3</sub>, CH<sub>2</sub> and CH radicals, which can combine to produce lower hydrocarbons (Xu and Tu, 2013; Chiremba *et al.*, 2017) via the following reactions:

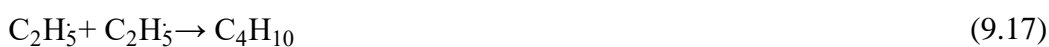
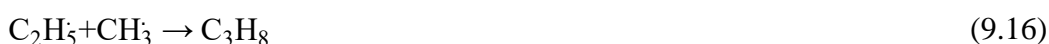
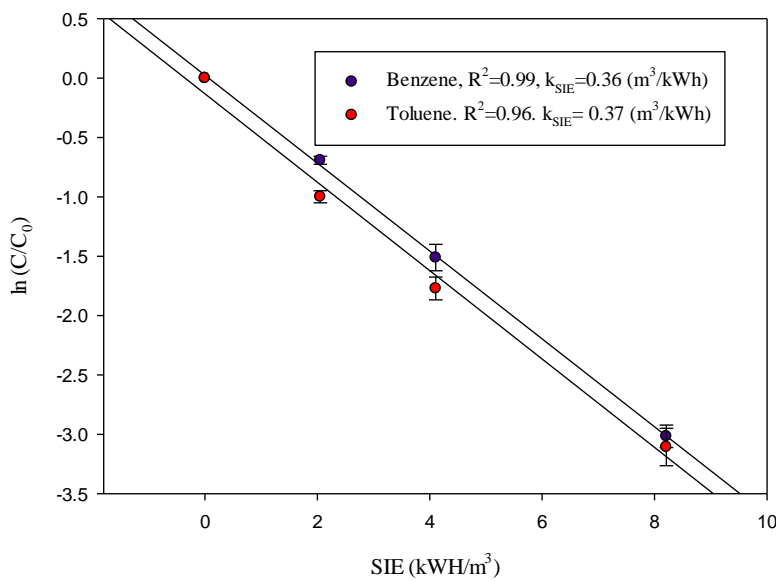
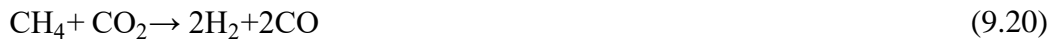


Fig. 9.2, (c) and (d) show that the decomposition of CO<sub>2</sub> and CH<sub>4</sub> increases with increasing specific input energy for all species. The reason is that with increasing the power decomposition of CO<sub>2</sub> to CO and O increases (Yu *et al.*, 2012), while CH<sub>4</sub> decomposition promotes the agglomeration of, CH<sub>3</sub>, CH<sub>2</sub>, and CH radicals (Chiremba *et al.*, 2017). In addition, it has previously been shown that dry reforming of CH<sub>4</sub> and CO<sub>2</sub> can cause decomposition of these two gaseous compounds (Tu and Whitehead, 2012).



**Figure 9.3. Effect of specific input energy (SIE) on the remaining fraction of toluene and benzene. Reaction conditions: concentration, 33 g/Nm<sup>3</sup>; temperature, ambient; and residence time, 2.82 s.**

It has been observed that the non-thermal plasma processes are energy dependent instead of time dependent due to very quick plasma chemical reactions (within 0.1ms) (Yu *et al.*, 2012). Figure 9.3 shows that the decomposition reactions of benzene and toluene in non-thermal plasmas are clearly energy dependent. It shows that the natural log of the remaining fraction of toluene and benzene with respect to SIE follows a straight line trend. Therefore, it can be concluded that the decomposition of the tar analogues benzene and toluene in this DBD reactor exhibits first order behaviour with respect to SIE

The value of the energy constants for toluene and benzene were found to be 0.37 and 0.36 m<sup>3</sup>/kWh respectively.

$$\ln \frac{[C]}{[C]_0} = -k_{SIE} \times SIE \quad (9.21)$$

The decomposition of benzene and toluene produced a significant amount of light yellow solid residue. The decomposition of toluene could be initiated through the abstraction of an H atom from methyl group, which produces the benzyl radicals. These radicals can react together in the presence of CH<sub>2</sub> and phenyl radicals to form solid residue. Similarly, the formation of solid residue also occurred in benzene due to reactions between phenyl radicals. These solid residues would produce operational problems, via fouling and eventual blockage of pipework. Therefore, it is very important to resolve this problem. It has been observed that increasing temperature in the presence of H could eliminate the formation of solid residue (see 7.2.4).

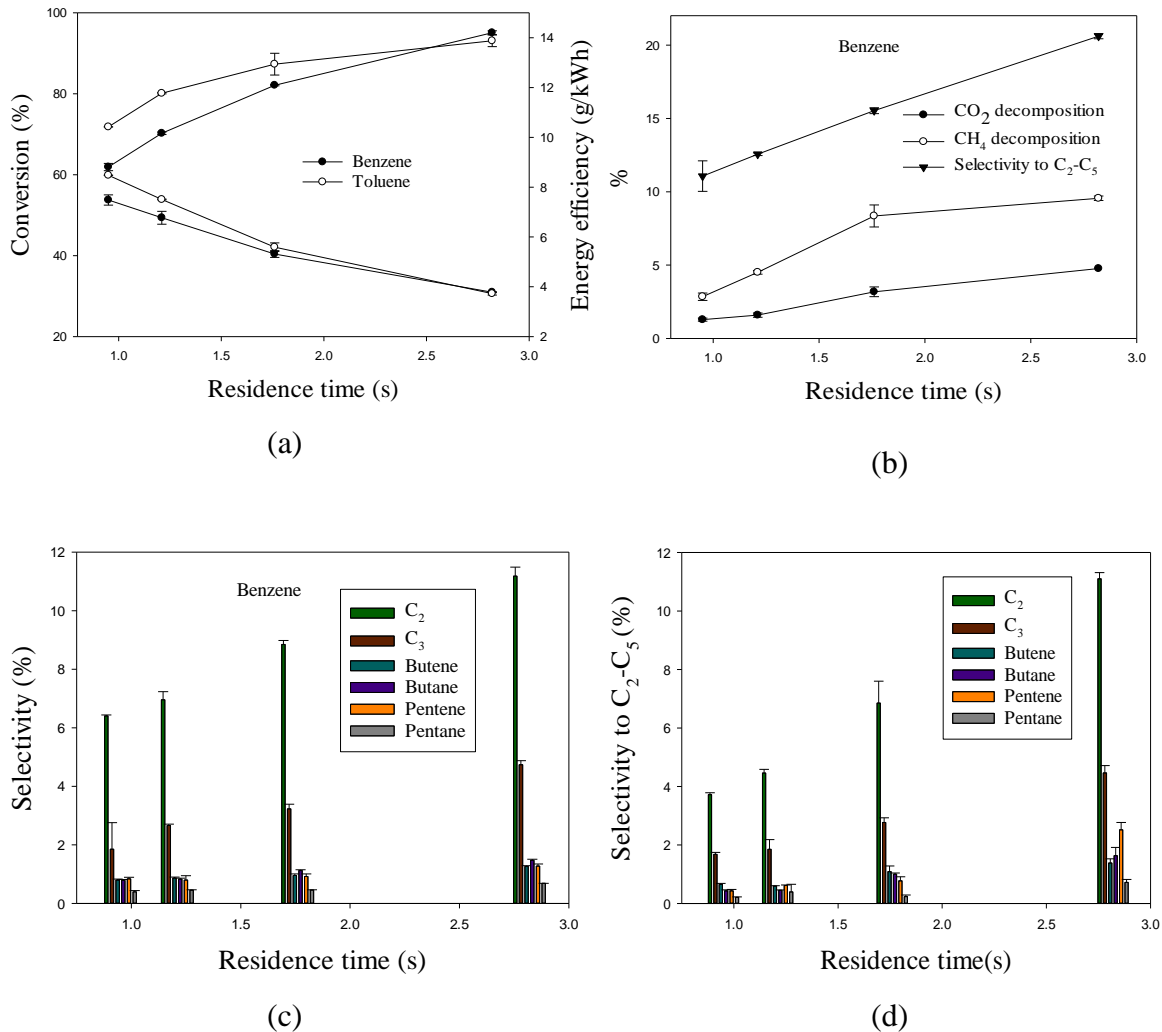
Carrier gas	Tar conversion (%)	Gaseous Products	Solid residue at 20 °C	Solid residue at 400 °C
CO <sub>2</sub>	>98	CO, H <sub>2</sub> and LHC	Black and brown	Black
H <sub>2</sub>	>98	LHC	Light yellow	Disappeared
N <sub>2</sub>	>98	H <sub>2</sub> and LHC	Black	Black
Mixture 1	>98	LHC	Yellowish	Disappeared
Mixture 2	>98	LHC	Yellowish	Disappeared

**Table 9.1: Formation of products in different carrier gases.**

### 9.2.2 Effect of residence time

Figure 9.4(a) shows how the conversions of the various species vary with residence time. Generally, the decomposition of tar representatives increases with increasing residence time because of high number of collisions with reactive species. However, the energy efficiency decreases, as the production rate per unit energy input decreases, due to the lower flowrate. The trends are consistent with previous experimental studies of decomposition of tar analogues using DBD reactors (see 7.2.2).

Fig. 9.4(b) shows the effect of residence time on the decomposition of CO<sub>2</sub> and CH<sub>4</sub>. It can be seen that decomposition of methane and CO<sub>2</sub> increases from 2.8 to 9.5% and 2.25 to 4.76% respectively, as the residence time increases.



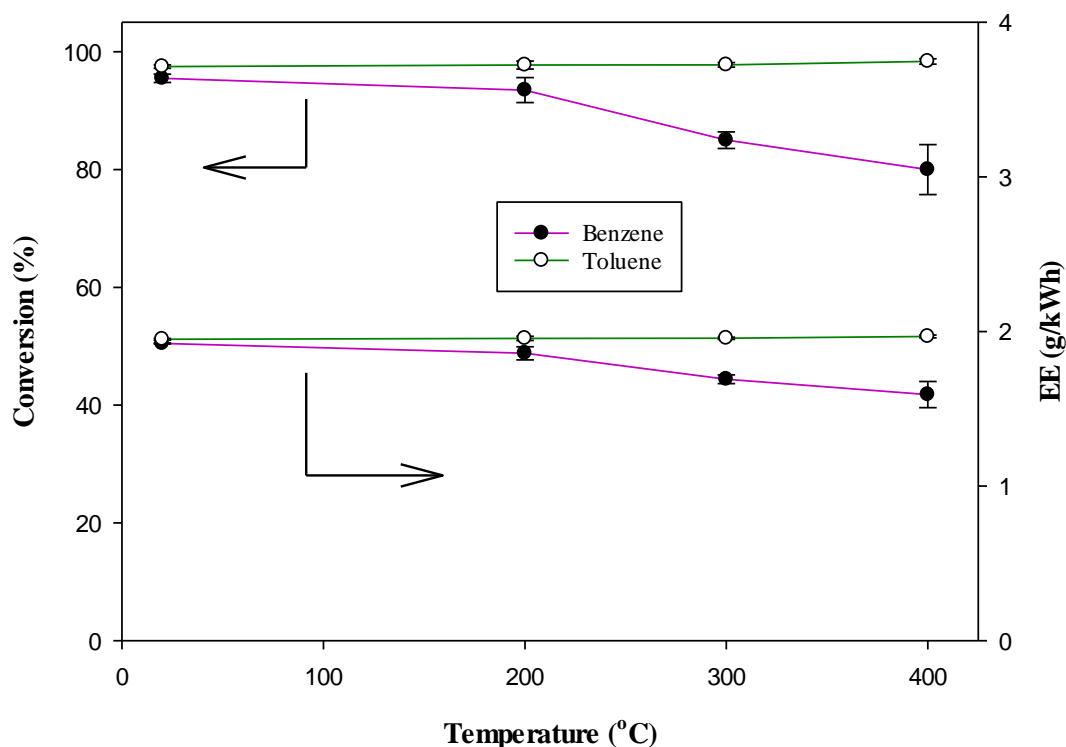
**Figure 9.4. Effect of residence time on (a) the conversion of toluene, benzene and energy efficiency, (b) Decomposition of CO<sub>2</sub> and CH<sub>4</sub> and selectivity to LHC, (c) Individual selectivity to LHC for benzene, and (d) individual selectivity to LHC for toluene; bars represent standard deviation. Reaction conditions: concentration, 33 g/Nm<sup>3</sup>; flow rate, 40.6-120 ml/min; ambient temperature; and power, 20 W.**

Fig. 9.4 (c) and (d) show the selectivities to lower hydrocarbons (C<sub>1</sub>-C<sub>5</sub>) in benzene and toluene respectively. It can be noted that the selectivity to conversion to lower hydrocarbons increases with increasing residence time. At lower flow rates, the probability of ring-opening products increases due to the higher number of collisions with more reactive species. Moreover, the decomposition of methane also increases with time, and it was reported that methane decomposition produces C<sub>2</sub>-C<sub>5</sub> hydrocarbons (Chiremba *et al.*, 2017). Therefore, at

higher residence times, the cracking of aromatic rings and the decomposition of methane both contribute to lower hydrocarbon formation.

### 9.2.3 Effect of temperature

The synergistic effect of temperatures and input discharge power was studied on the product distribution as well as the tar removal efficiency. Fig. 9.5 shows the conversion of tar representatives with respect to temperature at 40 W. It can be observed that conversion of toluene is not affected by temperature. However, for benzene, it decreases with increasing temperature. This may be due to recombination reactions of phenyl radicals and H atoms. In previous study, it was observed that formation of benzene increased with increasing temperatures under constant plasma power during the decomposition of toluene (see 5.2.4). The benzene formation occurred due to reactions of H radicals with phenyl radicals. Therefore, the decomposition efficiency has decreased at elevated temperatures, due to formation reactions of benzene.



**Figure 9.5. Effect of temperature on the conversion of toluene and benzene. Reaction conditions: concentration, 33 g/Nm<sup>3</sup>; residence time, 2.82 s; flow rate, 40.6 ml/min, SIE, 16.40 kWh/m<sup>3</sup>.**

Fig. 9.6 (a) and (b) show the effect of temperature on the decomposition of CH<sub>4</sub> and CO<sub>2</sub>. It can be observed that the decomposition of methane decreases with increasing temperature.

This is probably due to the formation of CH<sub>4</sub> from the decomposition of aromatic compounds in the presence of plasma at elevated temperatures (see 7.2.4). It has previously been reported that selectivity to methane increases to 60 % during the plasma-assisted decomposition of toluene in H<sub>2</sub> carrier gas at elevated temperature (see 5.2.4). The decomposition of CO<sub>2</sub> also decreases with increasing temperature. This may be due to the recombination reactions of O and CO radicals (Cenian *et al.*, 1995).

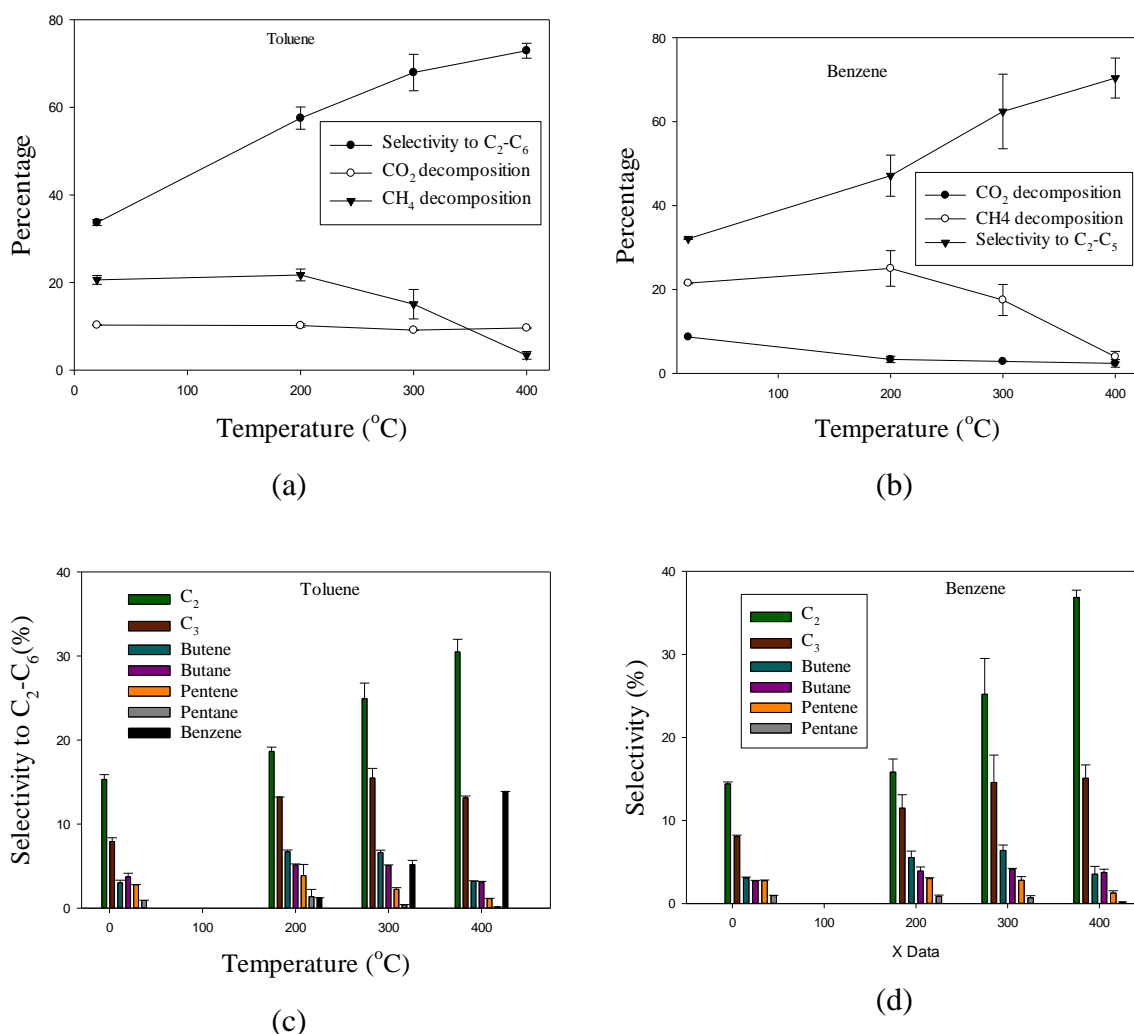


**Figure 9.6. Effect of temperature on (a) the products distribution (toluene), (b) the product distribution (benzene); (c) the individual selectivity to LHC (toluene); (d) the individual selectivity to LHC (benzene). Reaction conditions: concentration, 33 g/Nm<sup>3</sup>; residence time, 2.82 s; flow rate, 40.6 ml/min.**

It can be observed from Figures 9.6 (a) and (b) that the selectivity of C<sub>2</sub>-C<sub>6</sub> increases to nearly 77% for both benzene and toluene. However, in a previous study it was observed that selectivity to C<sub>2</sub>-C<sub>6</sub> decreases with increasing the temperature due to formation of methane

(see 5.2.4). The study was conducted in the absence of methane and it was observed that conversion of C<sub>2</sub>-C<sub>6</sub> to methane took place at 400 °C at 40 W (see 7.2.4). In this study, methane was present, and it has been previously reported that methane decomposition can lead to formation of C<sub>2</sub>-C<sub>5</sub> hydrocarbons (Chiremba *et al.*, 2017). Therefore, the total production of C<sub>2</sub>-C<sub>5</sub> depends upon the decomposition of the benzene and toluene and CH<sub>4</sub> decomposition.

Fig.9.6 (c) and (d) show that the selectivity to C<sub>2</sub> (C<sub>2</sub>H<sub>6</sub>+C<sub>2</sub>H<sub>4</sub>) increases with increasing temperature. However, in a previous study it was observed that selectivity to C<sub>2</sub> decreases after 300 °C in pure H<sub>2</sub> carrier gas (see 5.2.4). This, again, perhaps implies that methane is acting as a source of C<sub>2</sub>. The selectivity to C<sub>3</sub>-C<sub>5</sub> started to decrease after 300 °C due to cracking into lower hydrocarbons. However, formation of benzene increased to 13 % at 400 °C during the cracking of toluene. It is possible due to radical substitution reactions at elevated temperature (Amano *et al.*, 1972).

### 9.3 Conclusions

Cracking of benzene and toluene as analogues for gasification tars was investigated in a non-thermal plasma DBD reactor using a mixture of simulated product gas (H<sub>2</sub>:41%, CO<sub>2</sub>:23% and CO:23.5%, CH<sub>4</sub>: 12.5%). The performance was investigated as a function of: SIE (2.05–16.4 kWh/m<sup>3</sup>), residence time (0.95-2.82 s) and temperature (20-400 °C).

The main findings were:

- i. At lower SIE < 7 kWh/m<sup>3</sup>, toluene had a higher conversion than benzene. However, at high SIE > 7 kWh/m<sup>3</sup> both gave same conversion about 98%.
- ii. Significant formation of solids was observed for both benzene and toluene at normal temperature. However, it was shown that this could be eliminated by increasing the operating temperature up to 400 °C.
- iii. The presence of methane in the mixture of carrier gases significantly increased (>32%) the selectivity to C<sub>2</sub> (C<sub>2</sub>H<sub>6</sub>+C<sub>2</sub>H<sub>4</sub>) hydrocarbons when increasing the temperature up to 400 °C at constant power.
- iv. Decomposition of methane decreased to nearly 2 % with increasing temperature due to formation of methane at elevated temperatures.
- v. Selectivity to lower hydrocarbons (<C<sub>7</sub>) increased to about 77 % as the temperature was increased to 400 °C.

The results demonstrate that high temperature eliminates the formation of solid residues and convert them largely into C<sub>2</sub>-C<sub>5</sub>. Hence, the coupling of temperature and plasma effects could resolve the problem of formation of solid residue.



## Chapter 10. Conclusions and Further Work

### 10.1 Conclusions

The cracking of toluene and benzene in non-thermal plasmas was studied in various carrier gases and gas mixtures to study the effects on the decomposition of tar analogue compounds and the resultant product distributions. It was observed that the conversion of both tar analogues (toluene and benzene) increased with increasing power and residence time in all carrier gases, and selectivities to gaseous products (CO, H<sub>2</sub>, and LHC) also showed increasing trend due to increase in reactive species and collision frequency at high power and residence time.

In CO<sub>2</sub> carrier gas the major products were lower hydrocarbons (“LHC”: C<sub>1</sub> - C<sub>6</sub>), CO and solid residues. At elevated temperature (400 °C) toluene conversion decreased due to recombination reactions of O and CO radicals, which reduced the amount of reactive species. The yields of H<sub>2</sub> and CO also decreased. However, selectivity to lower hydrocarbons increased (3.5 to 12.8%) with increasing temperature. The significant amount of solid formation occurring when operating in CO<sub>2</sub> carrier gas was a negative outcome and must be resolved. However, it should be noted that the presence of other gases, such as CO, N<sub>2</sub>, and H<sub>2</sub>, reduces the solid residue.

In H<sub>2</sub> carrier gas at ambient temperature, solid residues and lower hydrocarbons were also formed in the reactor. It was observed that the toluene conversion was not a function of temperature when increasing the temperature from 20 to 400 °C. This was partially because nearly complete removal of tar took place at 40 W. However, it should be noted that in the absence of plasma, no decomposition of toluene was observed at these temperatures. The selectivity to lower hydrocarbons increased with increasing temperature, reaching 99.9 % at 400 °C, without formation of solid deposits or heavy hydrocarbons (>C<sub>6</sub>). At higher temperatures (200-400°C), hydrocracking caused increased selectivity to lower hydrocarbons. Hydrogen could work as a scavenger for methyl, benzyl and phenyl radicals. The major products were methane (60%) and benzene (28%) at 40 W and 400 °C. Clearly, there are benefits to combining thermal and non-thermal effects in this particular application. Here, “adding in” thermal effects allowed high selectivity to LHCs, without solid residue formation, which are both desirable outcomes.

Using N<sub>2</sub> as a carrier gas, at ambient conditions, the selectivity to lower hydrocarbons reached a maximum of only 6%. However, it increased to 14.5% when the temperature was increased to 400 °C. Solid deposits were again formed inside the reactor. This is generally an undesirable effect, but it can be substantially reduced by introducing H<sub>2</sub>. At elevated temperatures in the presence of H<sub>2</sub>, the selectivity to lower hydrocarbons increased with increasing hydrogen concentration. It reached 57 % at a concentration of H<sub>2</sub> of 35% at 400 °C. The main product in these conditions was CH<sub>4</sub>, which reached a maximum selectivity of 45 %. This occurred due to plasma-assisted hydrocracking of hydrocarbons in the presence of excess H<sub>2</sub> at elevated temperatures.

In synthetic fuel gas mixtures (CO<sub>2</sub>: 30 %; CO: 20 %; H<sub>2</sub>: 50 %), the conversion of toluene was as high as 99%. The major products were CO, lower hydrocarbons (LHC) and solid residues. Again, as for H<sub>2</sub>, solid formation could be eliminated by increasing the wall temperature. A further benefit of increasing the temperature was that it increased both selectivity and yield of the lower hydrocarbons. Formation of methane increased with increasing temperature and power. The highest yield of methane in this study was 7.5 %, at 400 °C and 40 W.

The conversion of benzene, as another tar analogue, was also investigated in the DBD reactor, in CO<sub>2</sub> and H<sub>2</sub> carrier gases. At high SIEs, the conversion of benzene was similar in both carrier gases. However, at lower SIEs (<30 kJ/L), there was a clear difference: the H<sub>2</sub> exhibited significantly higher conversions of benzene than the CO<sub>2</sub>. This was due to the higher reactivity of the H· free radical. The wall temperature of the reactor was identified as an important parameter in controlling the product distribution. Importantly, it was noted that solid formation completely disappeared in H<sub>2</sub> carrier gas at 400 °C, and the selectivity to LHC was as high as 91%. The presence of H· radicals at elevated temperatures in the presence of plasma promoted a new reaction route: cracking of the aromatic ring and intermediates to lower hydrocarbons. Therefore these reactors can be operated without solid residue formation in the presence of H<sub>2</sub> carrier gas at elevated temperatures along with NTP. At higher powers and temperatures (40 W and 400 °C) selectivity to methane increased from 15 to 81 % in H<sub>2</sub> carrier gas, whereas, the selectivity to C<sub>2</sub>-C<sub>4</sub> decreased from 38% to 12% with increasing temperature from 300 to 400 °C at 40 W. Clearly, hydrocarbon chain length can be controlled by judicious choice of wall temperature and power: chain lengths decrease as temperature and power increases.

Comparative decomposition of benzene and toluene as tar representatives was investigated in a non-thermal plasma DBD reactor using a mixture of synthetic “product gas” (H<sub>2</sub>:41%, CO<sub>2</sub>:23% and CO: 23.5%, CH<sub>4</sub>: 12.5 %). At lower SIE < 7 kWh/m<sup>3</sup>, toluene exhibited greater conversion than benzene. However, at high SIE (>7 kWh/m<sup>3</sup>) both gave similar conversions (about 98%). The products included lower hydrocarbons and solid residues. Solid formation occurred in both benzene and toluene at normal temperature. However, the problem of formation of solid residue could be resolved by increasing the reactor wall temperatures. Decomposition of methane decreased with increasing temperature. Selectivity to lower hydrocarbons (<C<sub>7</sub>) increased to about 77 % as the temperature was increased to 400 °C.

These results illustrate the opportunities for combining thermal effects with non-thermal plasma effects for operation of gas phase reactors. In this case, judicious choice of temperature, atmosphere and power could be used to operate the reactor such that no solid residue was formed, and the “tar” was largely converted into lower hydrocarbons (C<sub>1</sub>-C<sub>6</sub>).

## **10.2 Future recommendations**

### ***10.2.1 Kinetic and scale up study***

The results (chapter 5-9) have shown that the synergetic effect of temperature and plasma power promotes the conversion of tar analogues (benzene and toluene) to lower hydrocarbons in the presence of hydrogen. The conversion of aromatics to lower hydrocarbons at elevated temperatures (20-400 °C) was studied at constant residence time. It should also be studied at different residence times by changing flow rates to investigate the activation energy and rate constants of lower hydrocarbons formation in a non-thermal plasma dielectric barrier discharge reactor at elevated temperature. Kinetic information could be used to feed into pragmatic reaction engineering design issues, such as scale up studies. Suitable chemical kinetic models could then be developed to allow design of dielectric barrier discharge reactors in order to obtain maximum conversion of tar at minimal cost. Scale-up is a considerable challenge for the successful application of this technique. Understanding the impact of reactor hydrodynamics in the performance of the process is also an important step to overcoming this problem. The chemical engineering concepts could be applied to investigate the impact of reactor configurations and flow regimes (laminar/turbulent) on the performance of dielectric barrier discharge reactor.

### ***10.2.2 Formation of valuable lower hydrocarbons (C<sub>1</sub>-C<sub>5</sub>)***

In conventional hydrocracking, the conversion of heavy oils to light fuels in petroleum refineries requires catalyst and significant high temperatures. However, the synergetic effect of plasma and temperature could be used to convert heavy oils *without* catalyst and the attendant operational difficulties of using catalysts (particularly with ill-defined feedstocks). In Chapter 2, it was observed that an aromatic compound (toluene) could be completely converted to lower hydrocarbons (C<sub>1</sub>-C<sub>6</sub>), and that the product distribution strongly depended upon plasma power and wall temperature. At lower power and temperature, the major products were >C<sub>1</sub>, whereas methane was present in significant amount (60 %) at high temperatures (400 °C) and powers (40 W). Therefore, further study could be conducted to control the product distribution by changing power and wall temperature. A similar study could be performed for the conversion of heavy oils to light fuels by using non-thermal plasma dielectric barrier discharge reactor.

### ***10.2.3 Synthesis of nano crystals and valuable solid products using Non-thermal plasmas***

At ambient conditions significant amounts of solid residue formed due to polymerization reactions in all carrier gases at ambient conditions. The analysis of solid residues could be performed to investigate the properties and nature of these by products. It has been reported that plasma processes produce different types of carbon products including, carbon fibre amorphous carbon and polymers. The decomposition of chloroform via NTP polymerization in double dielectric barrier discharge reactor was studied at atmospheric pressure (Gaikwad *et al.*, 2018). It was observed that addition of additives (methane and hydrogen) increased the yield of non-cross linked polymer. Therefore, by changing/adding the reactants, the formation of useful polymers could be studied in the current system. In addition, nano crystals can be produced in non-thermal plasmas. These nanocrystals showed wide range of applications. It has been observed that Silicon nanocrystals produced in a NTP have luminescent properties with remarkable photoluminescence quantum yields (60-70 %) (Jurbergs *et al.*, 2006).

## References

- Abdelaziz, A.A., Seto, T., Abdel-Salam, M. and Otani, Y. (2013) 'Influence of nitrogen excited species on the destruction of naphthalene in nitrogen and air using surface dielectric barrier discharge', *Journal of hazardous materials*, 246, pp. 26-33.
- Amano, A., Horie, O. and Hanh, N.H. (1972) 'Reaction of toluene with hydrogen atoms at elevated temperatures', *Chemistry Letters*, 1(10), pp. 917-920.
- Amano, A., Tominaga, H. and Tokuhisa, H. (1965) 'Mechanism of Thermal Hydrogenolysis of Toluene', *Bulletin of The Japan Petroleum Institute*, 7, pp. 59-63.
- Ammendola, P., Lisi, L., Piriou, B. and Ruoppolo, G. (2009) 'Rh-perovskite catalysts for conversion of tar from biomass pyrolysis', *Chemical Engineering Journal*, 154(1-3), pp. 361-368.
- Anis, S. and Zainal, Z.A. (2011) 'Tar reduction in biomass producer gas via mechanical, catalytic and thermal methods: A review', *Renewable and Sustainable Energy Reviews*, 15(5), pp. 2355-2377.
- Arribas, M.A. and Martinez, A. (2002) 'The influence of zeolite acidity for the coupled hydrogenation and ring opening of 1-methylnaphthalene on Pt/USY catalysts', *Applied Catalysis A: General*, 230(1), pp. 203-217.
- Asadullah, M., Ito, S.-i., Kunimori, K., Yamada, M. and Tomishige, K. (2002) 'Biomass gasification to hydrogen and syngas at low temperature: novel catalytic system using fluidized-bed reactor', *Journal of Catalysis*, 208(2), pp. 255-259.
- Asadullah, M., Miyazawa, T., Ito, S.-i., Kunimori, K. and Tomishige, K. (2003) 'Demonstration of real biomass gasification drastically promoted by effective catalyst', *Applied Catalysis A: General*, 246(1), pp. 103-116.
- Aznar, M.P. and Delgado, J. (1992) 'Biomass for energy and industry', *Amsterdam: Elsevier*.
- Baker, E.G., Brown, M.D., Moore, R.H., Mudge, L.K. and Elliott, D.C. (1986) *Engineering analysis of biomass gasifier product gas cleaning technology*. Pacific Northwest Lab., Richland, WA (USA).
- Basu, P. (2010) *Biomass gasification and pyrolysis: practical design and theory*. Academic press.
- Bellakhal, N., Draou, K. and Brisset, J.L. (1997) 'Electrochemical investigation of copper oxide films formed by oxygen plasma treatment', *Journal of applied electrochemistry*, 27(4), pp. 414-421.

Bityurin, V.A., Filimonova, E.A. and Naidis, G.V. (2009) 'Simulation of naphthalene conversion in biogas initiated by pulsed corona discharges', *IEEE Transactions on Plasma Science*, 37(6), pp. 911-919.

Blin-Simiand, N., Jorand, F., Magne, L., Pasquiers, S., Postel, C. and Vacher, J.R. (2008) 'Plasma reactivity and plasma-surface interactions during treatment of toluene by a dielectric barrier discharge', *Plasma Chemistry and Plasma Processing*, 28(4), pp. 429-466.

Bo, Z., Yan, J., Li, X., Chi, Y. and Cen, K. (2008) 'Scale-up analysis and development of gliding arc discharge facility for volatile organic compounds decomposition', *Journal of hazardous materials*, 155(3), pp. 494-501.

Bosmans, A.W., S; Helsen, L (2013) 'Waste to clean syngas: Avoiding Tar Problems', *2nd International Enhanced Landfill Mining Symposium*.

Brage, C., Yu, Q., Chen, G. and Sjöström, K. (2000) 'Tar evolution profiles obtained from gasification of biomass and coal', *Biomass and Bioenergy*, 18(1), pp. 87-91.

Bridgwater, A.V. (1984) 'Thermochemical processing of biomass'.

Bridgwater, A.V. (1995) 'The technical and economic feasibility of biomass gasification for power generation', *Fuel*, 74(5), pp. 631-653.

Bridgwater, A.V., Dick, C.M. and Hauge, R.A. (1996) 'The fast pyrolysis of oil seed rape'.

Bridgwater, A.V. and Evans, G.D. (1993) *An assessment of thermochemical conversion systems for processing biomass and refuse*. Energy Technology Support Unit Harwell, UK.

Bromberg, L., Cohn, D.R., Rabinovich, A. and Alexeev, N. (2001) 'Hydrogen manufacturing using low current, non-thermal plasma boosted fuel converters'.

Brooks, C.T., Peacock, S.J. and Reuben, B.G. (1979) 'Pyrolysis of benzene', *Journal of the Chemical Society, Faraday Transactions 1: Physical Chemistry in Condensed Phases*, 75, pp. 652-662.

Burr, J.G., Meyer, R.A. and Strong, J.D. (1964) 'The hydrogen carrier technique for the pyrolysis of toluene', *Journal of the American Chemical Society*, 86(18), pp. 3846-3850.

Castaño, P., Arandes, J.M., Pawelec, B., Olazar, M. and Bilbao, J. (2008) 'Kinetic modeling for assessing the product distribution in toluene hydrocracking on a Pt/HZSM-5 catalyst', *Industrial & Engineering Chemistry Research*, 47(4), pp. 1043-1050.

Cenian, A., Chernukho, A. and Borodin, V. (1995) 'Modeling of Plasma - Chemical Reactions in Gas Mixture of CO<sub>2</sub> lasers. II. Theoretical Model and its Verification', *Contributions to Plasma Physics*, 35(3), pp. 273-296.

Chang, J.S., Lawless, P.A. and Yamamoto, T. (1991) 'Corona discharge processes', *IEEE Transactions on plasma science*, 19(6), pp. 1152-1166.

- Chen, G.-Y., Liu, C., Ma, W.-C., Yan, B.-B. and Ji, N. (2015) 'Catalytic Cracking of Tar from Biomass Gasification over a HZSM-5-Supported Ni-MgO Catalyst', *Energy & Fuels*, 29(12), pp. 7969-7974.
- Chen, H.L., Lee, H.M., Chen, S.H., Chang, M.B., Yu, S.J. and Li, S.N. (2009) 'Removal of volatile organic compounds by single-stage and two-stage plasma catalysis systems: a review of the performance enhancement mechanisms, current status, and suitable applications', *Environmental science & technology*, 43(7), pp. 2216-2227.
- Chen, Y. (2016) 'Electrical Breakdown of Gases in Subatmospheric Pressure'.
- Chiremba, E., Zhang, K., Kazak, C. and Akay, G. (2017) 'Direct nonoxidative conversion of methane to hydrogen and higher hydrocarbons by dielectric barrier discharge plasma with plasma catalysis promoters', *AIChE Journal*, 63(10), pp. 4418-4429.
- Cho, I.J., Park, H.-W., Park, D.-W. and Choi, S. (2015) 'Enhancement of synthesis gas production using gasification-plasma hybrid system', *International Journal of hydrogen Energy*, 40(4), pp. 1709-1716.
- Chun, Y.N., Kim, S.C. and Yoshikawa, K. (2012) 'Removal characteristics of tar benzene using the externally oscillated plasma reformer', *Chemical Engineering and Processing: Process Intensification*, 57, pp. 65-74.
- Chun, Y.N., Kim, S.C. and Yoshikawa, K. (2013) 'Decomposition of benzene as a surrogate tar in a gliding Arc plasma', *Environmental Progress & Sustainable Energy*, 32(3), pp. 837-845.
- Chun, Y.N. and Lim, M.S. (2012) 'Light tar decomposition of product pyrolysis gas from sewage sludge in a gliding arc plasma reformer', *Environmental Engineering Research*, 17(2), pp. 89-94.
- Coll, R., Salvado, J., Farriol, X. and Montane, D. (2001) 'Steam reforming model compounds of biomass gasification tars: conversion at different operating conditions and tendency towards coke formation', *Fuel Processing Technology*, 74(1), pp. 19-31.
- Corella, J., Herguido, J., Gonzalez-Saiz, J., Alday, F.J. and Rodriguez-Trujillo, J.L. (1988) 'Fluidized bed steam gasification of biomass with dolomite and with a commercial FCC catalyst', in *Research in thermochemical biomass conversion*. Springer, pp. 754-765.
- Corella, J., Orió, A. and Toledo, J.-M. (1999) 'Biomass gasification with air in a fluidized bed: exhaustive tar elimination with commercial steam reforming catalysts', *Energy & Fuels*, 13(3), pp. 702-709.
- Czernichowski, A. (1994) 'Gliding arc: applications to engineering and environment control', *Pure and Applied Chemistry*, 66(6), pp. 1301-1310.

- Darwent, B.d. (1970) 'Bond dissociation energies in simple molecules', *NSRDS-NBS NO. 31, U. S. DEPT. COMMERCE, WASHINGTON, D. C. JAN. 1970, 48 P.*
- Dayton, D. (2002) *Review of the literature on catalytic biomass tar destruction: Milestone completion report*. National Renewable Energy Lab., Golden, CO (US).
- De Filippis, P., Borgianni, C., Paolucci, M. and Pochetti, F. (2004) 'Gasification process of Cuban bagasse in a two-stage reactor', *Biomass and Bioenergy*, 27(3), pp. 247-252.
- de Jong, W., Ünal, Ö., Andries, J., Hein, K.R.G. and Spliethoff, H. (2003) 'Biomass and fossil fuel conversion by pressurised fluidised bed gasification using hot gas ceramic filters as gas cleaning', *Biomass and Bioenergy*, 25(1), pp. 59-83.
- Demidiouk, V., Moon, S.I. and Chae, J.O. (2003) 'Toluene and butyl acetate removal from air by plasma-catalytic system', *Catalysis Communications*, 4(2), pp. 51-56.
- Devi, L., Ptasiński, K.J. and Janssen, F.J.J.G. (2003) 'A review of the primary measures for tar elimination in biomass gasification processes', *Biomass and bioenergy*, 24(2), pp. 125-140.
- Diaz, G., Sharma, N., Leal-Quiros, E. and Munoz-Hernandez, A. (2015) 'Enhanced hydrogen production using steam plasma processing of biomass: experimental apparatus and procedure', *International Journal of Hydrogen Energy*, 40(5), pp. 2091-2098.
- Dou, B., Gao, J., Sha, X. and Baek, S.W. (2003) 'Catalytic cracking of tar component from high-temperature fuel gas', *Applied Thermal Engineering*, 23(17), pp. 2229-2239.
- Draelants, D.J., Zhao, H.B. and Baron, G.V. (2000) 'Catalytic conversion of tars in biomass gasification fuel gases with nickel-activated ceramic filters', in *Studies in surface science and catalysis*. Elsevier, pp. 1595-1600.
- Ekstrom, C., Lindman, N. and Petersson, R. (1988) 'Fundamentals of thermochemical biomass conversion', *London and New York: Elsevier Applied Science*.
- El-Rub, Z.A., Bramer, E.A. and Brem, G. (2008) 'Experimental comparison of biomass chars with other catalysts for tar reduction', *Fuel*, 87(10-11), pp. 2243-2252.
- Elliott, R.M., Nogueira, M.F.M., Silva Sobrinho, A.S., Couto, B.A.P., Maciel, H.S. and Lacava, P.T. (2013) 'Tar reforming under a microwave plasma torch', *Energy & Fuels*, 27(2), pp. 1174-1181.
- Engelen, K., Zhang, Y., Draelants, D.J. and Baron, G.V. (2003) 'A novel catalytic filter for tar removal from biomass gasification gas: Improvement of the catalytic activity in presence of H<sub>2</sub>S', *Chemical Engineering Science*, 58(3-6), pp. 665-670.
- Fagbemi, L., Khezami, L. and Capart, R. (2001) 'Pyrolysis products from different biomasses: application to the thermal cracking of tar', *Applied energy*, 69(4), pp. 293-306.

- Fassinou, W.F., Van de Steene, L., Toure, S., Volle, G. and Girard, P. (2009) 'Pyrolysis of Pinus pinaster in a two-stage gasifier: Influence of processing parameters and thermal cracking of tar', *Fuel processing technology*, 90(1), pp. 75-90.
- Ferreira, C.M. and Moisan, M. (2013) *Microwave discharges: fundamentals and applications*. Springer Science & Business Media.
- Fjellerup, J., Ahrenfeldt, J., Henriksen, U. and Gøbel, B. (2005) *Formation, Decomposition and Cracking of Biomass Tars in Gasification* (87-7475-326-6). Technical University of Denmark. Department of Mechanical Engineering.
- Freel, J. and Galwey, A.K. (1968) 'Hydrocarbon cracking reactions on nickel', *Journal of Catalysis*, 10(3), pp. 277-289.
- Fridman, A. (2008) *Plasma chemistry*. Cambridge university press.
- Fridman, A., Chirokov, A. and Gutsol, A. (2005) 'Non-thermal atmospheric pressure discharges', *Journal of Physics D: Applied Physics*, 38(2), p. R1.
- Fridman, A., Nester, S., Kennedy, L.A., Saveliev, A. and Mutaf-Yardimci, O. (1999) 'Gliding arc gas discharge', *Progress in Energy and Combustion Science*, 25(2), pp. 211-231.
- Fridman, A.A., Petrousov, A., Chapelle, J., Cormier, J.M., Czernichowski, A., Lesueur, H. and Stevefelt, J. (1994) 'Model of the gliding arc', *Journal de Physique III*, 4(8), pp. 1449-1465.
- Furusawa, T. and Tsutsumi, A. (2005) 'Comparison of Co/MgO and Ni/MgO catalysts for the steam reforming of naphthalene as a model compound of tar derived from biomass gasification', *Applied Catalysis A: General*, 278(2), pp. 207-212.
- Gai, C., Dong, Y., Fan, P., Zhang, Z., Liang, J. and Xu, P. (2015) 'Kinetic study on thermal decomposition of toluene in a micro fluidized bed reactor', *Energy Conversion and Management*, 106, pp. 721-727.
- Gaikwad, V., Kennedy, E., Mackie, J., Holdsworth, C., Molloy, T., Kundu, S., Stockenhuber, M. and Dlugogorski, B. (2018) 'Process for chloroform decomposition: Nonthermal plasma polymerization with methane and hydrogen', *Industrial & Engineering Chemistry Research*, 57(28), pp. 9075-9082.
- Gandhi, M.S., Ananth, A., Mok, Y.S., Song, J.-I. and Park, K.-H. (2013) 'Time dependence of ethylene decomposition and byproducts formation in a continuous flow dielectric-packed plasma reactor', *Chemosphere*, 91(5), pp. 685-691.
- Gil, J., Caballero, M.A., Martín, J.A., Aznar, M.-P. and Corella, J. (1999) 'Biomass gasification with air in a fluidized bed: effect of the in-bed use of dolomite under different operation conditions', *Industrial & Engineering Chemistry Research*, 38(11), pp. 4226-4235.

- Guo, T., Li, X., Li, J., Peng, Z., Xu, L., Dong, J., Cheng, P. and Zhou, Z. (2018) 'On-line quantification and human health risk assessment of organic by-products from the removal of toluene in air using non-thermal plasma', *Chemosphere*, 194, pp. 139-146.
- Guo, Y.-F., Ye, D.-Q., Chen, K.-F., He, J.-C. and Chen, W.-L. (2006) 'Toluene decomposition using a wire-plate dielectric barrier discharge reactor with manganese oxide catalyst in situ', *Journal of Molecular Catalysis A: Chemical*, 245(1), pp. 93-100.
- Gusta, E., Dalai, A.K., Uddin, M.A. and Sasaoka, E. (2009) 'Catalytic decomposition of biomass tars with dolomites', *Energy & Fuels*, 23(4), pp. 2264-2272.
- Hallgren, A. (1997) *Improved technologies for the gasification of energy crops. Publishable Final Report (TPS AB), European Commission JOULE III Programme, Project no. JOR3-CT97-0125.*
- Han, J. and Kim, H. (2008) 'The reduction and control technology of tar during biomass gasification/pyrolysis: an overview', *Renewable and sustainable energy reviews*, 12(2), pp. 397-416.
- Harding, L.B., Georgievskii, Y. and Klippenstein, S.J. (2005) 'Predictive theory for hydrogen atom– hydrocarbon radical association kinetics', *The Journal of Physical Chemistry A*, 109(21), pp. 4646-4656.
- Hasler, P., Buehler, R. and Nussbaumer, T. (1997) *Evaluation of Gas Cleaning Technologies for Small Scale Biomass Gasifiers: Biomass Programme; Final Report.* Bundesamt für Energiewirtschaft.
- Hasler, P.H. and Nussbaumer, T. (1999) 'Gas cleaning for IC engine applications from fixed bed biomass gasification', *Biomass and Bioenergy*, 16(6), pp. 385-395.
- He, M., Hu, Z., Xiao, B., Li, J., Guo, X., Luo, S., Yang, F., Feng, Y., Yang, G. and Liu, S. (2009) 'Hydrogen-rich gas from catalytic steam gasification of municipal solid waste (MSW): influence of catalyst and temperature on yield and product composition', *International Journal of Hydrogen Energy*, 34(1), pp. 195-203.
- Hepola, J., McCarty, J., Krishnan, G. and Wong, V. (1999) 'Elucidation of behavior of sulfur on nickel-based hot gas cleaning catalysts', *Applied Catalysis B: Environmental*, 20(3), pp. 191-203.
- Hlina, M., Hrabovsky, M., Kavka, T. and Konrad, M. (2014) 'Production of high quality syngas from argon/water plasma gasification of biomass and waste', *Waste management*, 34(1), pp. 63-66.

- Hosoya, T., Kawamoto, H. and Saka, S. (2008) 'Pyrolysis gasification reactivities of primary tar and char fractions from cellulose and lignin as studied with a closed ampoule reactor', *Journal of Analytical and Applied Pyrolysis*, 83(1), pp. 71-77.
- Hsiao, M.C., Penetrante, B.M., Merritt, B.T., Vogtlin, G.E. and Wallman, P.H. (1997) 'Effect of gas temperature on pulsed corona discharge processing of acetone, benzene and ethylene', *Journal of Advanced Oxidation Technologies*, 2(2), pp. 306-311.
- Huang, H., Ye, D., Leung, D.Y.C., Feng, F. and Guan, X. (2011) 'Byproducts and pathways of toluene destruction via plasma-catalysis', *Journal of Molecular Catalysis A: Chemical*, 336(1), pp. 87-93.
- Huang, Y., Yin, X., Wu, C., Wang, C., Xie, J., Zhou, Z., Ma, L. and Li, H. (2009) 'Effects of metal catalysts on CO<sub>2</sub> gasification reactivity of biomass char', *Biotechnology advances*, 27(5), pp. 568-572.
- Jamróz, P., Kordylewski, W. and Wnukowski, M. (2018) 'Microwave plasma application in decomposition and steam reforming of model tar compounds', *Fuel Processing Technology*, 169, pp. 1-14.
- Jegers, H.E. and Klein, M.T. (1985) 'Primary and secondary lignin pyrolysis reaction pathways', *Industrial & Engineering Chemistry Process Design and Development*, 24(1), pp. 173-183.
- Jess, A. (1996) 'Mechanisms and kinetics of thermal reactions of aromatic hydrocarbons from pyrolysis of solid fuels', *Fuel*, 75(12), pp. 1441-1448.
- Jiménez, R., García, X., López, T. and Gordon, A.L. (2008) 'Catalytic combustion of soot. Effects of added alkali metals on CaO–MgO physical mixtures', *Fuel Processing Technology*, 89(11), pp. 1160-1168.
- Jurbergs, D., Rogojina, E., Mangolini, L. and Kortshagen, U. (2006) 'Silicon nanocrystals with ensemble quantum yields exceeding 60%', *Applied Physics Letters*, 88(23), p. 233116.
- Karatum, O. and Deshusses, M.A. (2016) 'A comparative study of dilute VOCs treatment in a non-thermal plasma reactor', *Chemical Engineering Journal*, 294, pp. 308-315.
- Kim, H.-H. (2004a) 'Nonthermal Plasma Processing for Air-Pollution Control: A Historical Review, Current Issues, and Future Prospects', *Plasma Processes and Polymers*, 1(2), pp. 91-110.
- Kim, H.H. (2004b) 'Nonthermal plasma processing for air - pollution control: a historical review, current issues, and future prospects', *Plasma Processes and Polymers*, 1(2), pp. 91-110.

- Kinoshita, C.M., Wang, Y. and Zhou, J. (1994) 'Tar formation under different biomass gasification conditions', *Journal of Analytical and Applied Pyrolysis*, 29(2), pp. 169-181.
- Kinoshita, C.M., Wang, Y. and Zhou, J. (1995) 'Effect of Reformer Conditions on Catalytic Reforming of Biomass-Gasification Tars', *Industrial & Engineering Chemistry Research*, 34(9), pp. 2949-2954.
- Knight, R.A. (2000) 'Experience with raw gas analysis from pressurized gasification of biomass', *Biomass and Bioenergy*, 18(1), pp. 67-77.
- Kogelschatz, U. (2003) 'Dielectric-barrier discharges: their history, discharge physics, and industrial applications', *Plasma chemistry and plasma processing*, 23(1), pp. 1-46.
- Kohno, H., Berezin, A.A., Chang, J.-S., Tamura, M., Yamamoto, T., Shibuya, A. and Honda, S. (1998) 'Destruction of volatile organic compounds used in a semiconductor industry by a capillary tube discharge reactor', *IEEE Transactions on Industry Applications*, 34(5), pp. 953-966.
- Kortshagen, U.R., Sankaran, R.M., Pereira, R.N., Girshick, S.L., Wu, J.J. and Aydil, E.S. (2016) 'Nonthermal plasma synthesis of nanocrystals: fundamental principles, materials, and applications', *Chemical reviews*, 116(18), pp. 11061-11127.
- Kumar, A., Jones, D.D. and Hanna, M.A. (2009) 'Thermochemical biomass gasification: a review of the current status of the technology', *Energies*, 2(3), pp. 556-581.
- Lappas, A.A., Samolada, M.C., Iatridis, D.K., Voutetakis, S.S. and Vasalos, I.A. (2002) 'Biomass pyrolysis in a circulating fluid bed reactor for the production of fuels and chemicals', *Fuel*, 81(16), pp. 2087-2095.
- Lebedev, Y.A. (1998) 'Plasma chemistry of nonequilibrium microwave discharges. Status and tendency', *Le Journal de Physique IV*, 8(PR7), pp. Pr7-369-Pr7-380.
- Lebedev, Y.A. (2010) *Journal of Physics: Conference Series*. IOP Publishing.
- Lee, B.-K., Jung, K.-R. and Park, S.-H. (2008) 'Development and application of a novel swirl cyclone scrubber—(1) Experimental', *Journal of Aerosol Science*, 39(12), pp. 1079-1088.
- Lee, H.M. and Chang, M.B. (2003) 'Abatement of gas-phase p-xylene via dielectric barrier discharges', *Plasma chemistry and plasma processing*, 23(3), pp. 541-558.
- Lettner, F., Timmerer, H. and Haselbacher, P. (2007) *Biomass gasification—state of the art description, Guideline for safe and eco-friendly biomass gasification Intelligent Energy—Europe (IEE), 2007, Report. EIE/06/078/SI2. 447511.*
- Li, C., Yamamoto, Y., Suzuki, M., Hirabayashi, D. and Suzuki, K. (2009) 'Study on the combustion kinetic characteristics of biomass tar under catalysts', *Journal of thermal analysis and calorimetry*, 95(3), pp. 991-997.

- Liang, W.-J., Ma, L., Liu, H. and Li, J. (2013) 'Toluene degradation by non-thermal plasma combined with a ferroelectric catalyst', *Chemosphere*, 92(10), pp. 1390-1395.
- Liu, C.-j., Xu, G.-h. and Wang, T. (1999) 'Non-thermal plasma approaches in CO<sub>2</sub> utilization', *Fuel Processing Technology*, 58(2-3), pp. 119-134.
- Liu, L., Wang, Q., Song, J., Yang, X. and Sun, Y. (2018) 'Dry reforming of model biomass pyrolysis products to syngas by dielectric barrier discharge plasma', *International Journal of Hydrogen Energy*, 43(22), pp. 10281-10293.
- Liu, S., Mei, D., Wang, L. and Tu, X. (2017a) 'Steam reforming of toluene as biomass tar model compound in a gliding arc discharge reactor', *Chemical Engineering Journal*, 307, pp. 793-802.
- Liu, S.Y., Mei, D.H., Nahil, M.A., Gadkari, S., Gu, S., Williams, P.T. and Tu, X. (2017b) 'Hybrid plasma-catalytic steam reforming of toluene as a biomass tar model compound over Ni/Al<sub>2</sub>O<sub>3</sub> catalysts', *Fuel Processing Technology*, 166, pp. 269-275.
- Livingston, W.R., McGhee, B.F. and Cooke, S. (1997) 'Studies on the thermal processing of biomass and waste materials'.
- Locht, R. and Davister, M. (1995) 'The dissociative electroionization of carbon dioxide by low-energy electron impact. The C<sup>+</sup>, O<sup>+</sup> and CO<sup>+</sup> dissociation channels', *International journal of mass spectrometry and ion processes*, 144(1-2), pp. 105-129.
- Luo, S., Xiao, B., Hu, Z., Liu, S., Guo, X. and He, M. (2009) 'Hydrogen-rich gas from catalytic steam gasification of biomass in a fixed bed reactor: Influence of temperature and steam on gasification performance', *International Journal of hydrogen energy*, 34(5), pp. 2191-2194.
- Magureanu, M., Mandache, N.B., Gaigneaux, E., Paun, C. and Parvulescu, V.I. (2006) 'Toluene oxidation in a plasma-catalytic system', *Journal of applied physics*, 99(12), p. 123301.
- Magureanu, M., Piroi, D., Mandache, N.B., Pârvulescu, V.I., Pârvulescu, V., Cojocaru, B., Cadigan, C., Richards, R., Daly, H. and Hardacre, C. (2011) 'In situ study of ozone and hybrid plasma Ag–Al catalysts for the oxidation of toluene: evidence of the nature of the active sites', *Applied Catalysis B: Environmental*, 104(1), pp. 84-90.
- Marino, F.J., Cerrella, E.G., Duhalde, S., Jobbagy, M. and Laborde, M.A. (1998) 'Hydrogen from steam reforming of ethanol. Characterization and performance of copper-nickel supported catalysts', *International Journal of Hydrogen Energy*, 23(12), pp. 1095-1101.

- Materazzi, M., Lettieri, P., Taylor, R. and Chapman, C. (2016) 'Performance analysis of RDF gasification in a two stage fluidized bed–plasma process', *Waste Management*, 47, pp. 256-266.
- McKendry, P. (2002a) 'Energy production from biomass (part 1): overview of biomass', *Bioresource technology*, 83(1), pp. 37-46.
- McKendry, P. (2002b) 'Energy production from biomass (part 2): conversion technologies', *Bioresource technology*, 83(1), pp. 47-54.
- Michelmore, A., Steele, D.A., Whittle, J.D., Bradley, J.W. and Short, R.D. (2013) 'Nanoscale deposition of chemically functionalised films via plasma polymerisation', *Rsc Advances*, 3(33), pp. 13540-13557.
- Milne, T.A., Evans, R.J. and Abatzoglou, N. (1998) *Biomass Gasifier "Tars": Their Nature, Formation, and Conversion*. National Renewable Energy Laboratory, Golden, CO (US).
- Miyazawa, T., Kimura, T., Nishikawa, J., Kunimori, K. and Tomishige, K. (2005) 'Catalytic properties of Rh/CeO<sub>2</sub>/SiO<sub>2</sub> for synthesis gas production from biomass by catalytic partial oxidation of tar', *Science and technology of Advanced Materials*, 6(6), pp. 604-614.
- Miziolek, A.W., Herron, J.T., Mallard, W.G., Hudgens, J.W., Green, D.S., Tsang, W. and Chang, J.S. (1994) *Proc. ELMECO94*.
- Moreau, M., Orange, N. and Feuilloley, M.G.J. (2008) 'Non-thermal plasma technologies: new tools for bio-decontamination', *Biotechnology advances*, 26(6), pp. 610-617.
- Morf, P., Hasler, P. and Nussbaumer, T. (2002) 'Mechanisms and kinetics of homogeneous secondary reactions of tar from continuous pyrolysis of wood chips', *Fuel*, 81(7), pp. 843-853.
- Myrén, C., Hörnell, C., Björnbom, E. and Sjöström, K. (2002) 'Catalytic tar decomposition of biomass pyrolysis gas with a combination of dolomite and silica', *Biomass and Bioenergy*, 23(3), pp. 217-227.
- Nair, S.A., Pemen, A.J.M., Yan, K., Van Gompel, F.M., Van Leuken, H.E.M., Van Heesch, E.J.M., Ptasinski, K.J. and Drinkenburg, A.A.H. (2003a) 'Tar removal from biomass-derived fuel gas by pulsed corona discharges', *Fuel Processing Technology*, 84(1), pp. 161-173.
- Nair, S.A., Pemen, A.J.M., Yan, K., Van Gompel, F.M., Van Leuken, H.E.M., Van Heesch, E.J.M., Ptasinski, K.J. and Drinkenburg, A.A.H. (2003b) 'Tar removal from biomass-derived fuel gas by pulsed corona discharges', *Fuel Processing Technology*, 84(1-3), pp. 161-173.
- Nair, S.A., Pemen, A.J.M., Yan, K., Van Heesch, E.J.M., Ptasinski, K.J. and Drinkenburg, A.A.H. (2003c) 'Chemical processes in tar removal from biomass derived fuel gas by pulsed corona discharges', *Plasma chemistry and plasma processing*, 23(4), pp. 665-680.

Nair, S.A., Yan, K., Pemen, A.J.M., Van Heesch, E.J.M., Ptasinski, K.J. and Drinkenburg, A.A.H. (2004) 'Tar removal from biomass-derived fuel gas by pulsed corona discharges. A chemical kinetic study', *Industrial & engineering chemistry research*, 43(7), pp. 1649-1658.

Narvaez, I., Orío, A., Aznar, M.P. and Corella, J. (1996) 'Biomass gasification with air in an atmospheric bubbling fluidized bed. Effect of six operational variables on the quality of the produced raw gas', *Industrial & Engineering Chemistry Research*, 35(7), pp. 2110-2120.

Nunnally, T., Tsangaris, A., Rabinovich, A., Nirenberg, G., Chernets, I. and Fridman, A. (2014) 'Gliding arc plasma oxidative steam reforming of a simulated syngas containing naphthalene and toluene', *international journal of hydrogen energy*, 39(23), pp. 11976-11989.

Palma, C.F. (2013) 'Modelling of tar formation and evolution for biomass gasification: a review', *Applied Energy*, 111, pp. 129-141.

Park, H.J., Park, S.H., Sohn, J.M., Park, J., Jeon, J.-K., Kim, S.-S. and Park, Y.-K. (2010) 'Steam reforming of biomass gasification tar using benzene as a model compound over various Ni supported metal oxide catalysts', *Bioresource Technology*, 101(1), pp. S101-S103.

Parthasarathy, P. and Narayanan, K.S. (2014) 'Hydrogen production from steam gasification of biomass: influence of process parameters on hydrogen yield—a review', *Renewable Energy*, 66, pp. 570-579.

Pemen, A.J.M., Nair, S.A., Yan, K., van Heesch, E.J.M., Ptasinski, K.J. and Drinkenburg, A.A.H. (2003) 'Pulsed Corona Discharges for Tar Removal from Biomass Derived Fuel Gas', *Plasmas and Polymers*, 8(3), pp. 209-224.

Pérez, P., Aznar, P.M., Caballero, M.A., Gil, J., Martín, J.A. and Corella, J. (1997) 'Hot gas cleaning and upgrading with a calcined dolomite located downstream a biomass fluidized bed gasifier operating with steam– oxygen mixtures', *Energy & fuels*, 11(6), pp. 1194-1203.

Petitpas, G., Rollier, J.D., Darmon, A., Gonzalez-Aguilar, J., Metkemeijer, R. and Fulcheri, L. (2007) 'A comparative study of non-thermal plasma assisted reforming technologies', *International Journal of Hydrogen Energy*, 32(14), pp. 2848-2867.

Phuphuakrat, T., Nipattummakul, N., Namioka, T., Kerdsuwan, S. and Yoshikawa, K. (2010) 'Characterization of tar content in the syngas produced in a downdraft type fixed bed gasification system from dried sewage sludge', *Fuel*, 89(9), pp. 2278-2284.

Polychronopoulou, K., Costa, C.N. and Efstathiou, A.M. (2004) 'The steam reforming of phenol reaction over supported-Rh catalysts', *Applied Catalysis A: General*, 272(1-2), pp. 37-52.

Rabou, L.P.L.M., Zwart, R.W.R., Vreugdenhil, B.J. and Bos, L. (2009) 'Tar in biomass producer gas, the Energy research Centre of the Netherlands (ECN) experience: an enduring challenge', *Energy & Fuels*, 23(12), pp. 6189-6198.

Rampling, T.W.A. and Gill, P.J. (1994) 'Fundamental research on the thermal treatment of wastes and biomass'.

Richardson, Y., Blin, J. and Julbe, A. (2012) 'A short overview on purification and conditioning of syngas produced by biomass gasification: catalytic strategies, process intensification and new concepts', *Progress in Energy and Combustion Science*, 38(6), pp. 765-781.

Ruiz, J.A., Juárez, M.C., Morales, M.P., Muñoz, P. and Mendivil, M.A. (2013) 'Biomass gasification for electricity generation: Review of current technology barriers', *Renewable and Sustainable Energy Reviews*, 18, pp. 174-183.

Schmidt, S., Giesa, S., Drochner, A. and Vogel, H. (2011) 'Catalytic tar removal from bio syngas—catalyst development and kinetic studies', *Catalysis Today*, 175(1), pp. 442-449.

Seshadri, K.S. and Shamsi, A. (1998) 'Effects of temperature, pressure, and carrier gas on the cracking of coal tar over a char– dolomite mixture and calcined dolomite in a fixed-bed reactor', *Industrial & engineering chemistry research*, 37(10), pp. 3830-3837.

Šícha, M., Veselý, V., Šubertová, S. and Seifert, A. (1968) 'Microwave investigation of acoustic waves in low-pressure plasma', *Czechoslovak Journal of Physics B*, 18(1), pp. 86-91.

Simell, P.A., Hakala, N.A.K., Haario, H.E. and Krause, A.O.I. (1997a) 'Catalytic decomposition of gasification gas tar with benzene as the model compound', *Industrial & engineering chemistry research*, 36(1), pp. 42-51.

Simell, P.A., Hepola, J.O. and Krause, A.O.I. (1997b) 'Effects of gasification gas components on tar and ammonia decomposition over hot gas cleanup catalysts', *Fuel*, 76(12), pp. 1117-1127.

Simell, P.A., Hirvensalo, E.K., Smolander, V.T. and Krause, A.O.I. (1999) 'Steam reforming of gasification gas tar over dolomite with benzene as a model compound', *Industrial & Engineering Chemistry Research*, 38(4), pp. 1250-1257.

Sinağ, A., Sungur, M. and Canel, M. (2006) 'Effect of experimental conditions on the yields during the copyrolysis of Mustafa Kemal Paşa (MKP) lignite (Turkey) with low-density polyethylene', *Energy & fuels*, 20(4), pp. 1609-1613.

Skoblia, S., Koutsky, B., Malecha, J. and Marsak, J. (2015) *Nickel Catalyst for hot gas cleaning in biomass gasification*. Institute of Chemical Technology Prague, .

- Song, Y.-H., Kim, S.-J., Choi, K.-I. and Yamamoto, T. (2002) 'Effects of adsorption and temperature on a nonthermal plasma process for removing VOCs', *Journal of electrostatics*, 55(2), pp. 189-201.
- Stassen, H.E.M. (1993) 'Strategies for upgrading producer gas from fixed bed gasifier systems to internal combustion engine quality', *Biomass gasification: hot-gas clean-up. IEA Biomass Gasification Working Group*, p. 33.
- Strom, E., Linanki, L. and Sjoström, K. (1985) 'Biomass conversion'. London: Elsevier Applied Science.
- Sun, J., Wang, Q., Wang, W., Song, Z., Zhao, X., Mao, Y. and Ma, C. (2017) 'Novel treatment of a biomass tar model compound via microwave-metal discharges', *Fuel*, 207, pp. 121-125.
- Sutton, D., Kelleher, B. and Ross, J.R.H. (2001) 'Review of literature on catalysts for biomass gasification', *Fuel Processing Technology*, 73(3), pp. 155-173.
- Swierczynski, D., Courson, C. and Kiennemann, A. (2008) 'Study of steam reforming of toluene used as model compound of tar produced by biomass gasification', *Chemical Engineering and Processing: Process Intensification*, 47(3), pp. 508-513.
- Szwarc, M. (1948) 'The C-H bond energy in toluene and xylenes', *The Journal of Chemical Physics*, 16(2), pp. 128-136.
- Tamhankar, S.S., Tsuchiya, K. and Riggs, J.B. (1985) 'Catalytic cracking of benzene on iron oxide-silica: catalyst activity and reaction mechanism', *Applied Catalysis*, 16(1), pp. 103-121.
- Tao, K., Ohta, N., Liu, G., Yoneyama, Y., Wang, T. and Tsubaki, N. (2013) 'Plasma enhanced catalytic reforming of biomass tar model compound to syngas', *Fuel*, 104, pp. 53-57.
- Taralas, G. and Kontominas, M.G. (2004) 'Kinetic modelling of VOC catalytic steam pyrolysis for tar abatement phenomena in gasification/pyrolysis technologies', *Fuel*, 83(9), pp. 1235-1245.
- Taralas, G., Kontominas, M.G. and Kakatsios, X. (2003) 'Modeling the thermal destruction of toluene (C<sub>7</sub>H<sub>8</sub>) as tar-related species for fuel gas cleanup', *Energy & Fuels*, 17(2), pp. 329-337.
- Thambimuthu, K.V. (1993) 'Gas cleaning for advanced coal-based power generation', *EACR/53*.
- Tippayawong, N. and Inthasan, P. (2010) 'Investigation of light tar cracking in a gliding arc plasma system', *International Journal of Chemical Reactor Engineering*, 8(1).

- Tomishige, K., Asadullah, M. and Kunimori, K. (2004) 'Syngas production by biomass gasification using Rh/CeO<sub>2</sub>/SiO<sub>2</sub> catalysts and fluidized bed reactor', *Catalysis Today*, 89(4), pp. 389-403.
- Tu, X., Verheyde, B., Corthals, S., Paulussen, S. and Sels, B.F. (2011) 'Effect of packing solid material on characteristics of helium dielectric barrier discharge at atmospheric pressure', *Physics of Plasmas*, 18(8), p. 080702.
- Tu, X. and Whitehead, J.C. (2012) 'Plasma-catalytic dry reforming of methane in an atmospheric dielectric barrier discharge: Understanding the synergistic effect at low temperature', *Applied Catalysis B: Environmental*, 125, pp. 439-448.
- Tu, X. and Whitehead, J.C. (2014) 'Plasma dry reforming of methane in an atmospheric pressure AC gliding arc discharge: co-generation of syngas and carbon nanomaterials', *international journal of hydrogen energy*, 39(18), pp. 9658-9669.
- Uraahima, K., Chang, J.S. and Thompson, H. (1995) *Proc 12th int symp plasma chemistry (J. Heherlein, ed.)*. Minneapolis, MN: Univ. of Minnesota Press.
- Urashima, K. and Chang, J.-S. (2000) 'Removal of volatile organic compounds from air streams and industrial flue gases by non-thermal plasma technology', *IEEE Transactions on Dielectrics and Electrical Insulation*, 7(5), pp. 602-614.
- Urashima, K., Chang, J.S. and Ito, T. (1997) 'Reduction of NO<sub>x</sub> from combustion flue gases by superimposed barrier discharge plasma reactors', *IEEE Transactions on industry applications*, 33(4), pp. 879-886.
- Van Paasen, S.V.B., Rabou, L. and Bär, R. (2004) 'Tar removal with a wet electrostatic precipitator (ESP); a parametric study', *Acknowledgement/Preface*, p. 33.
- Walawender, W.P. and Fan, L.T. (1981) *Energy from biomass and wastes: symposium papers (USA)*.
- Walawender, W.P., Hoveland, D.A. and Fan, L.T. (1985) 'Steam Gasification of Alpha Cellulose in a Fluid Bed Reactor', in *Fundamentals of thermochemical biomass conversion*. Springer, pp. 897-910.
- Wang, B., Chi, C., Xu, M., Wang, C. and Meng, D. (2017a) 'Plasma-catalytic removal of toluene over CeO<sub>2</sub>-MnO<sub>x</sub> catalysts in an atmosphere dielectric barrier discharge', *Chemical Engineering Journal*, 322, pp. 679-692.
- Wang, B., Chi, C., Xu, M., Wang, C. and Meng, D. (2017b) 'Plasma-catalytic removal of toluene over CeO<sub>2</sub>-MnO<sub>x</sub> catalysts in an atmosphere dielectric barrier discharge', *Chemical Engineering Journal*, 322, pp. 679-692.

- Wang, T., Chang, J., Lv, P. and Zhu, J. (2005) 'Novel catalyst for cracking of biomass tar', *Energy & Fuels*, 19(1), pp. 22-27.
- Wang, W., Padban, N., Ye, Z., Olofsson, G., Andersson, A. and Bjerle, I. (2000) 'Catalytic hot gas cleaning of fuel gas from an air-blown pressurized fluidized-bed gasifier', *Industrial & engineering chemistry research*, 39(11), pp. 4075-4081.
- Wang, Z., Wang, F., Cao, J. and Wang, J. (2010) 'Pyrolysis of pine wood in a slowly heating fixed-bed reactor: potassium carbonate versus calcium hydroxide as a catalyst', *Fuel Processing Technology*, 91(8), pp. 942-950.
- Xie, Y.R., Shen, L.H., Xiao, J., Xie, D.X. and Zhu, J. (2009) 'Influences of additives on steam gasification of biomass. 1. Pyrolysis procedure', *Energy & Fuels*, 23(10), pp. 5199-5205.
- Xu, C. and Tu, X. (2013) 'Plasma-assisted methane conversion in an atmospheric pressure dielectric barrier discharge reactor', *Journal of Energy Chemistry*, 22(3), pp. 420-425.
- Yamamoto, T. and Futamura, S. (1998) 'Nonthermal plasma processing for controlling volatile organic compounds', *Combustion science and technology*, 133(1-3), pp. 117-133.
- Yan, K., Van Heesch, E.J.M., Pemen, A.J.M., Huijbrechts, P., Van Gompel, F.M., Van Leuken, H. and Matyas, Z. (2002) 'A high-voltage pulse generator for corona plasma generation', *IEEE Transactions on Industry Applications*, 38(3), pp. 866-872.
- Yang, Y.C. and Chun, Y.N. (2011) 'Naphthalene destruction performance from tar model compound using a gliding arc plasma reformer', *Korean Journal of Chemical Engineering*, 28(2), pp. 539-543.
- Yanik, J., Ebale, S., Kruse, A., Saglam, M. and Yüksel, M. (2008) 'Biomass gasification in supercritical water: II. Effect of catalyst', *International Journal of Hydrogen Energy*, 33(17), pp. 4520-4526.
- Yu, L., Li, X., Tu, X., Wang, Y., Lu, S. and Yan, J. (2009a) 'Decomposition of naphthalene by dc gliding arc gas discharge', *The Journal of Physical Chemistry A*, 114(1), pp. 360-368.
- Yu, L., Tu, X., Li, X., Wang, Y., Chi, Y. and Yan, J. (2010) 'Destruction of acenaphthene, fluorene, anthracene and pyrene by a dc gliding arc plasma reactor', *Journal of Hazardous Materials*, 180(1-3), pp. 449-455.
- Yu, Q., Brage, C., Chen, G. and Sjöström, K. (1997) 'Temperature impact on the formation of tar from biomass pyrolysis in a free-fall reactor', *Journal of Analytical and Applied Pyrolysis*, 40, pp. 481-489.
- Yu, Q., Kong, M., Liu, T., Fei, J. and Zheng, X. (2012) 'Characteristics of the decomposition of CO<sub>2</sub> in a dielectric packed-bed plasma reactor', *Plasma Chemistry and Plasma Processing*, 32(1), pp. 153-163.

- Yu, Q.Z., Brage, C., Nordgreen, T. and Sjöström, K. (2009b) 'Effects of Chinese dolomites on tar cracking in gasification of birch', *Fuel*, 88(10), pp. 1922-1926.
- Zhang, H., Du, C., Wu, A., Bo, Z., Yan, J. and Li, X. (2014a) 'Rotating gliding arc assisted methane decomposition in nitrogen for hydrogen production', *international journal of hydrogen energy*, 39(24), pp. 12620-12635.
- Zhang, H., Li, K., Shu, C., Lou, Z., Sun, T. and Jia, J. (2014b) 'Enhancement of styrene removal using a novel double-tube dielectric barrier discharge (DDBD) reactor', *Chemical Engineering Journal*, 256, pp. 107-118.
- Zhang, K., Eliasson, B. and Kogelschatz, U. (2002) 'Direct conversion of greenhouse gases to synthesis gas and C-4 hydrocarbons over zeolite HY promoted by a dielectric-barrier discharge', *Industrial & Engineering Chemistry Research*, 41(6), pp. 1462-1468.
- Zhang, K., Mukhriza, T., Liu, X., Greco, P.P. and Chiremba, E. (2015) 'A study on CO<sub>2</sub> and CH<sub>4</sub> conversion to synthesis gas and higher hydrocarbons by the combination of catalysts and dielectric-barrier discharges', *Appl. Catal., A*, 502, pp. 138-149.
- Zhang, K., Zhang, G., Liu, X., Phan, A.N. and Luo, K. (2017) 'A Study on CO<sub>2</sub> Decomposition to CO and O<sub>2</sub> by the Combination of Catalysis and Dielectric-Barrier Discharges at Low Temperatures and Ambient Pressure', *Industrial & Engineering Chemistry Research*, 56(12), pp. 3204-3216.
- Zhang, R., Brown, R.C., Suby, A. and Cummer, K. (2004) 'Catalytic destruction of tar in biomass derived producer gas', *Energy Conversion and Management*, 45(7-8), pp. 995-1014.
- Zhang, R., Wang, Y. and Brown, R.C. (2007) 'Steam reforming of tar compounds over Ni/olivine catalysts doped with CeO<sub>2</sub>', *Energy Conversion and Management*, 48(1), pp. 68-77.
- Zhang, Y., Kajitani, S., Ashizawa, M. and Oki, Y. (2010) 'Tar destruction and coke formation during rapid pyrolysis and gasification of biomass in a drop-tube furnace', *Fuel*, 89(2), pp. 302-309.
- Zhu, F., Li, X., Zhang, H., Wu, A., Yan, J., Ni, M., Zhang, H. and Buekens, A. (2016) 'Destruction of toluene by rotating gliding arc discharge', *Fuel*, 176, pp. 78-85.
- Zhu, T., Wan, Y.D., Li, J., He, X.W., Xu, D.Y., Shu, X.Q., Liang, W.J. and Jin, Y.Q. (2011) 'Volatile organic compounds decomposition using nonthermal plasma coupled with a combination of catalysts', *International Journal of Environmental Science & Technology*, 8(3), pp. 621-630.